Electronic Supplementary Information for Dalton Transactions

Supplementary Information

Diversity and Design of Metal-Based Carbon Monoxide-Releasing Molecules (CO-RMs) in Aqueous Systems: Revealing the Essential Trends

Wei-Qiang Zhang, Anthony J. Atkin, Robert J. Thatcher, Adrian C. Whitwood, Ian J. S. Fairlamb and Jason M. Lynam*

Department of Chemistry, University of York, Heslington, York, YO10 5DD, UK

1. CO-Release Tests

The release of CO from metal carbonyl compounds was studied spectrophotometrically by measuring the conversion of deoxy-myoglobin (deoxy-Mb) to carbonmonoxy myoglobin (Mb-CO).[1] The amount of Mb-CO formed was quantified by measuring the absorbance at 540 nm. A stock solution of myoglobin (lyophilised horse heart) (66 μM final concentration) was prepared fresh by dissolving the protein in phosphate buffered saline (PBS) (0.01M, pH = 7.4). Sodium dithionite (0.1%) was added to convert the myoglobin stock to deoxy-Mb. A 2 ml quantity of this was measured to obtain a deoxy-Mb spectrum and then bubbled with CO to get a Mb-CO spectrum. CO-RMs were dissolved in an appropriate solvent (DMSO or EtOH) (4, 8, 12 μM) and added to deoxy-Mb in the cuvette (to give a final CO-RM concentration of 20, 40, 60 μM), mixed using a pipette and then overlaid with 500 μL light mineral oil to prevent CO escaping or the myoglobin being oxygenated. This is the standard procedure; other experiments have been undertaken using different concentrations of myoglobin and different concentrations of DMSO.

The maximal absorption peak of deoxy-Mb at 560 nm is converted to the two maximal absorption peaks of Mb-CO at 540 and 578 nm. The concentration of myoglobin in the stock solution was calculated from the maximal absorption peak of the Mb-CO solution at 540 nm (Equation 1).

Equation 1. Equation for calculating total myoglobin concentration in a saturated solution of Mb-CO. ε = extinction coefficient of Mb-CO = 15.4 $mM^{-1}cm^{-1}$, OD_{540} = absorbance of Mb-CO solution at 540 nm.

$$Mb\text{-}CO_{max} = (OD_{540} / \varepsilon) \times 1000$$

Intermediate concentrations of Mb-CO are calculated from the OD_{540}. A new extinction coefficient (ε_2) must be calculated to take into account the change in absorbance at 540 nm (ΔOD_{540}). To aid in the accuracy of this calculation, another wavelength is used as a constant reference point. The deoxy-Mb and Mb-CO spectra share four isosbestic (OD_{iso}) points (510, 550, 570, 585 nm). The value at 510 nm (OD_{iso510}) was used in this set of experiments. The new extinction coefficient was calculated (Equation 2).

Equation 2. Equation needed to calculate unknown Mb-CO extinction coefficient. ΔOD_{iso510} = change in absorbance at the isosbestic point, ΔOD_{540} = change in absorbance at 540 nm, $Mb\text{-}CO_{max}$ = maximum concentration of myoglobin. ε_2 = new extinction coefficient.

$$\varepsilon_2 = (\Delta OD_{540} - \Delta OD_{iso510} \times 1000) / Mb\text{-}CO_{max}$$

From the new extinction coefficient and the change in absorbance at 540 and 510 nm will give the concentration of myoglobin in any unknown sample. (Equation 3)

Equation 3. Equation to calculate the Mb-CO concentration in samples. ΔOD_{540} = change in absorbance at 540 nm, ΔOD_{iso510} = change in absorbance at the isosbestic point, ε_2 = calculated absorption coefficient.

$$Mb\text{-}CO = 1000 \times (\Delta OD_{540} - \Delta OD_{iso510}) / \varepsilon_2$$

The resulting curves for the formation of Mb-CO verus time were fitted using non-linear regression routines in SigmaPlot,[2] resulting R^2 values were typically greater than 0.99. Half lives for CO-release were determined by extrapolating the equations generation from the non-linear regression to 30 μM, 20 μM and 10 μM Mb-CO for initial CO-RM concentrations of 60 μM, 40 μM and 20μM respectively. The same method was employed for CO-RM which exhibited slow release for Mb-CO concentrations of 15 μM, 10 μM and 5 μM respectively.

1 R. Motterlini, J. E Clark, R. Foresti, P. Sarathchandra, B. E. Mann and C. J. Green, *Circ. Res*., 2002, **90**, 1.
2 SigmaPlot Version 10.0 Systat Software, Inc

1.1. $[NEt_4][V(CO)_6]$

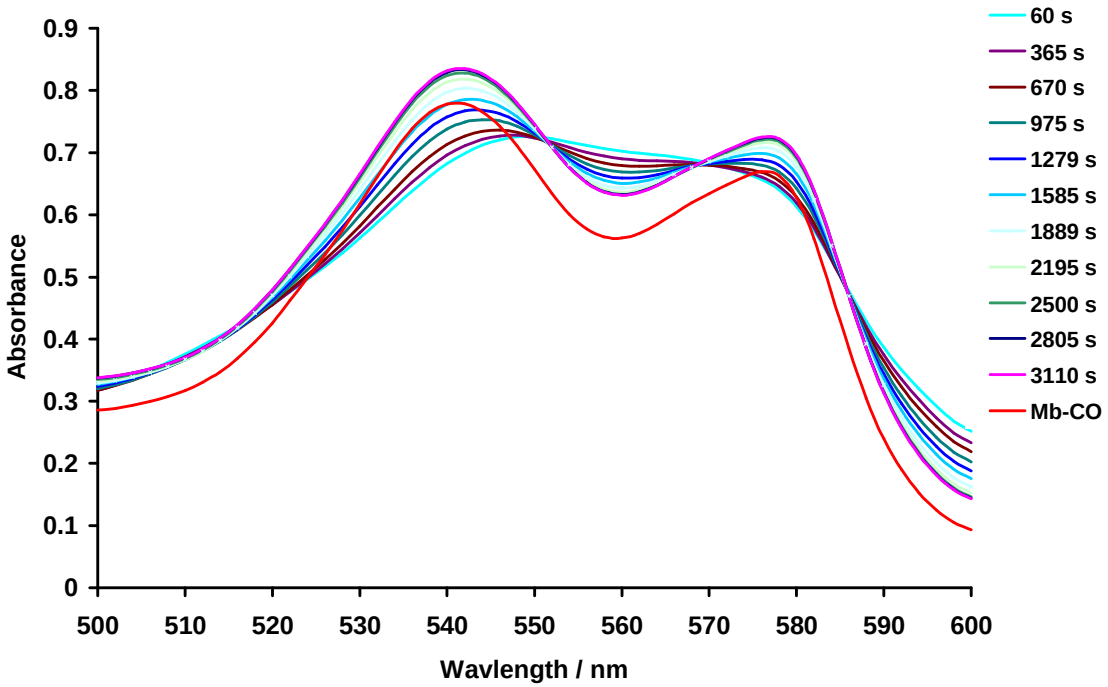

Fig. 1. The changes in the UV spectrum of myoglobin as CO is released from $[NEt_4][V(CO)_6]$ (60µm).

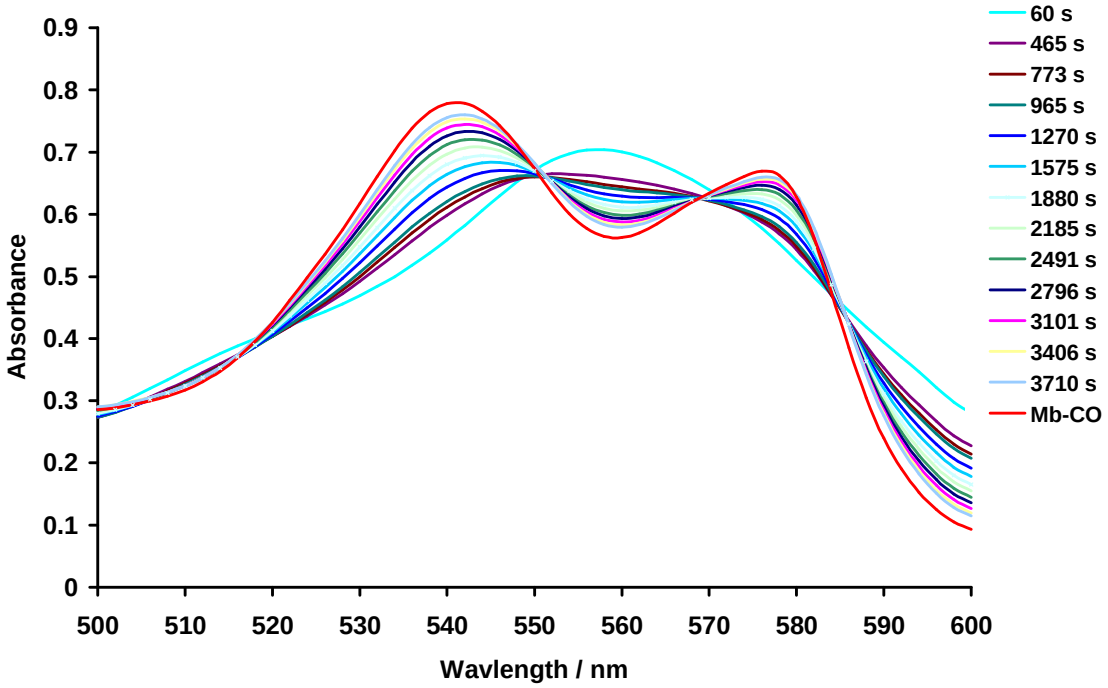

Fig. 2. The changes in the UV spectrum of myoglobin as CO is released from $[NEt_4][V(CO)_6]$ (40µm).

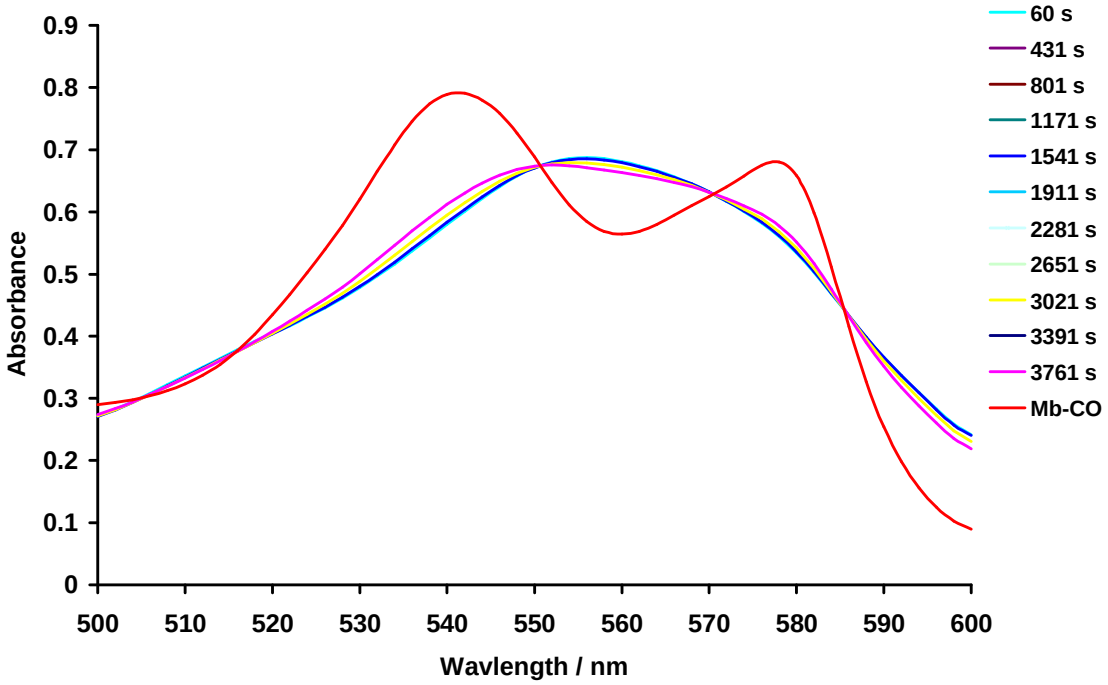

Fig. 3. The changes in the UV spectrum of myoglobin as CO is released from $[NEt_4][V(CO)_6]$ (20µm).

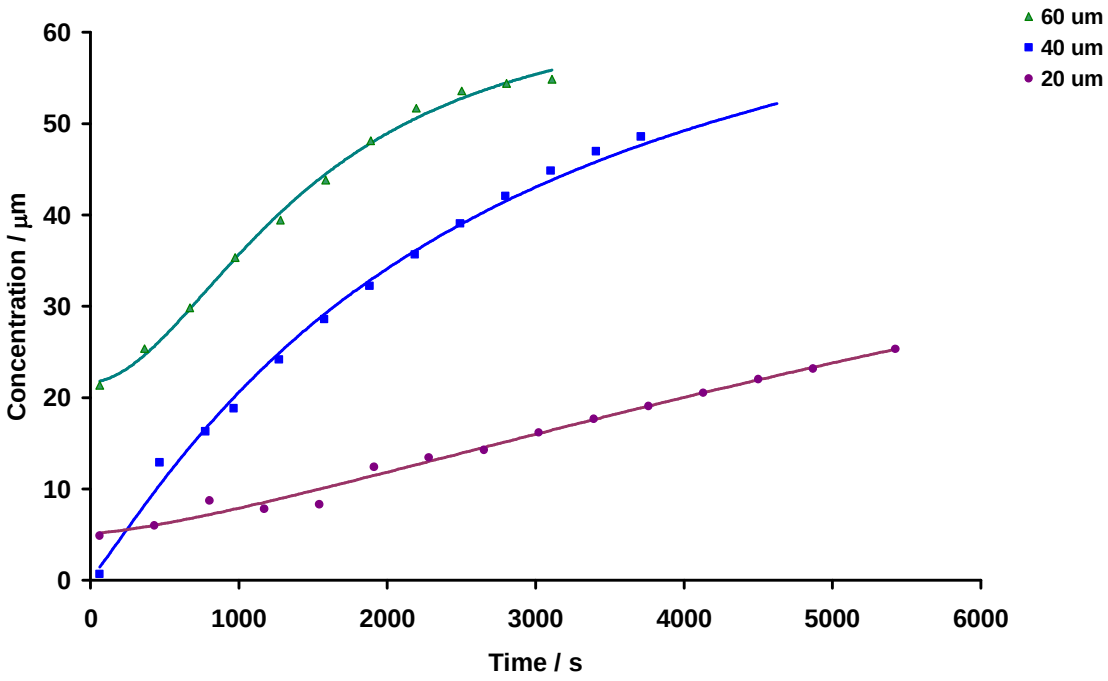

Fig. 4. Formation of MbCO over time after addition of 60 µM, 40µM and 20µM of $[NEt_4][V(CO)_6]$ in DMSO to an aqueous solution containing deoxy-myoglobin at pH 7.4.

1.2. $MnBr(CO)_5$

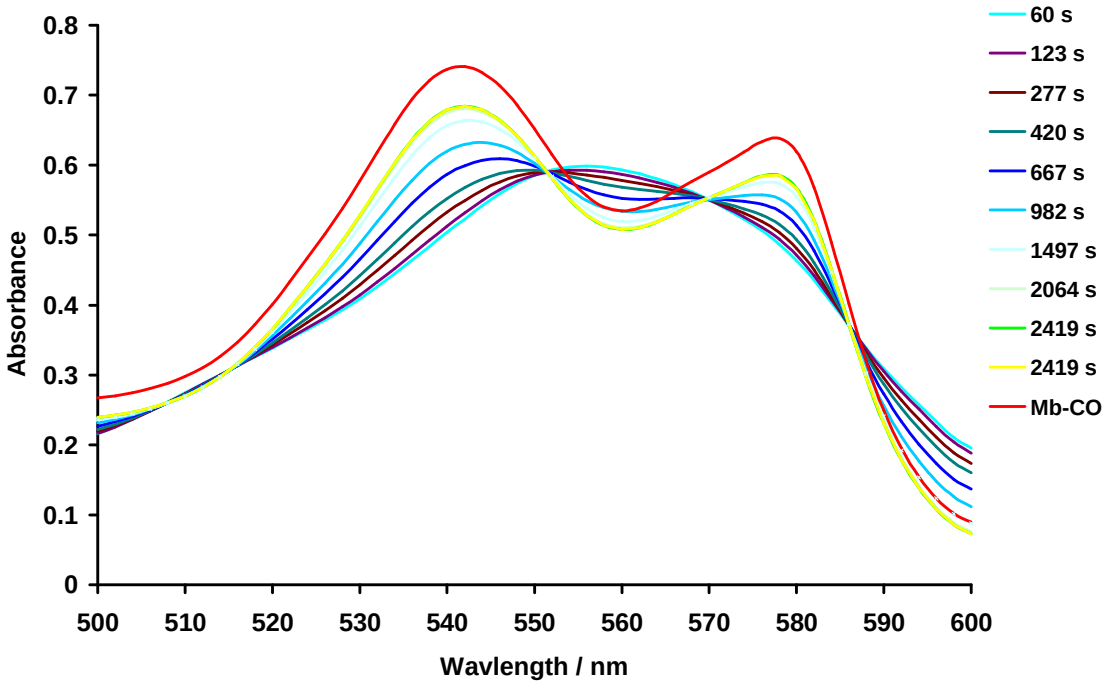

Fig. 5. The changes in the UV spectrum of myoglobin as CO is released from $MnBr(CO)_5$ (60µm).

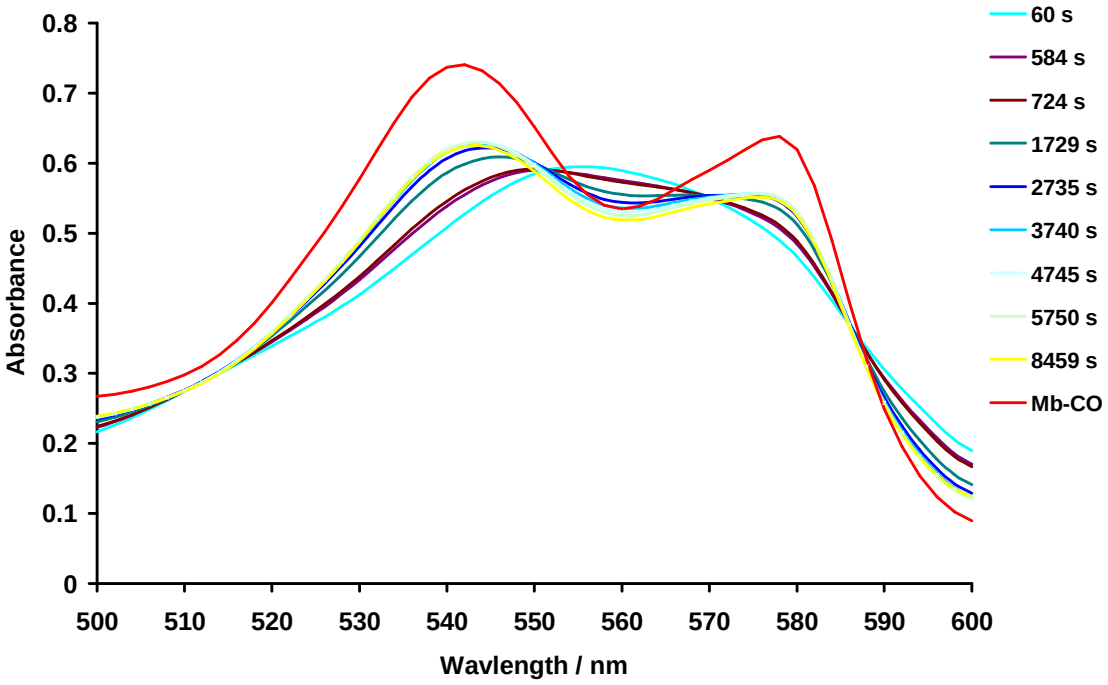

Fig. 6. The changes in the UV spectrum of myoglobin as CO is released from $MnBr(CO)_5$ (40µm).

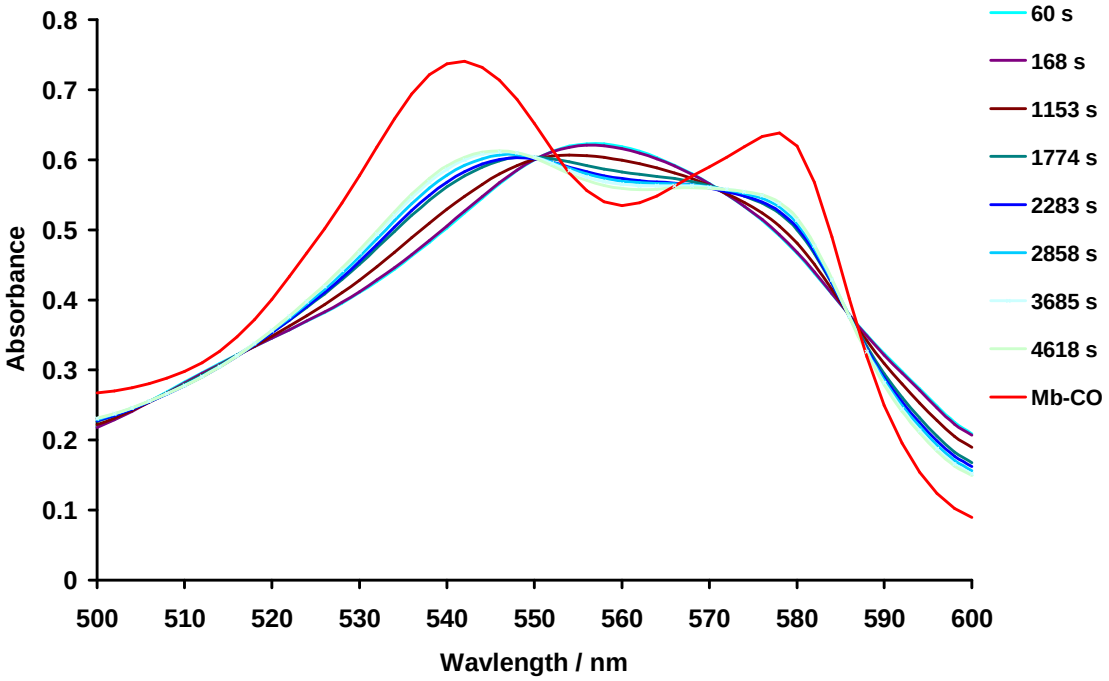

Fig. 7. The changes in the UV spectrum of myoglobin as CO is released from $MnBr(CO)_5$ (20µm).

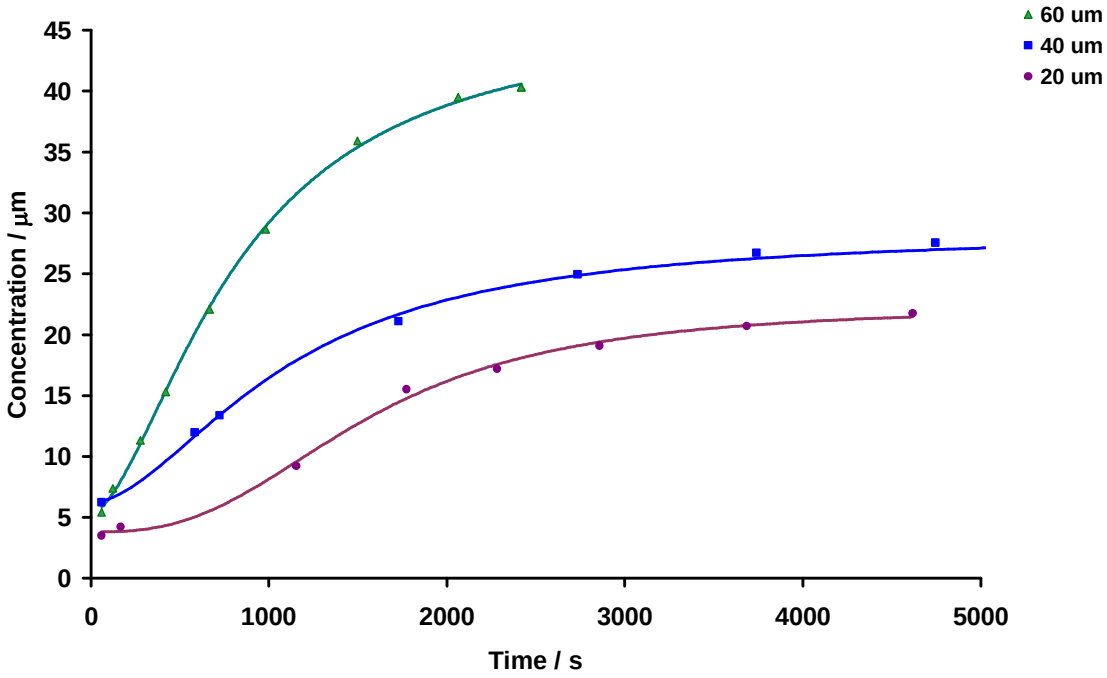

Fig. 8. Formation of MbCO over time after addition of 60 µM, 40µM and 20µM of $[Mn(CO)_5Br]$ in DMSO to an aqueous solution containing deoxy-myoglobin at pH 7.4.

1.3. $FeI_2(CO)_4$

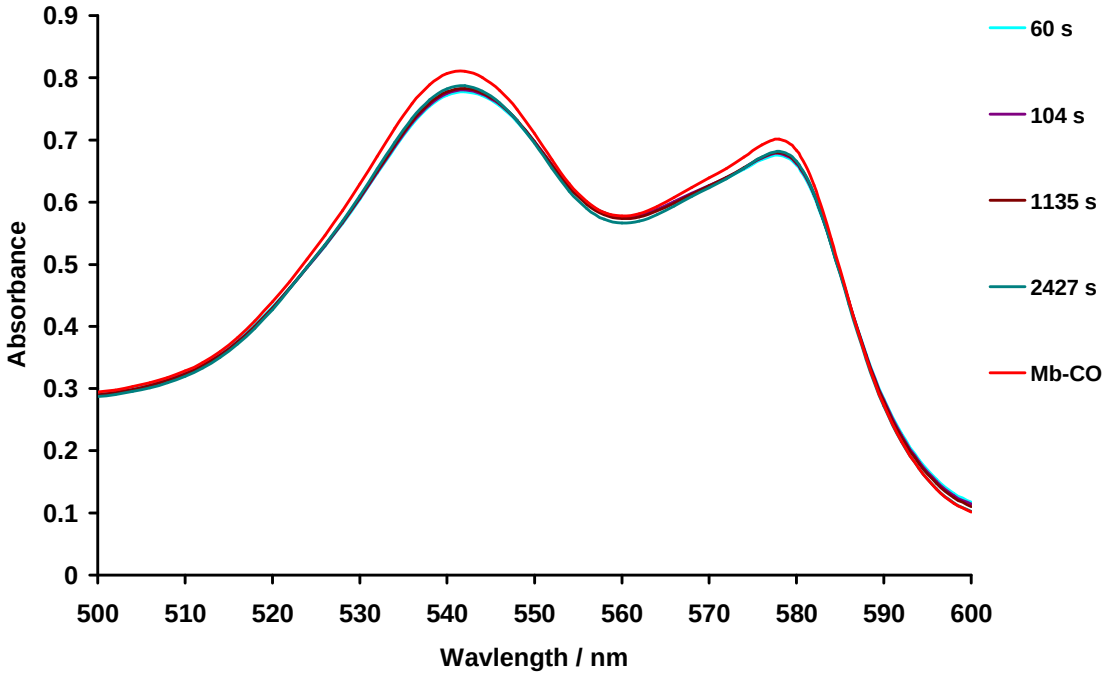

Fig. 9. The changes in the UV spectrum of myoglobin as CO is released from $FeI_2(CO)_5$ (60μm).

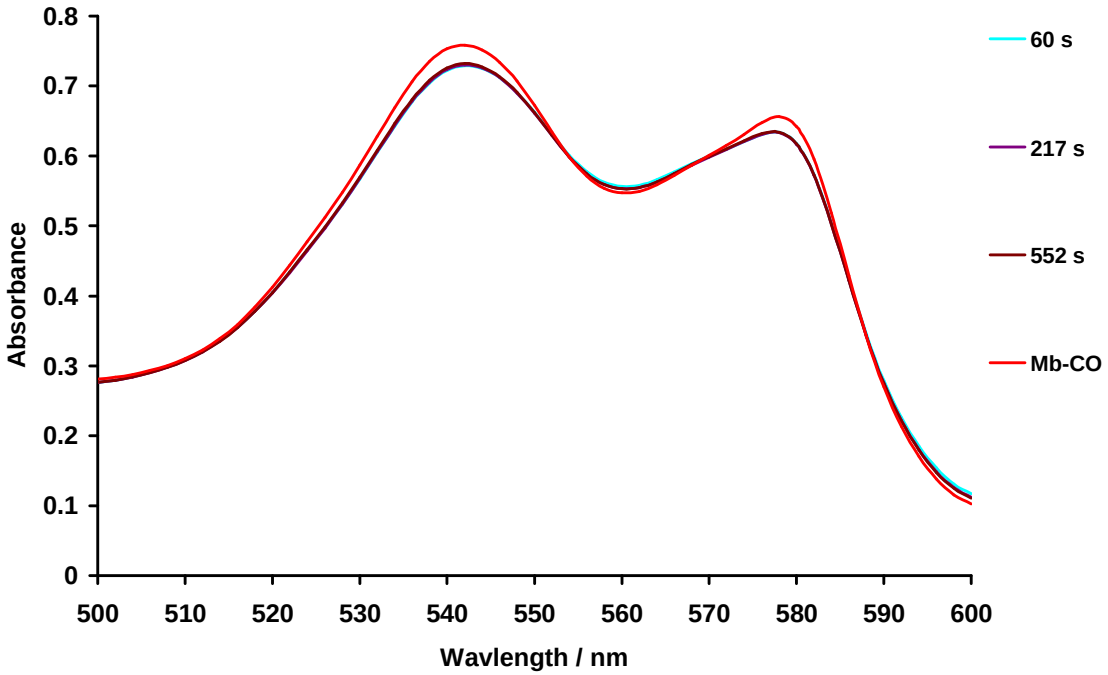

Fig. 10. The changes in the UV spectrum of myoglobin as CO is released from $FeI_2(CO)_5$ (40μm).

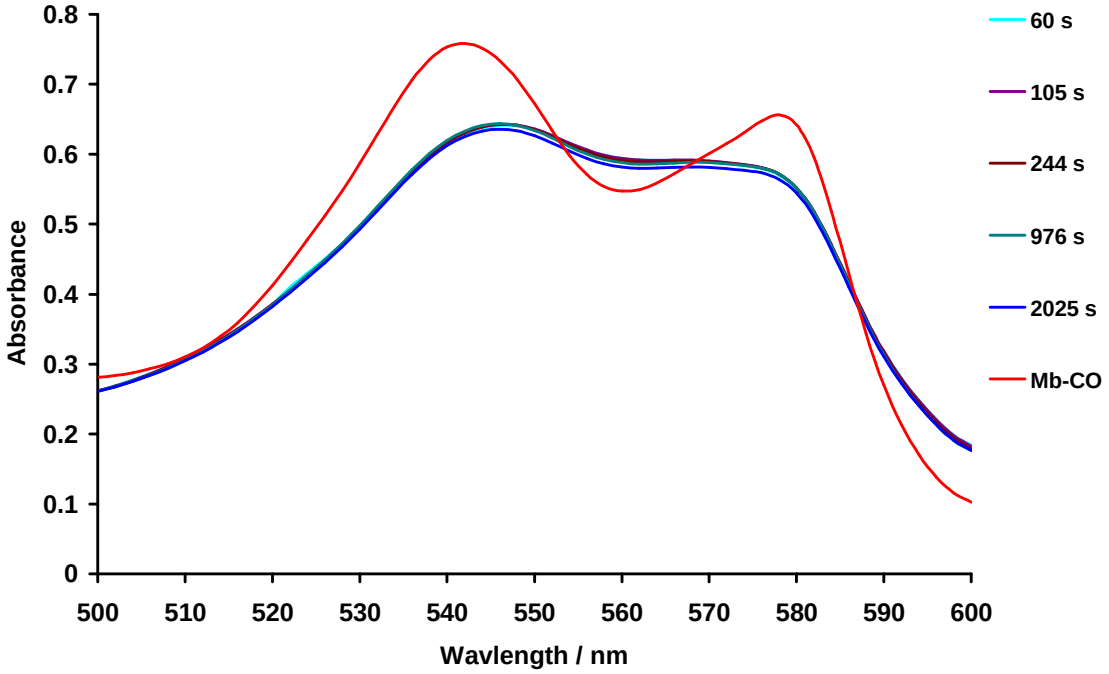

Fig. 11. The changes in the UV spectrum of myoglobin as CO is released from $FeI_2(CO)_5$ (20µm).

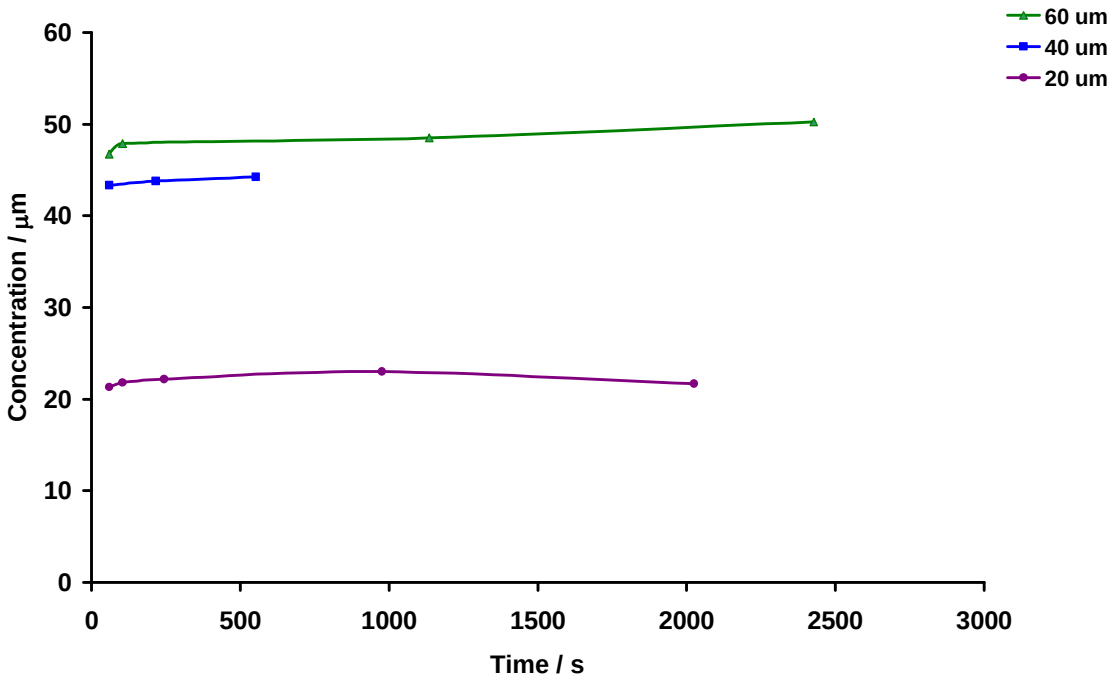

Fig. 12. Formation of MbCO over time after addition of 60 µM, 40µM and 20µM of $FeI_2(CO)_5$ in EtOH to an aqueous solution containing deoxy-myoglobin at pH 7.4.

1.4. mer-$FeI_2(CO)_3(P\{OCH_3\}_3)$

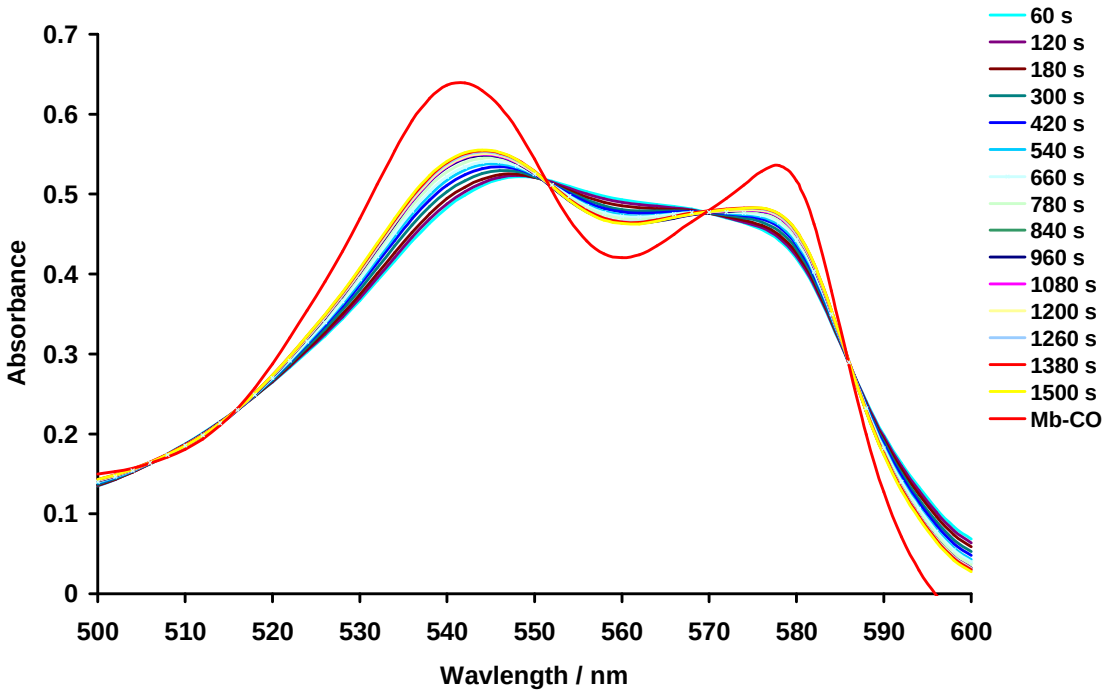

Fig. 13. The changes in the UV spectrum of myoglobin as CO is released from *mer*-$FeI_2(CO)_3(P\{OCH_3\}_3)$ (60μm).

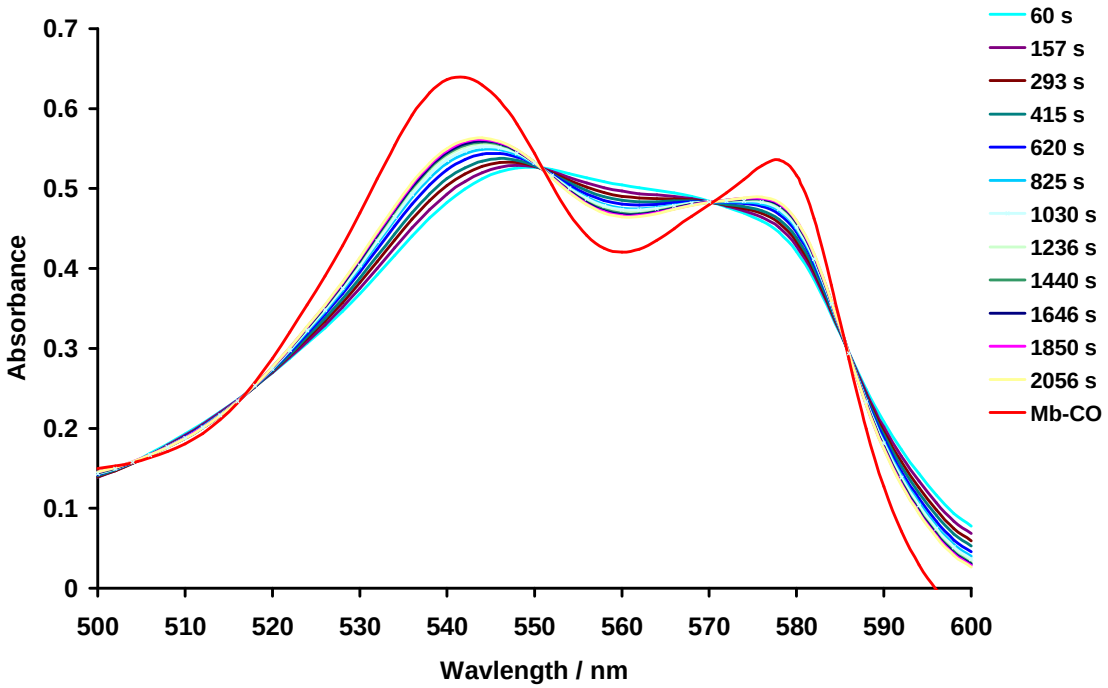

Fig. 14. The changes in the UV spectrum of myoglobin as CO is released from *mer*-$FeI_2(CO)_3(P\{OCH_3\}_3)$ (40μm).

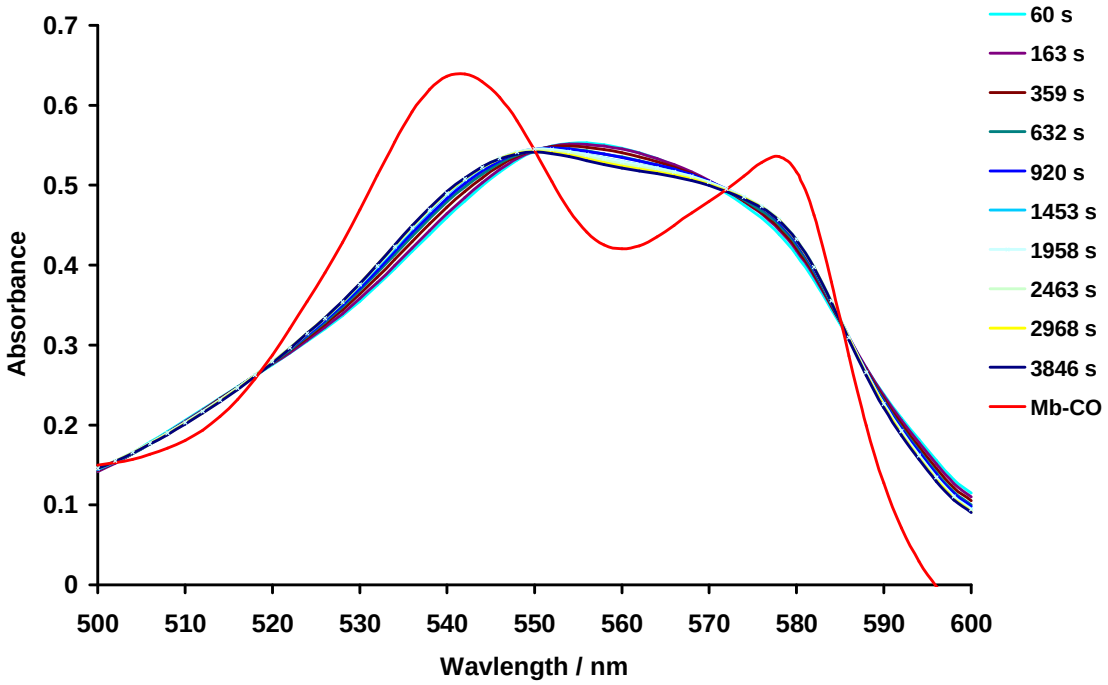

Fig. 15. The changes in the UV spectrum of myoglobin as CO is released from *mer*-$FeI_2(CO)_3(P\{OCH_3\}_3)$ (20μm).

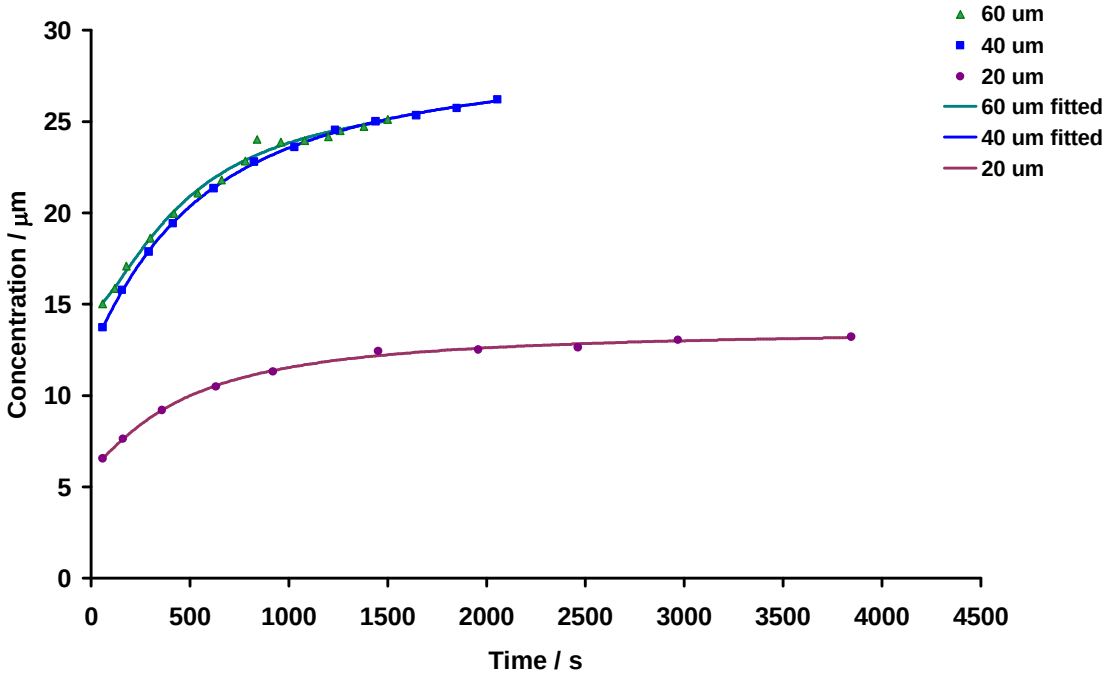

Fig. 16. Formation of MbCO over time after addition of 60 μM, 40μM and 20μM of *mer*-$FeI_2(CO)_3(P\{OCH_3\}_3)$ in DMSO to an aqueous solution containing deoxy-myoglobin at pH 7.4.

1.5. mer-$FeI_2(CO)_3(P\{CH_2OH\}_3)$

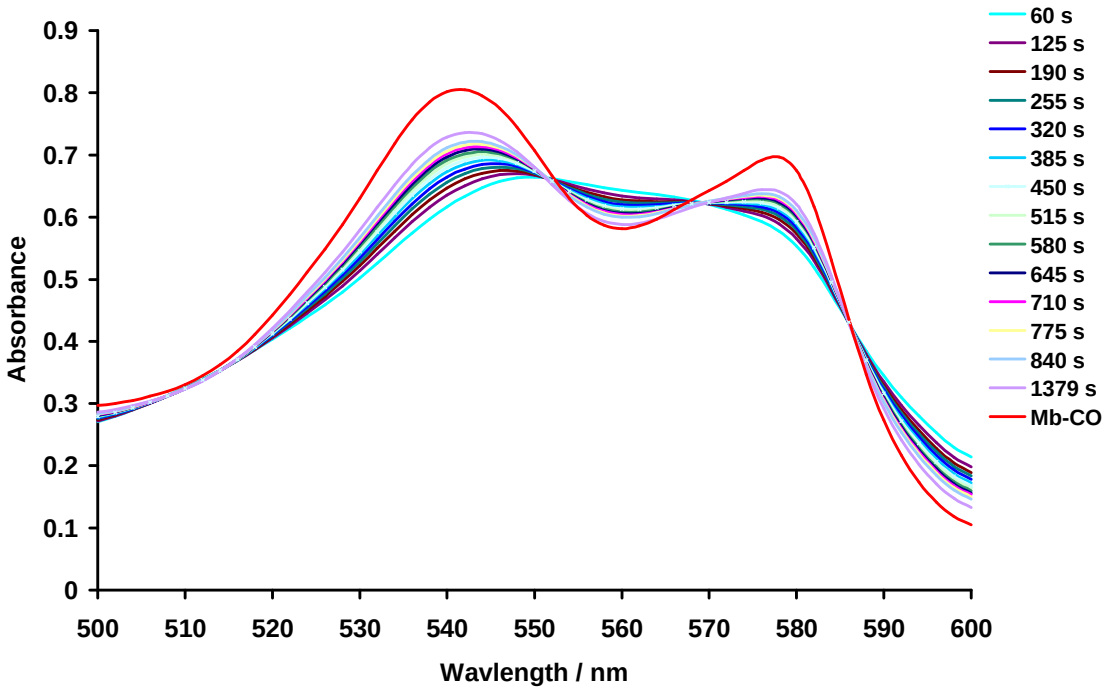

Fig. 17. The changes in the UV spectrum of myoglobin as CO is released from *mer*-$FeI_2(CO)_3(P\{CH_2OH\}_3)$ (60μm).

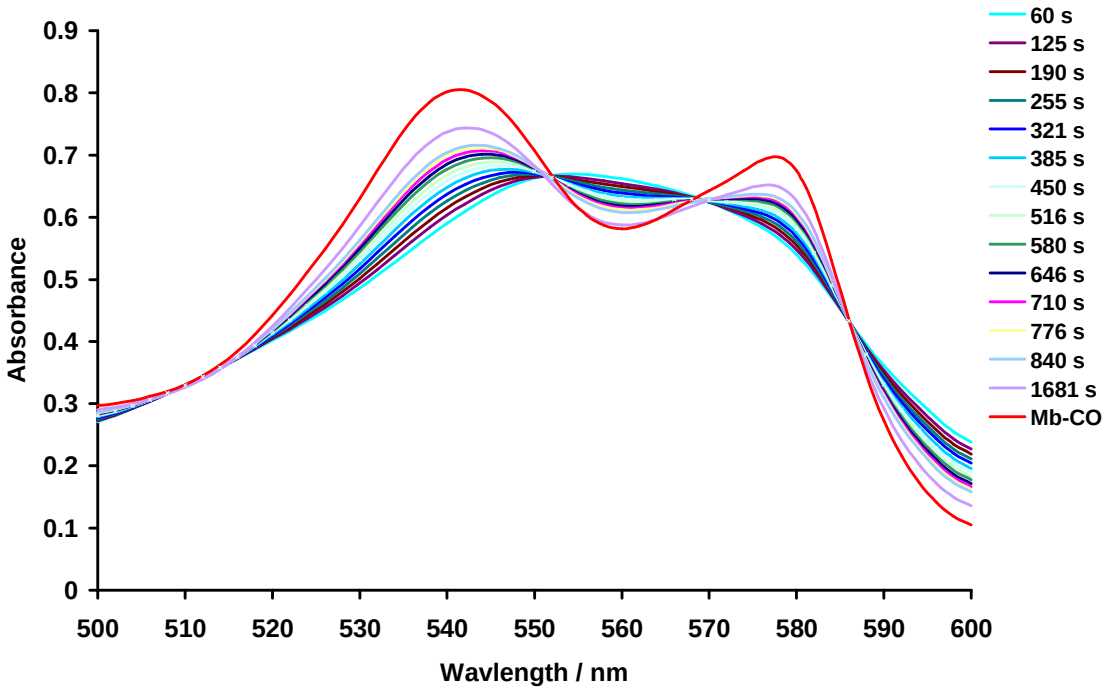

Fig. 18. The changes in the UV spectrum of myoglobin as CO is released from *mer*-$FeI_2(CO)_3(P\{CH_2OH\}_3)$ (40μm).

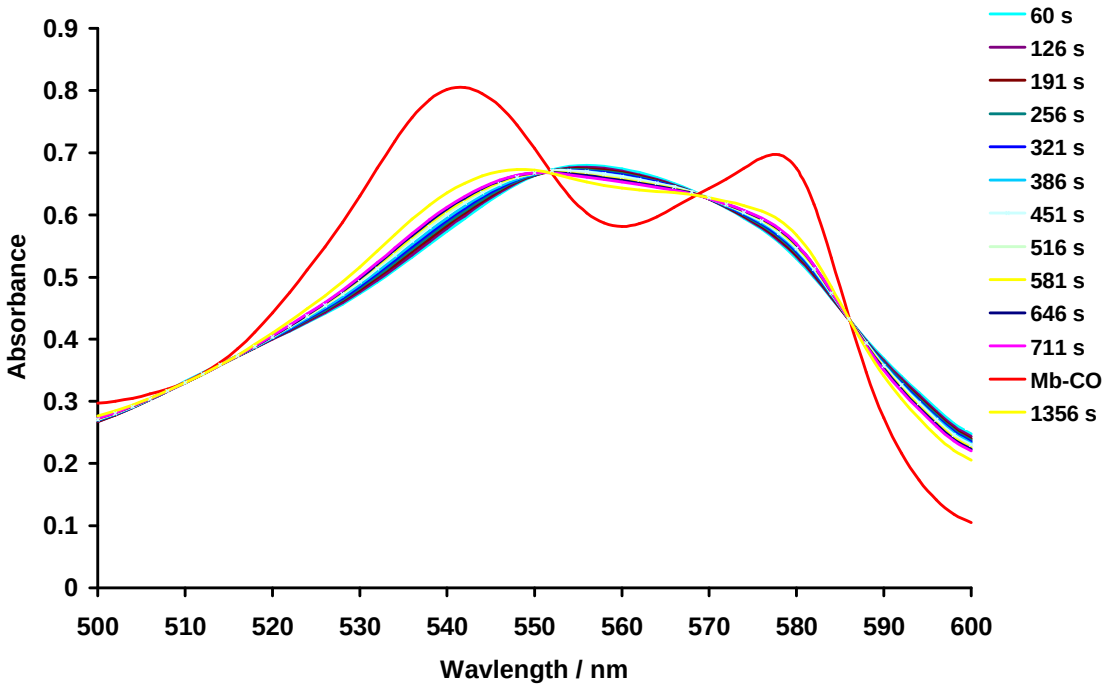

Fig. 19. The changes in the UV spectrum of myoglobin as CO is released from *mer*-$FeI_2(CO)_3(P\{CH_2OH\}_3)$ (20μm).

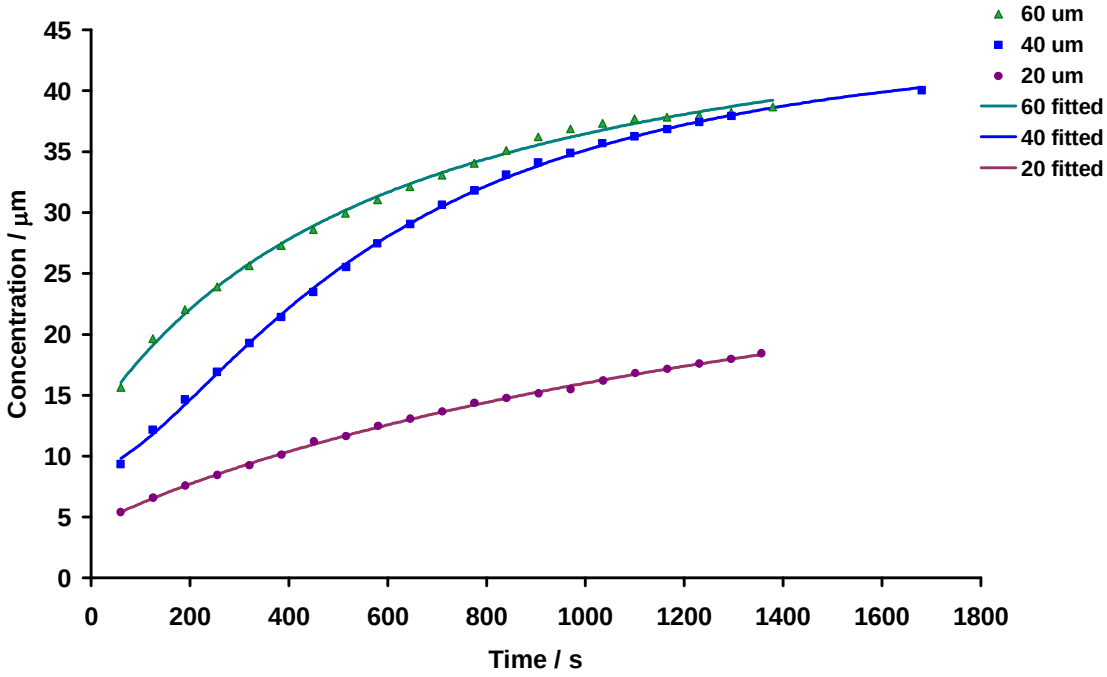

Fig. 20. Formation of MbCO over time after addition of 60 μM, 40μM and 20μM of *mer*-$FeI_2(CO)_3(P\{CH_2OH\}_3)$ in DMSO to an aqueous solution containing deoxy-myoglobin at pH 7.4.

1.6. all cis-$FeI_2(CO)_2(P\{OCH_3\}_3)_2$

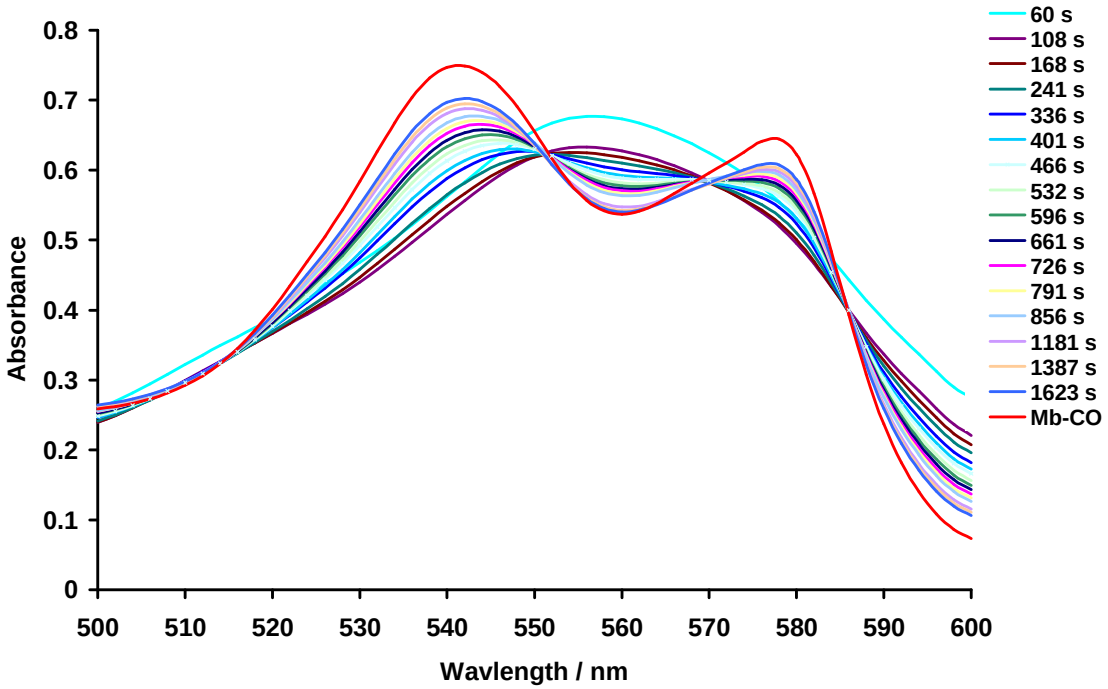

Fig. 21. The changes in the UV spectrum of myoglobin as CO is released from *all cis*-$FeI_2(CO)_2(P\{OCH_3\})_2$ (60μm).

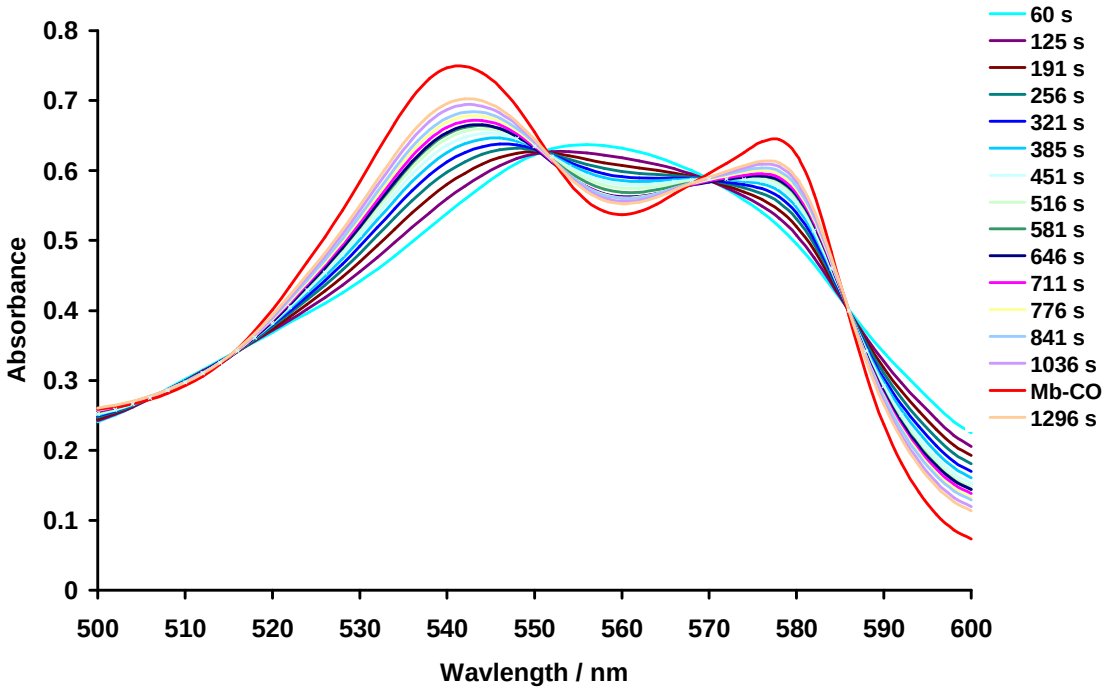

Fig. 22. The changes in the UV spectrum of myoglobin as CO is released from *all cis*-$FeI_2(CO)_2(P\{OCH_3\})_2$ (40μm).

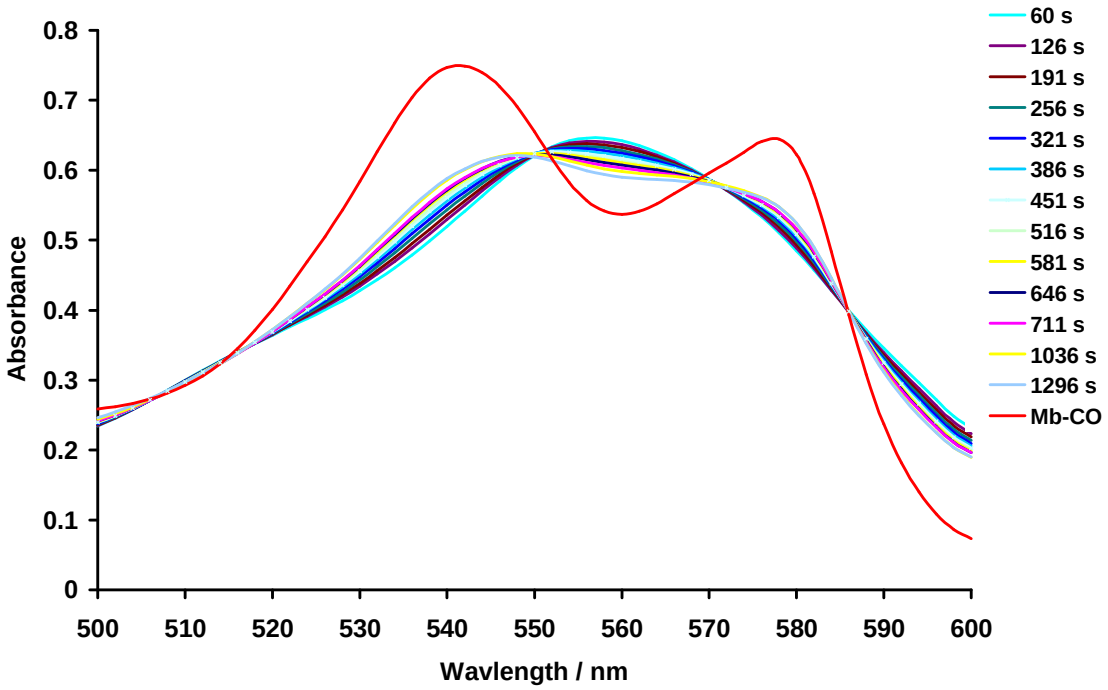

Fig. 23. The changes in the UV spectrum of myoglobin as CO is released from *all cis*-$FeI_2(CO)_2(P\{OCH_3\})_2$ (20µm).

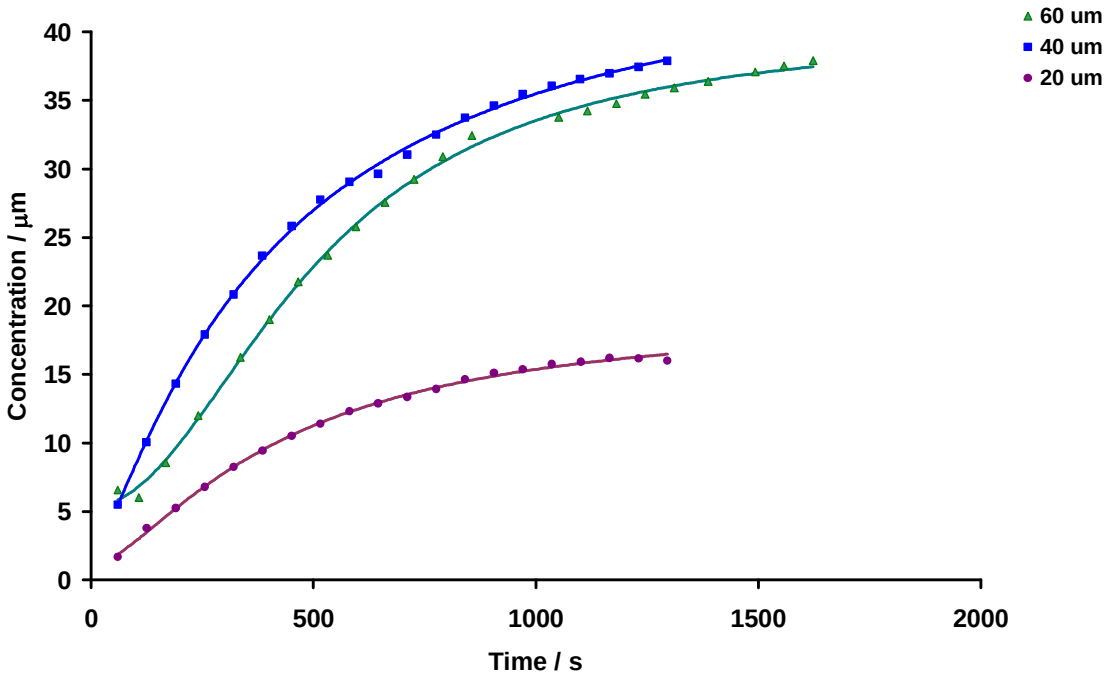

Fig. 24. Formation of MbCO over time after addition of 60 µM, 40µM and 20µM of *all cis*-$FeI_2(CO)_2(P\{OCH_3\})_2$ in DMSO to an aqueous solution containing deoxy-myoglobin at pH 7.4.

1.7. cis,cis,trans-$FeI_2(CO)_2(P\{OCH_3\}_3)_2$

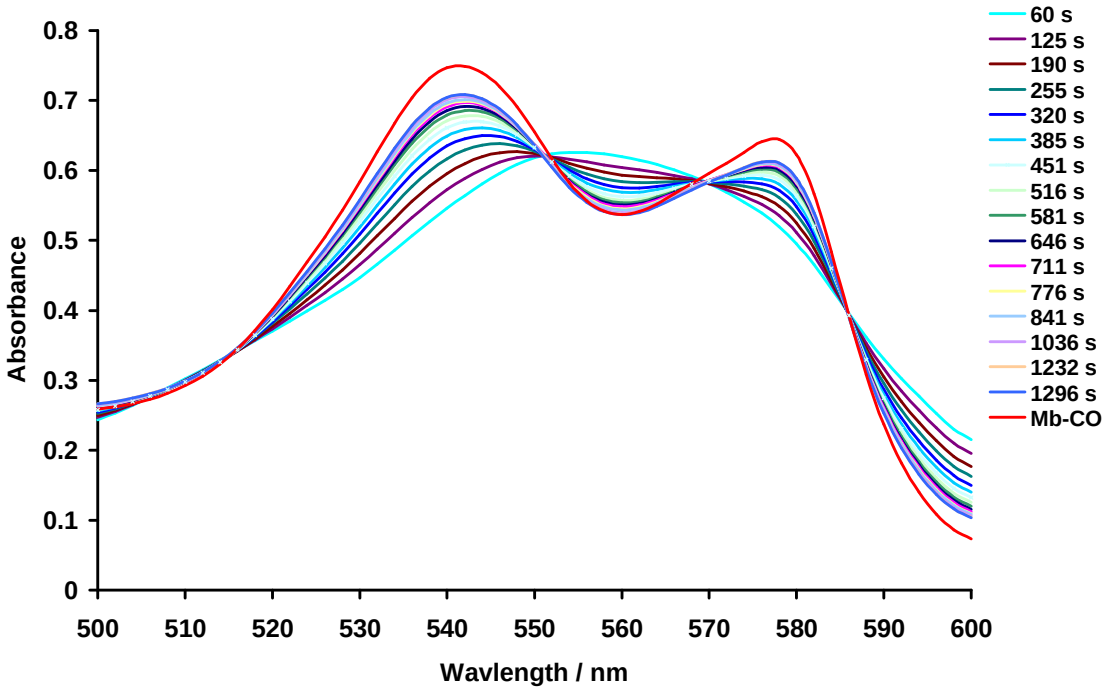

Fig. 25. The changes in the UV spectrum of myoglobin as CO is released from *cis,cis,trans*-$FeI_2(CO)_2(P\{OCH_3\})$ (60µm).

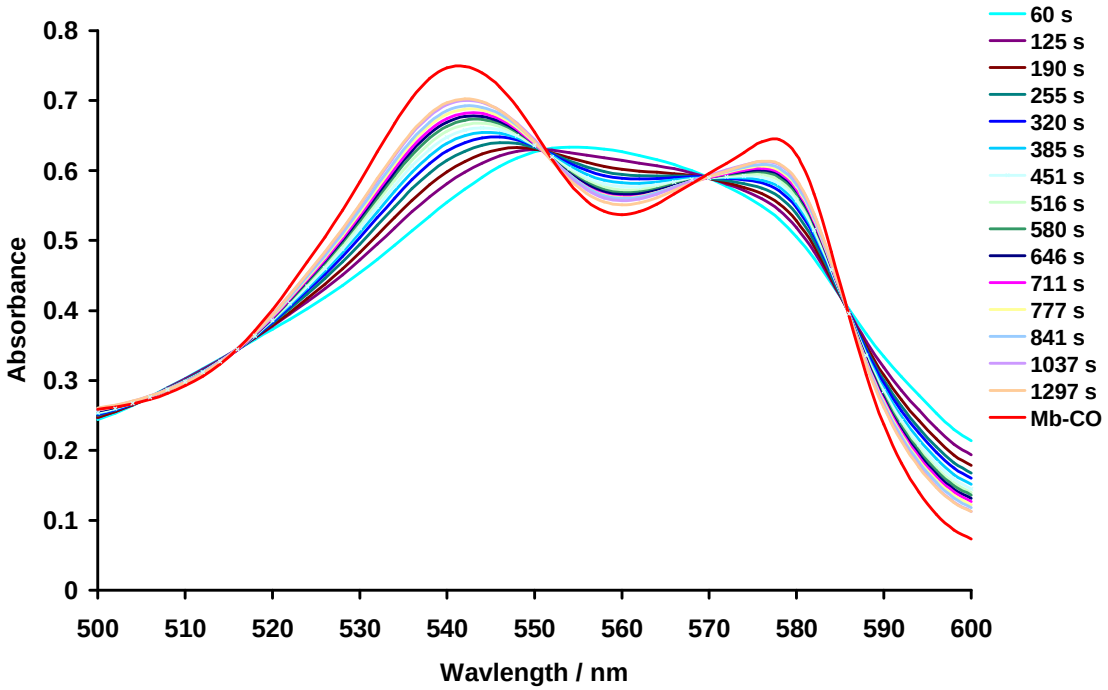

Fig. 26. The changes in the UV spectrum of myoglobin as CO is released from *cis,cis,trans*-$FeI_2(CO)_2(P\{OCH_3\})$ (40µm).

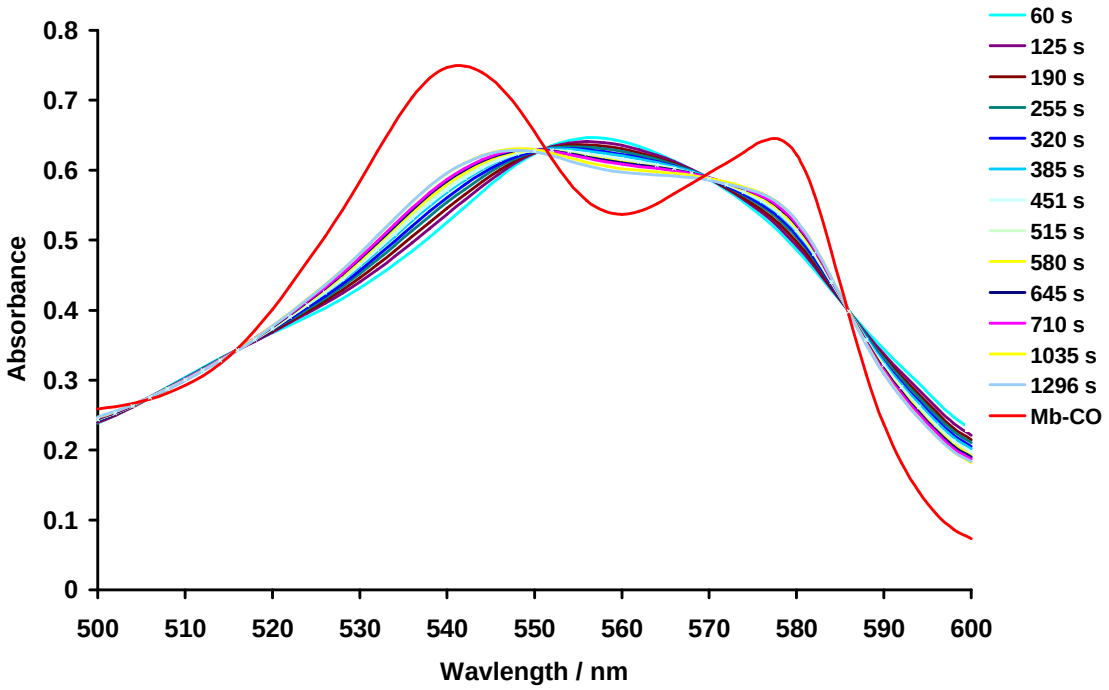

Fig. 27. The changes in the UV spectrum of myoglobin as CO is released from *cis,cis,trans*-$FeI_2(CO)_2(P\{OCH_3\})$ (20µm).

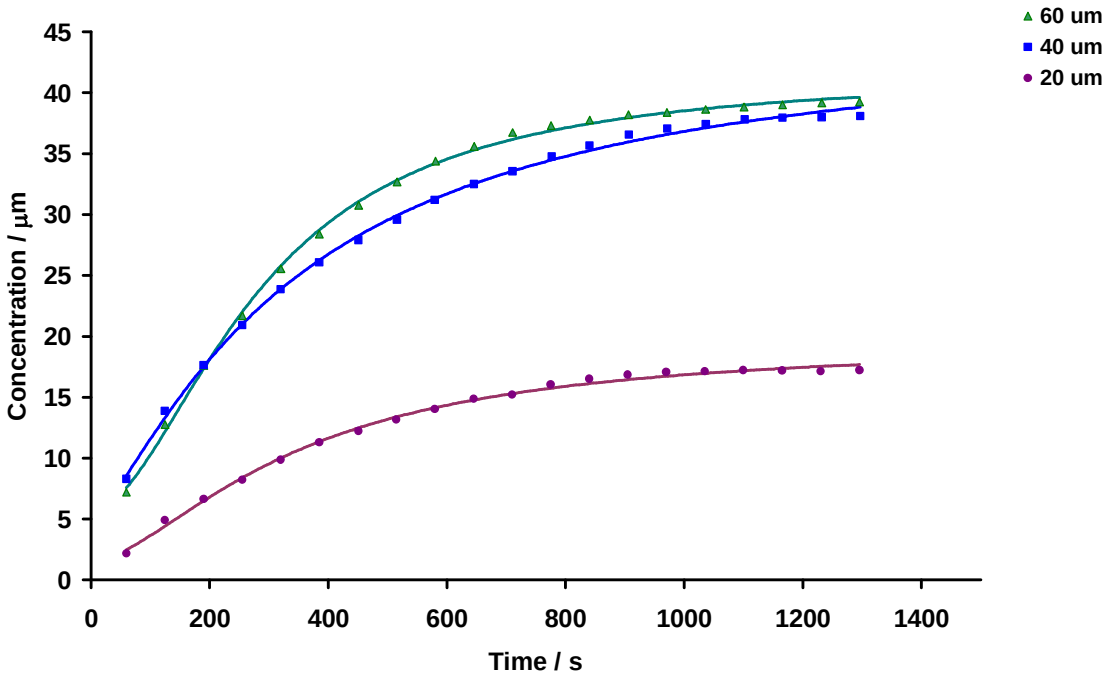

Fig. 28. Formation of MbCO over time after addition of 60 µM, 40µM and 20µM of *cis,cis,trans*-$FeI_2(CO)_2(P\{OCH_3\})_2$ in DMSO to an aqueous solution containing deoxy-myoglobin at pH 7.4.

1.8. Comparison of CO-release Data for Iron Phosphine Complexes

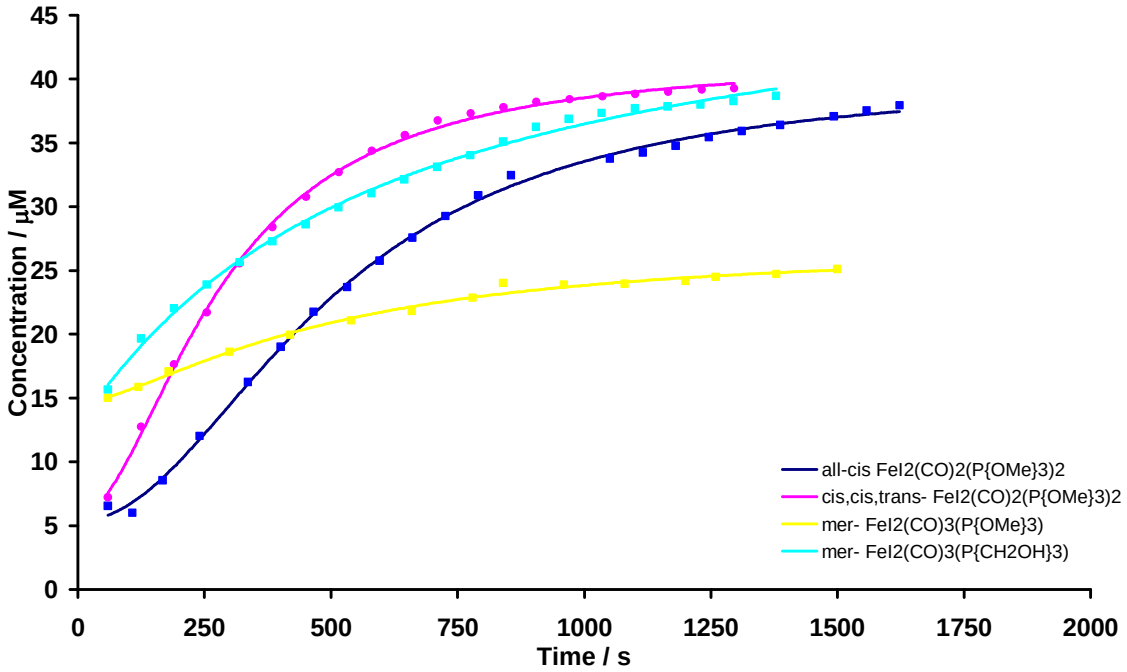

Fig. 29. Formation of MbCO over time after addition of 60 µM solutions of *mer*-$FeI_2(CO)_3(P\{OCH_3\})$, *mer*-$FeI_2(CO)_3(P\{CH_2OH\})$, *cis,cis, trans*-$FeI_2(CO)_2(P\{OCH_3\})_2$ and *all-cis*-$FeI_2(CO)_3(P\{OCH_3\})_2$ in DMSO to an aqueous solution containing deoxy-myoglobin at pH 7.4.

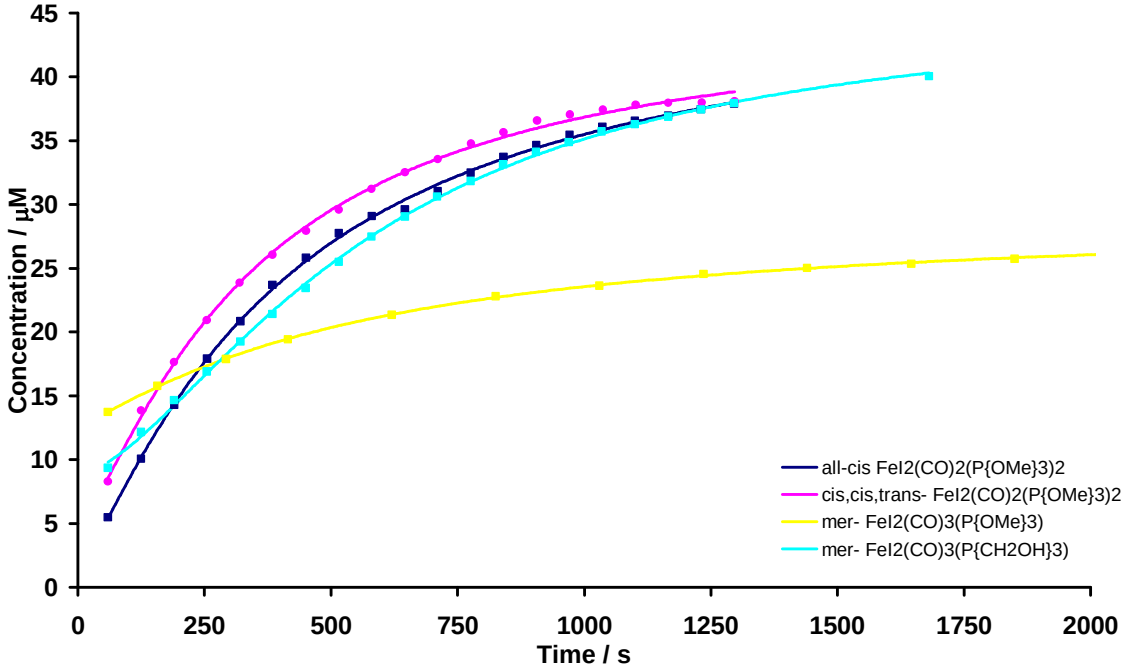

Fig. 30. Formation of MbCO over time after addition of 40 µM solutions of *mer*-$FeI_2(CO)_3(P\{OCH_3\})$, *mer*-$FeI_2(CO)_3(P\{CH_2OH\})$, *cis,cis, trans*-$FeI_2(CO)_2(P\{OCH_3\})_2$ and *all-cis*-$FeI_2(CO)_3(P\{OCH_3\})_2$ in DMSO to an aqueous solution containing deoxy-myoglobin at pH 7.4.

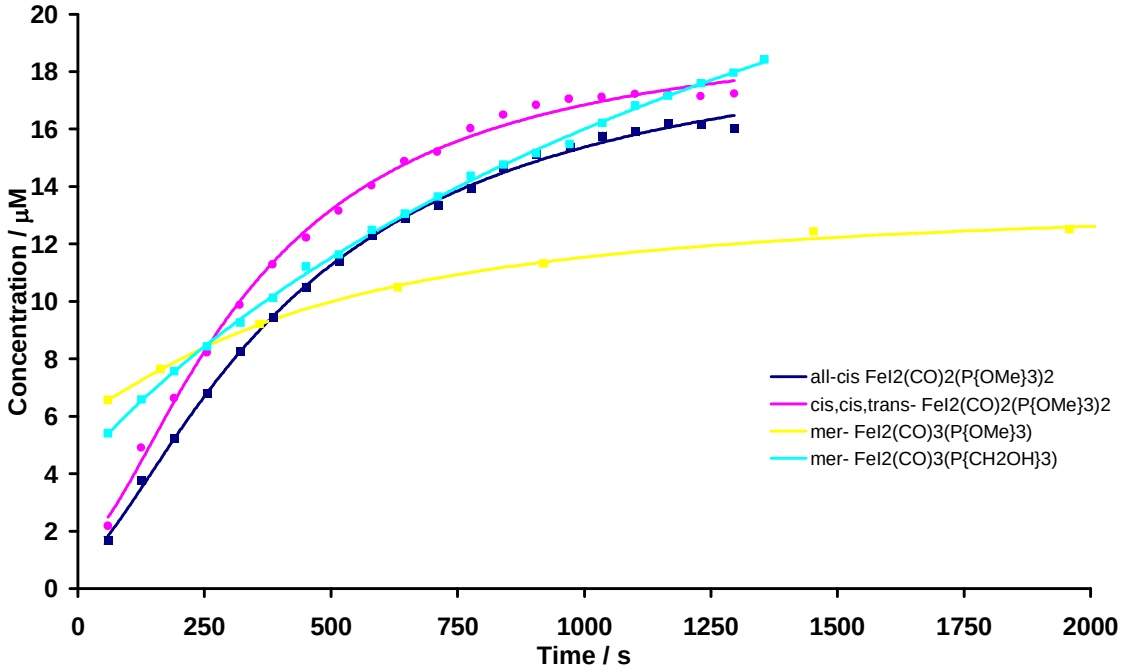

Fig. 31. Formation of MbCO over time after addition of 20 µM solutions of *mer*-$FeI_2(CO)_3(P\{OCH_3\})$, *mer*-$FeI_2(CO)_3(P\{CH_2OH\})$, *cis,cis, trans*-$FeI_2(CO)_2(P\{OCH_3\})_2$ and *all-cis*-$FeI_2(CO)_3(P\{OCH_3\})_2$ in DMSO to an aqueous solution containing deoxy-myoglobin at pH 7.4.

1.9. $[NEt_4][CrCl(CO)_5]$

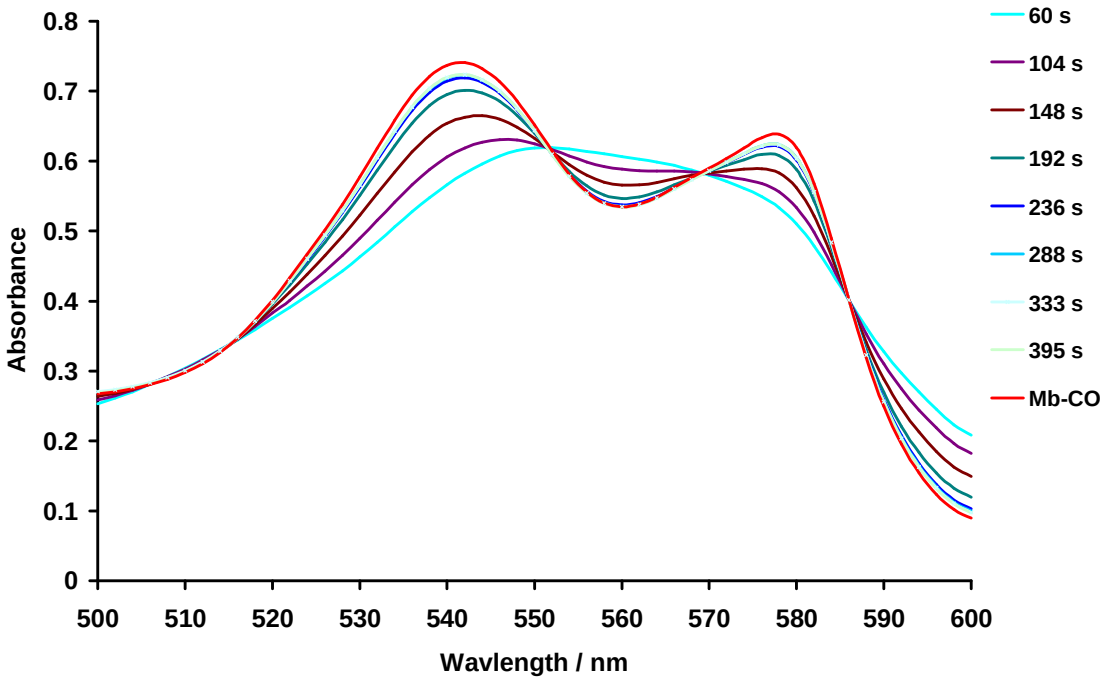

Fig. 32. The changes in the UV spectrum of myoglobin as CO is released from $[NEt_4][CrCl(CO)_5]$ (60µm).

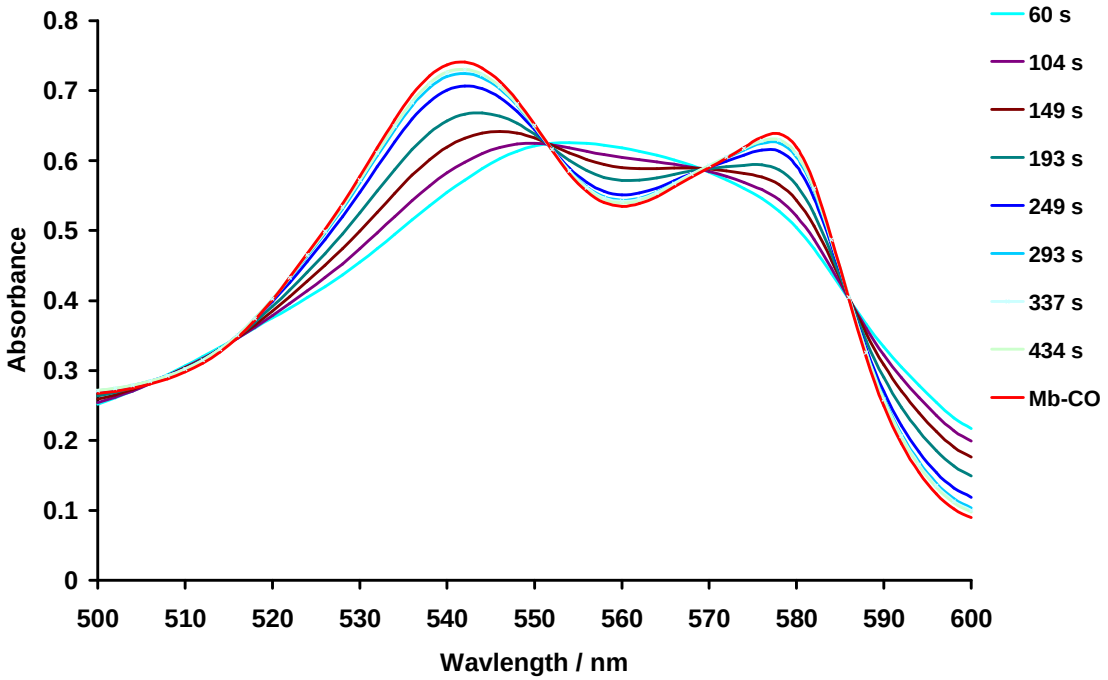

Fig. 33. The changes in the UV spectrum of myoglobin as CO is released from $[NEt_4][CrCl(CO)_5]$ (40µm).

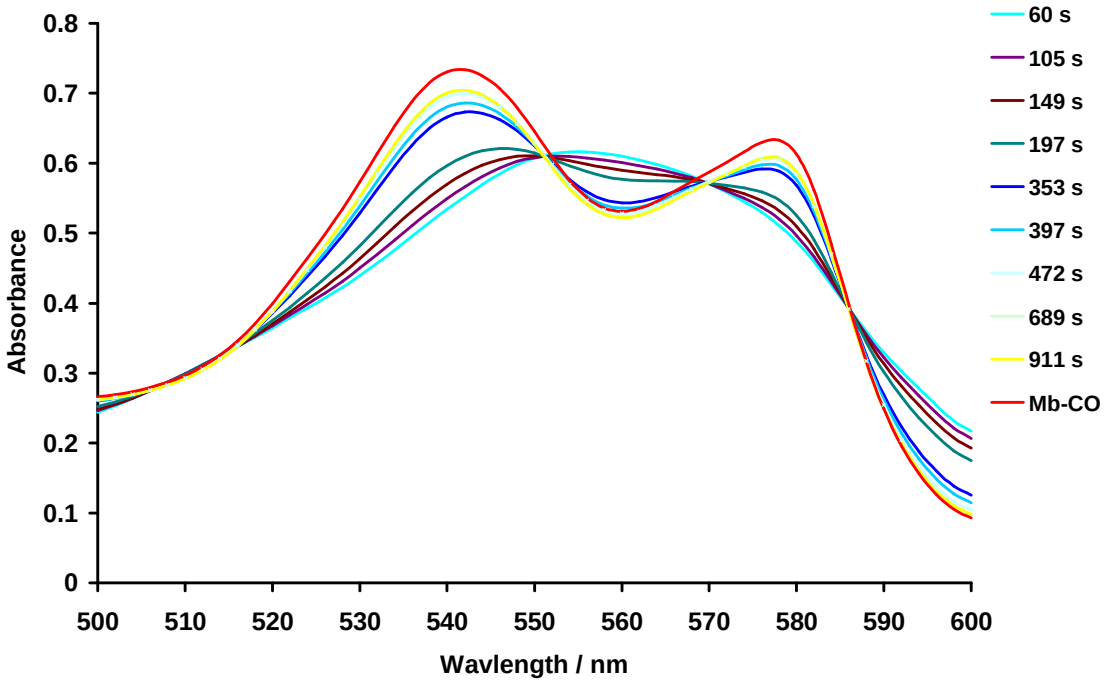

Fig. 34. The changes in the UV spectrum of myoglobin as CO is released from $[NEt_4][CrCl(CO)_5]$ (20µm).

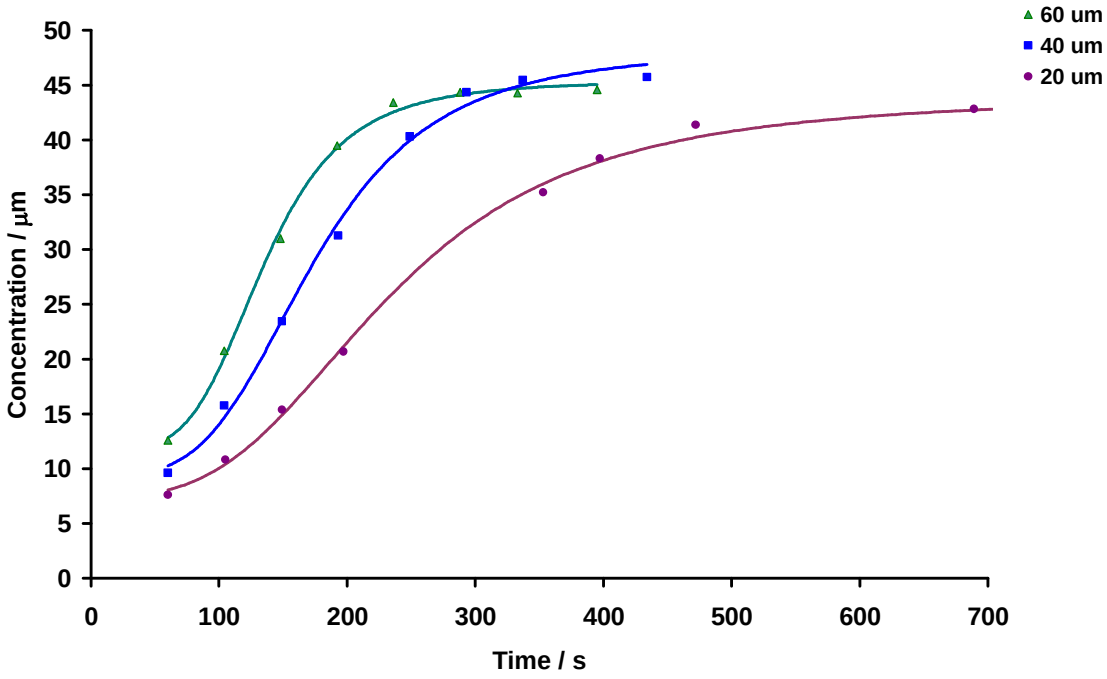

Fig. 35. Formation of MbCO over time after addition of 60 µM, 40µM and 20µM of $[NEt_4][CrCl(CO)_5]$ in DMSO to an aqueous solution containing deoxy-myoglobin at pH 7.4.

1.10. [NEt$_4$][CrBr(CO)$_5$]

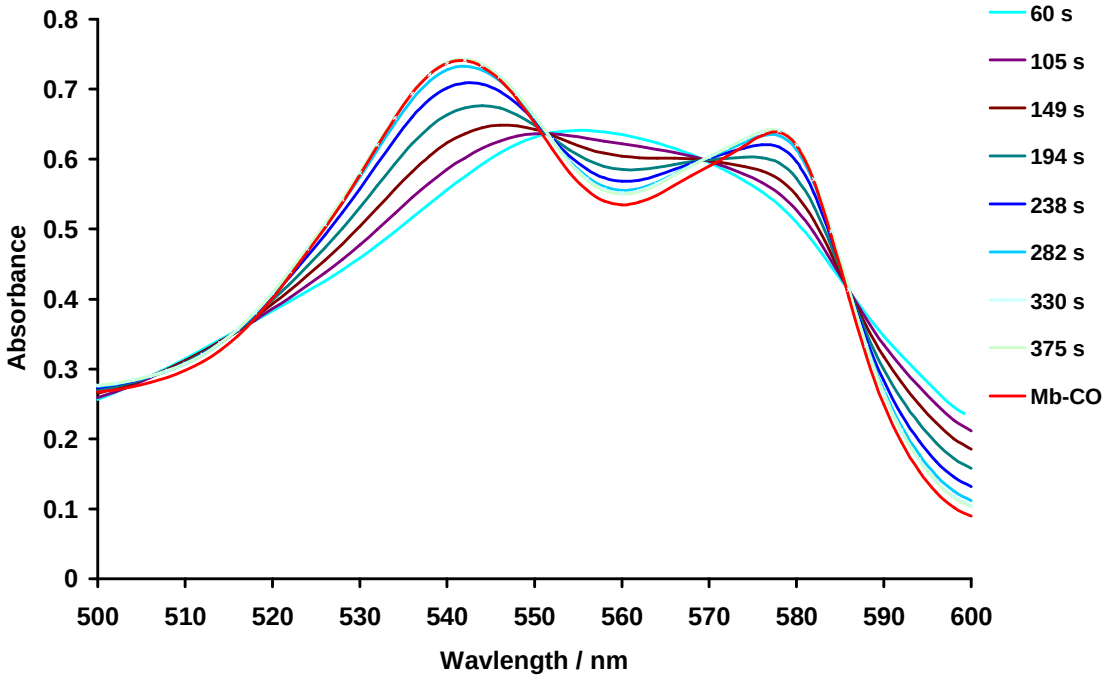

Fig. 36. The changes in the UV spectrum of myoglobin as CO is released from [NEt$_4$][CrBr(CO)$_5$] (60µm).

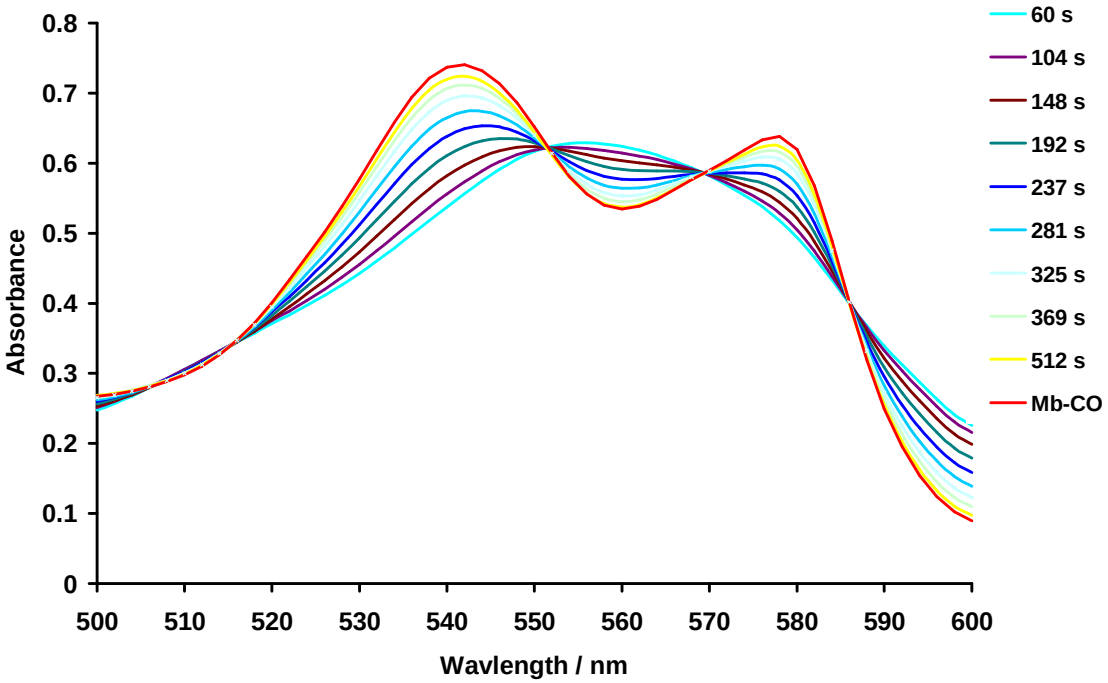

Fig. 37. The changes in the UV spectrum of myoglobin as CO is released from [NEt$_4$][CrBr(CO)$_5$] (40µm).

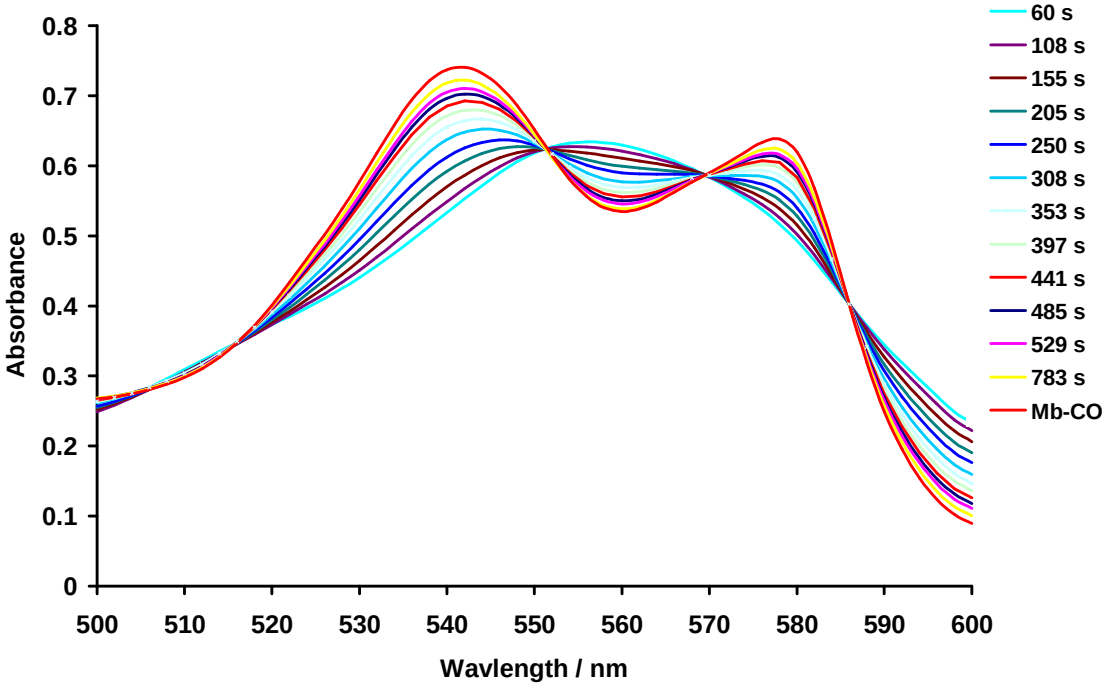

Fig. 38. The changes in the UV spectrum of myoglobin as CO is released from $[NEt_4][CrBr(CO)_5]$ (20µm).

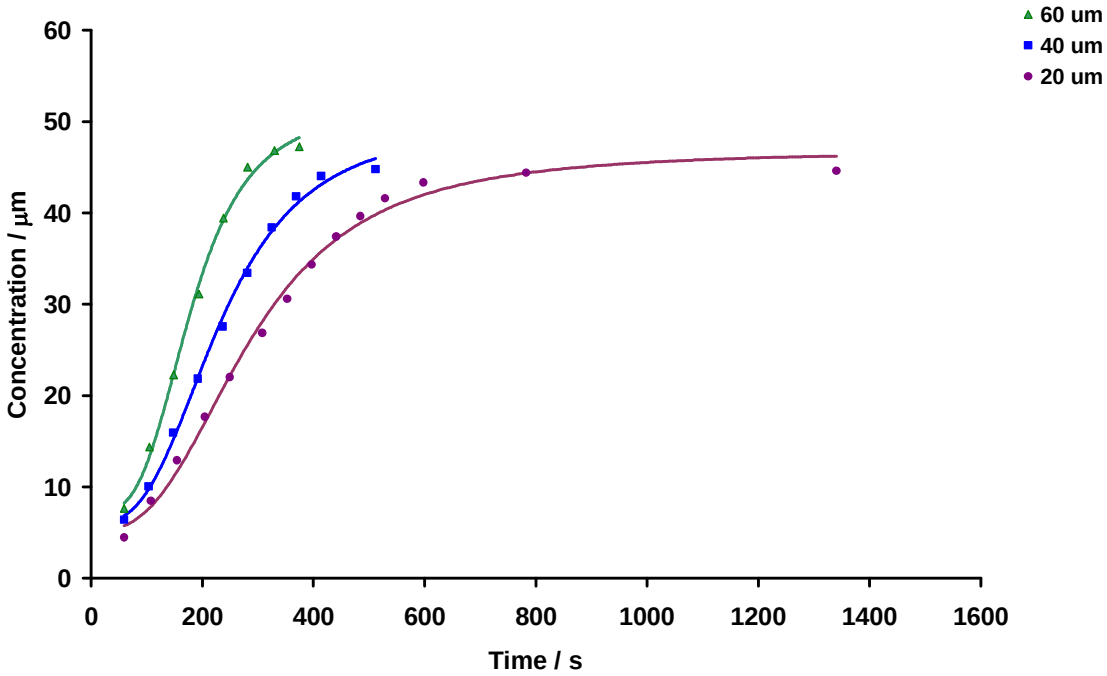

Fig. 39. Formation of MbCO over time after addition of 60 µM, 40µM and 20µM of $[NEt_4][CrBr(CO)_5]$ in DMSO to an aqueous solution containing deoxy-myoglobin at pH 7.4.

1.11. [NEt$_4$][CrI(CO)$_5$]

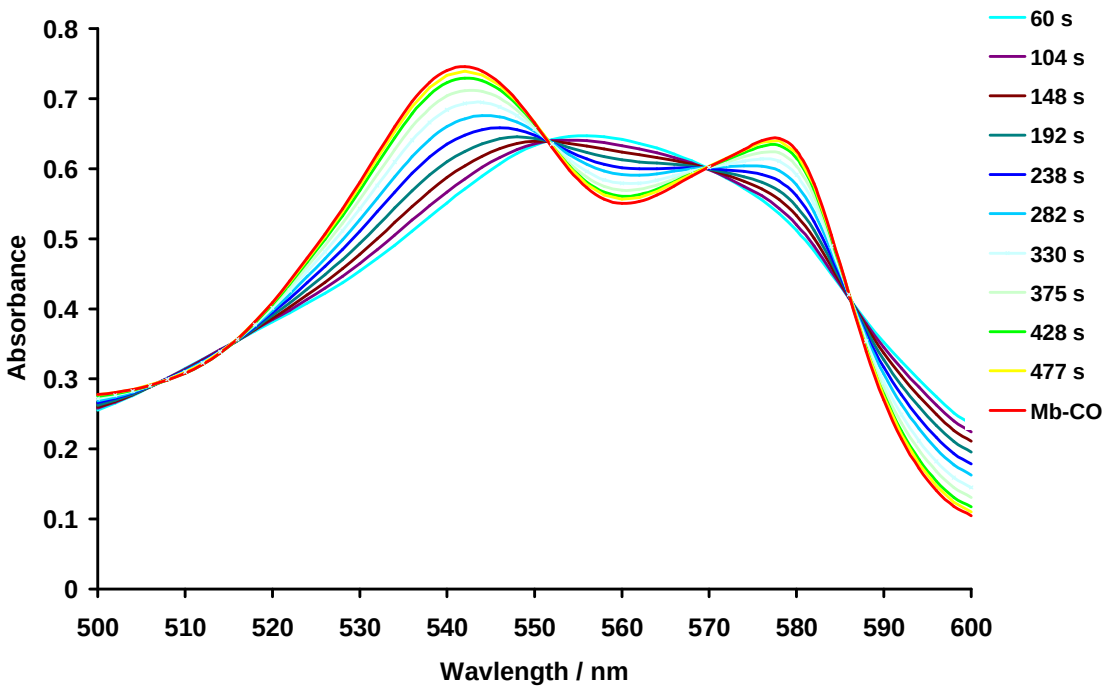

Fig. 40. The changes in the UV spectrum of myoglobin as CO is released from [NEt$_4$][CrI(CO)$_5$] (60μm).

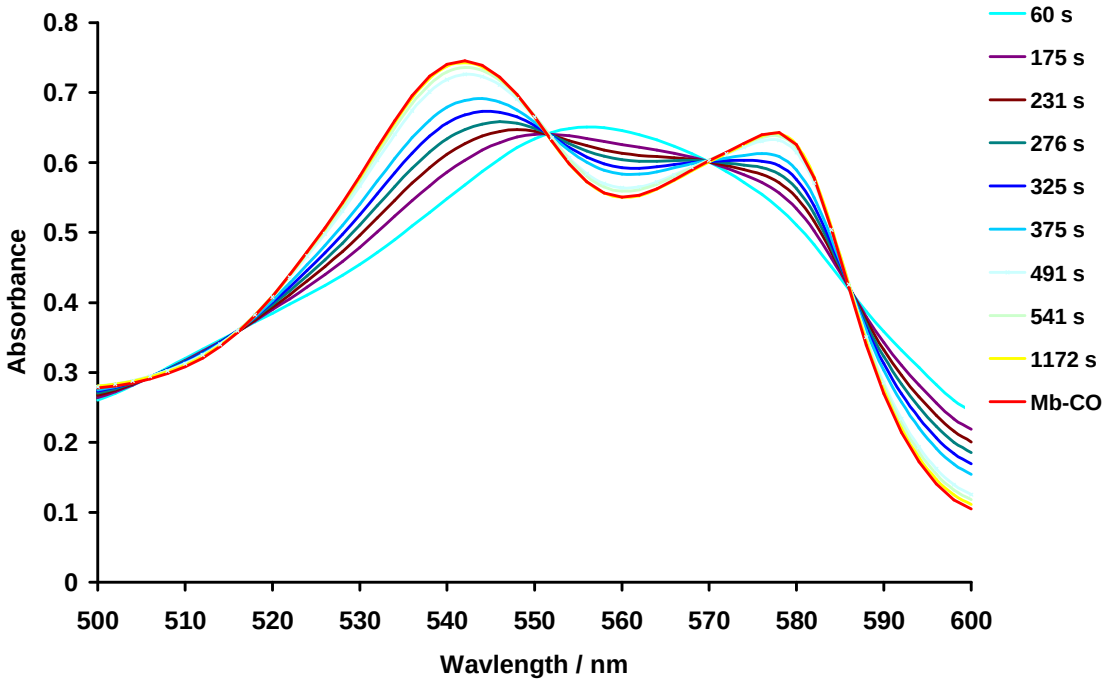

Fig. 41. The changes in the UV spectrum of myoglobin as CO is released from [NEt$_4$][CrI(CO)$_5$] (40μm).

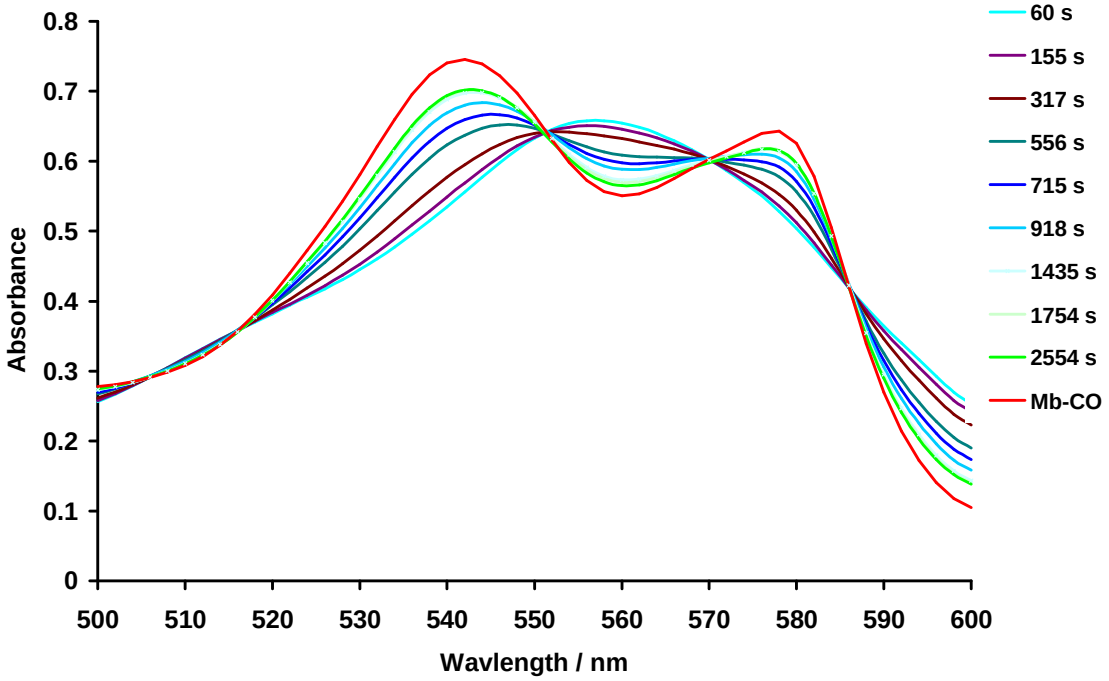

Fig. 42. The changes in the UV spectrum of myoglobin as CO is released from $[NEt_4][CrI(CO)_5]$ (20µm).

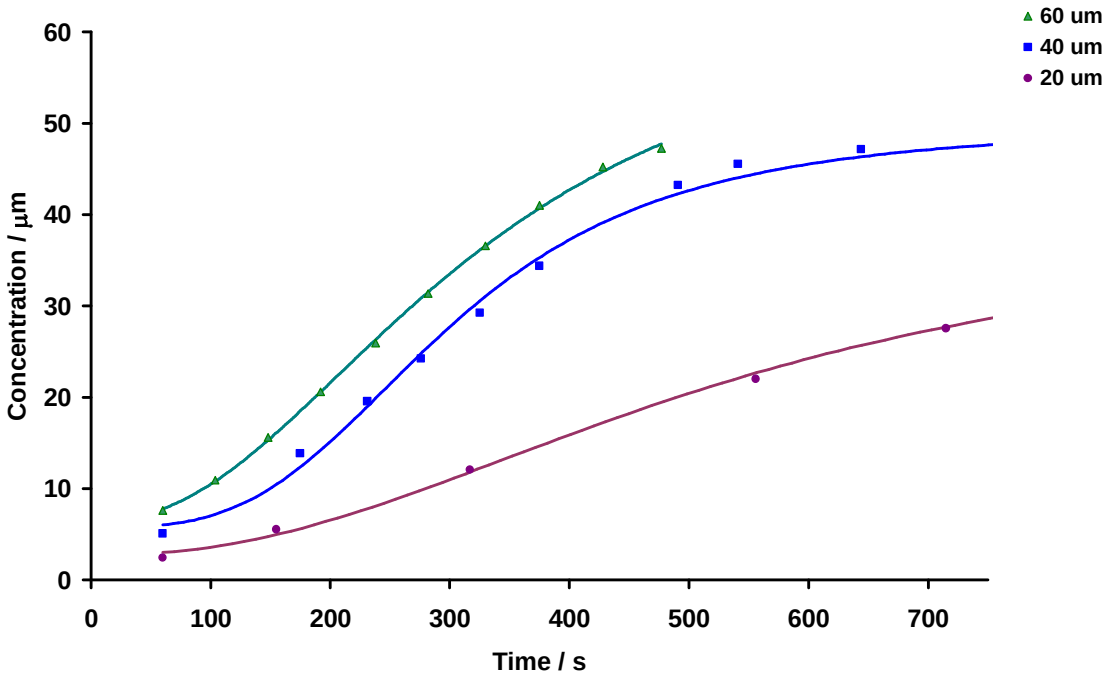

Fig. 43. Formation of MbCO over time after addition of 60 µM, 40µM and 20µM of $[NEt_4][CrI(CO)_5]$ in DMSO to an aqueous solution containing deoxy-myoglobin at pH 7.4.

1.12. [NEt$_4$][MoCl(CO)$_5$]

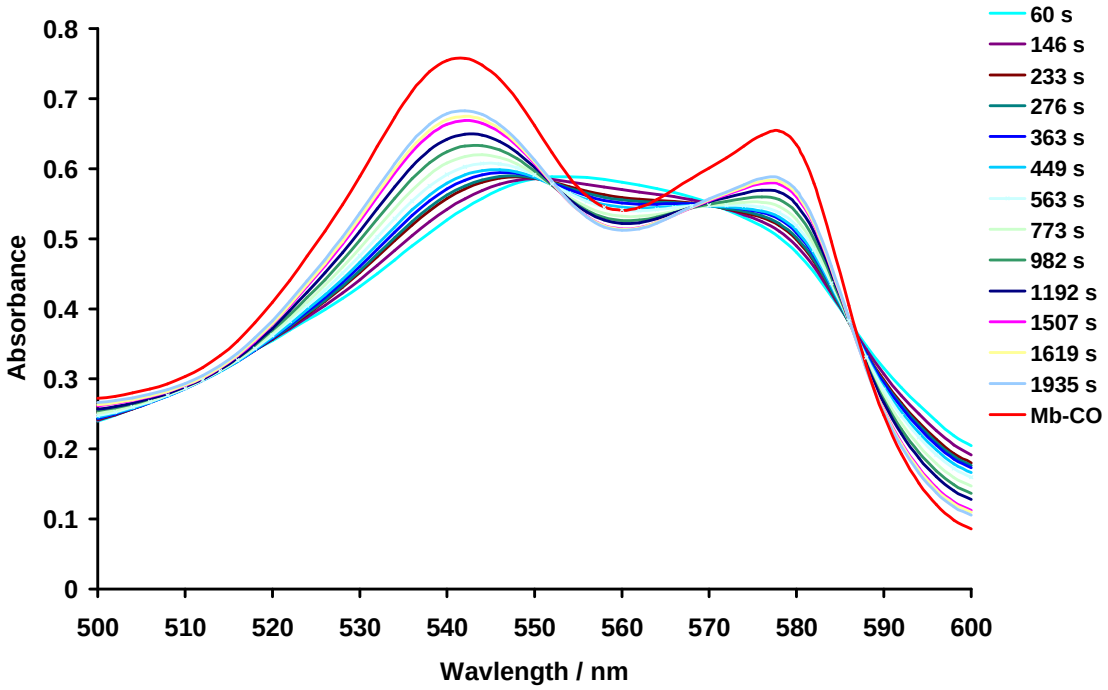

Fig. 44. The changes in the UV spectrum of myoglobin as CO is released from [NEt$_4$][MoCl(CO)$_5$] (60µm).

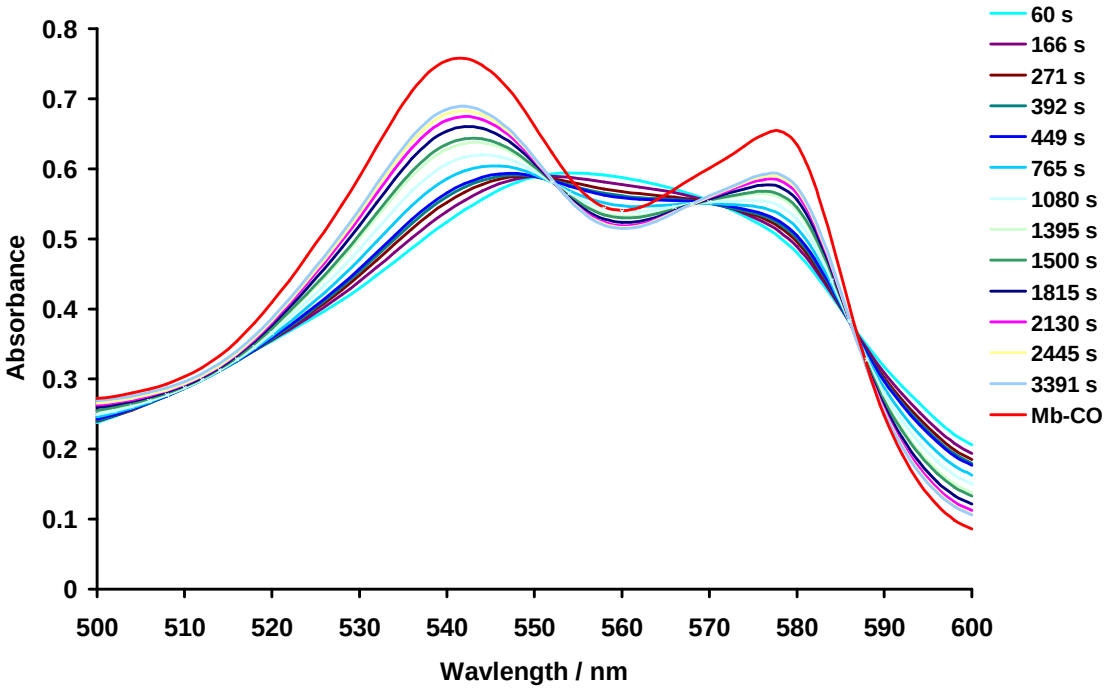

Fig. 45. The changes in the UV spectrum of myoglobin as CO is released from [NEt$_4$][MoCl(CO)$_5$] (40µm).

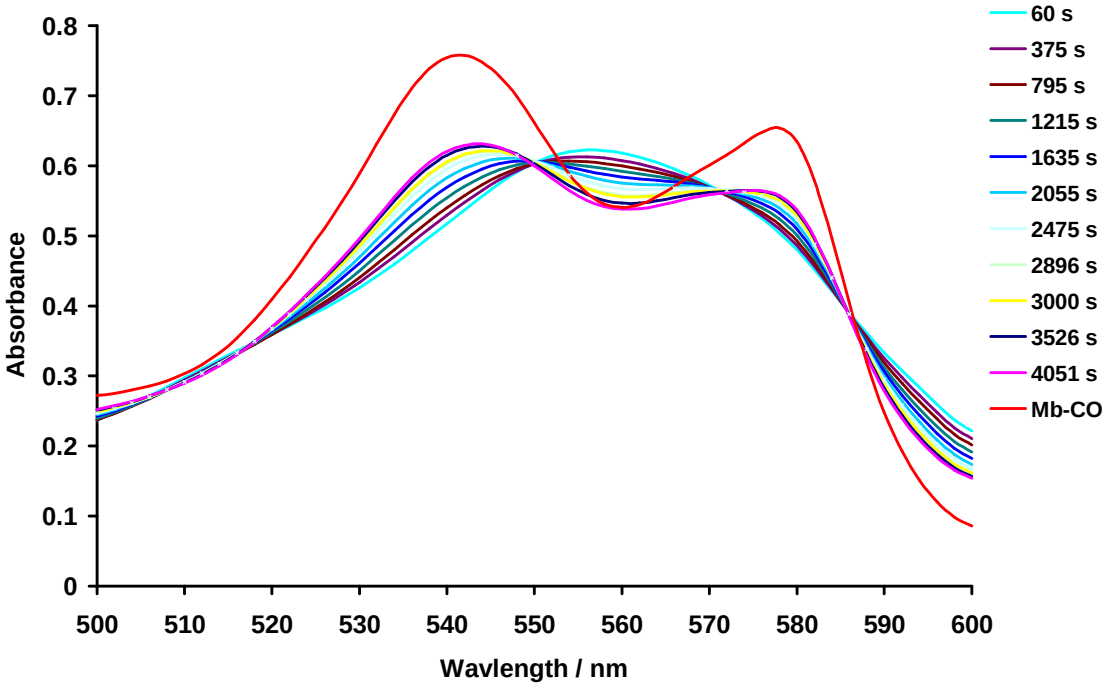

Fig. 46. The changes in the UV spectrum of myoglobin as CO is released from $[NEt_4][MoCl(CO)_5]$ (20µm).

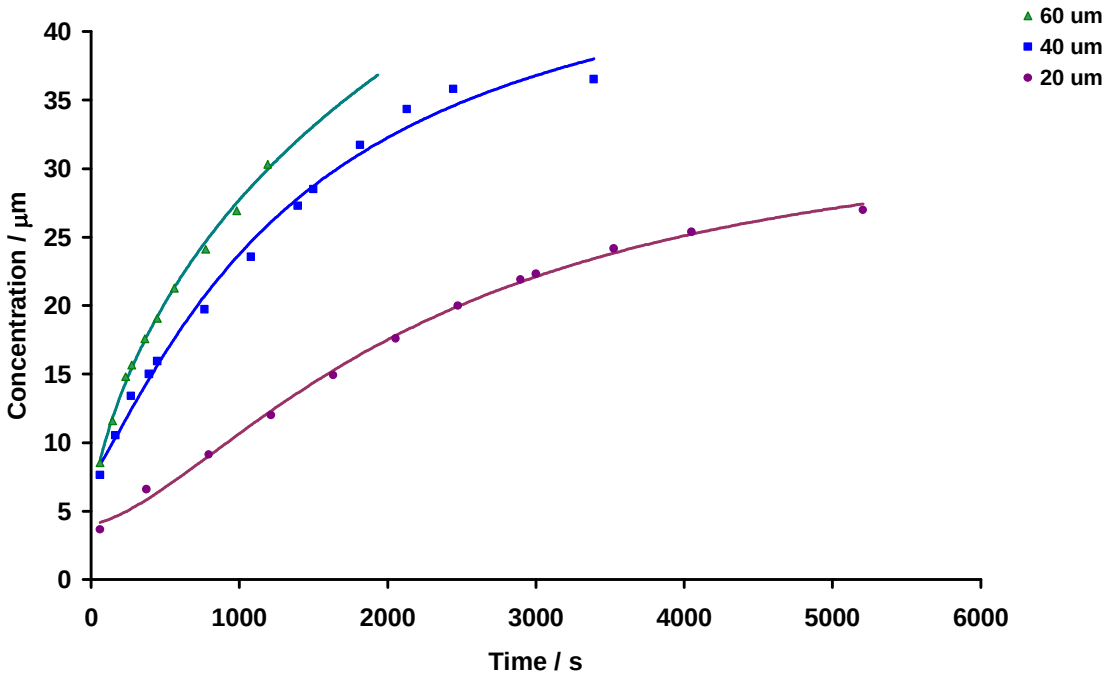

Fig. 47. Formation of MbCO over time after addition of 60 µM, 40µM and 20µM of $[NEt_4][[MoCl(CO)_5]$ in DMSO to an aqueous solution containing deoxy-myoglobin at pH 7.4.

1.13. [NEt$_4$][MoBr(CO)$_5$]

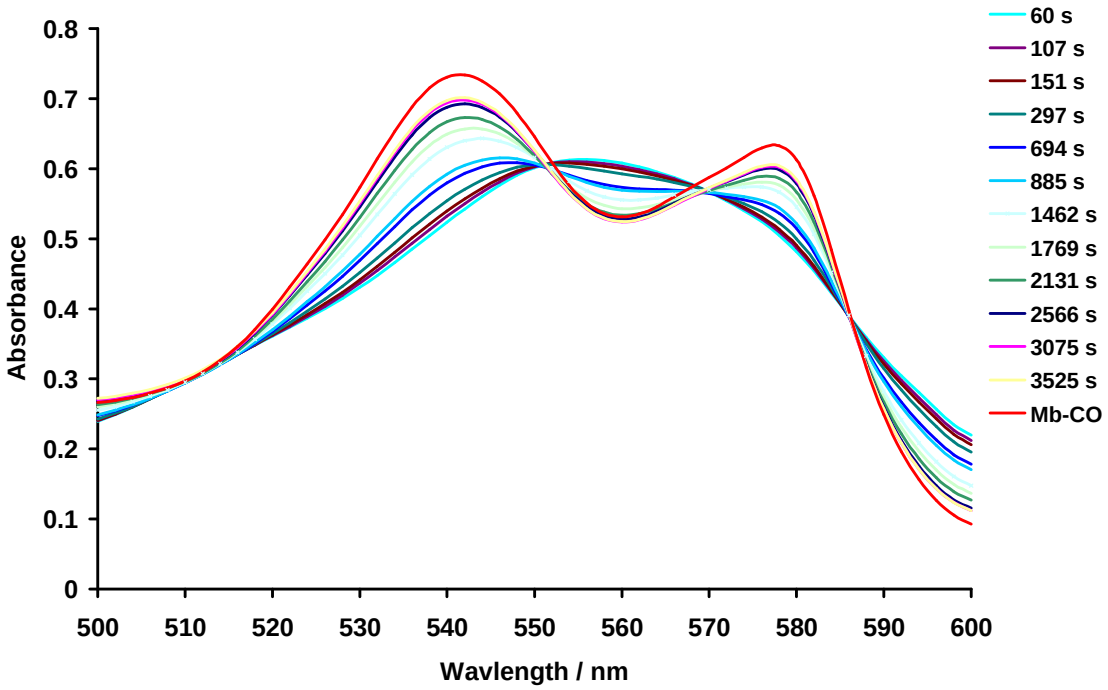

Fig. 48. The changes in the UV spectrum of myoglobin as CO is released from [NEt$_4$][MoBr(CO)$_5$] (60µm).

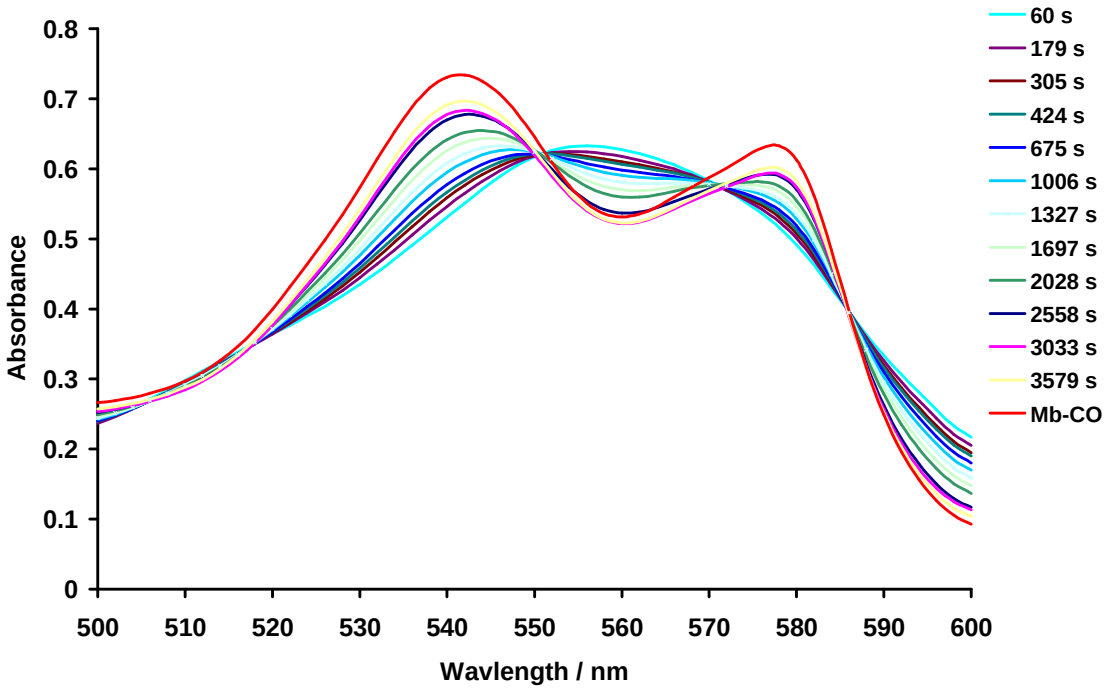

Fig. 49. The changes in the UV spectrum of myoglobin as CO is released from [NEt$_4$][MoBr(CO)$_5$] (40µm).

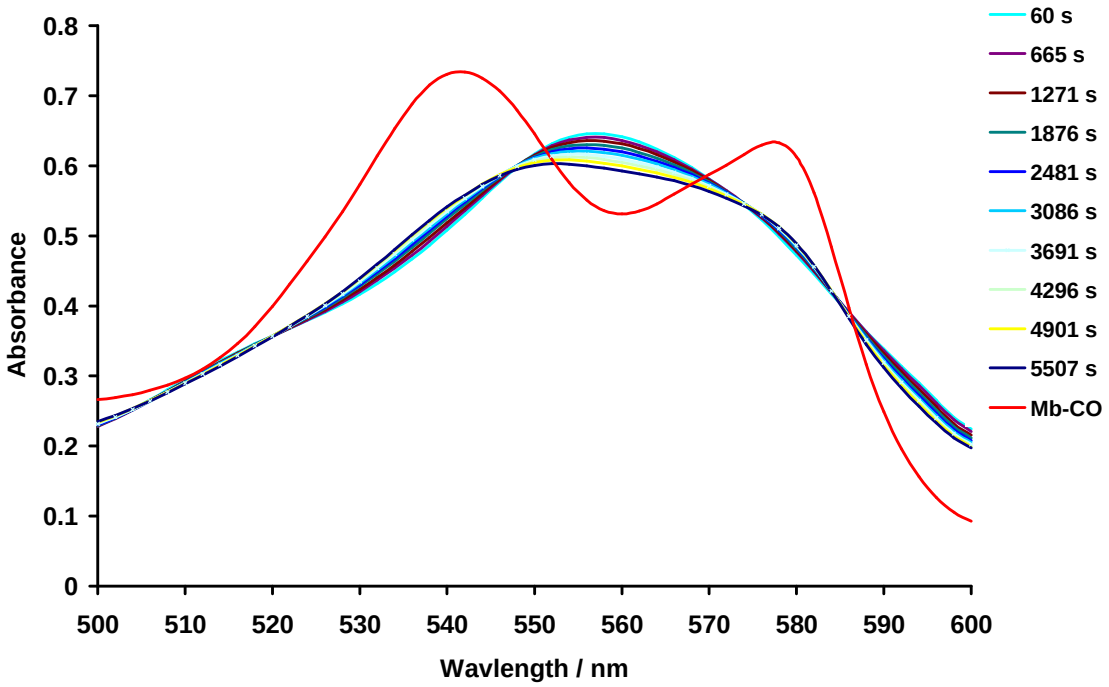

Fig. 50. The changes in the UV spectrum of myoglobin as CO is released from $[NEt_4][MoBr(CO)_5]$ (20µm).

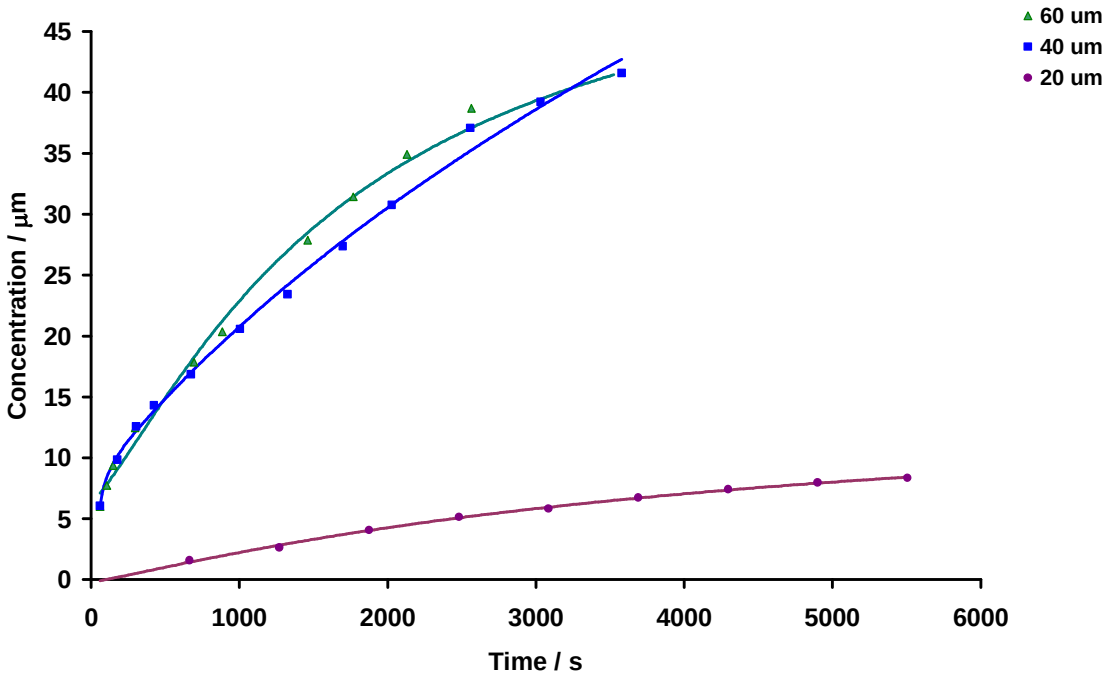

Fig. 51. Formation of MbCO over time after addition of 60 µM, 40µM and 20µM of $[NEt_4][[MoBr(CO)_5]$ in DMSO to an aqueous solution containing deoxy-myoglobin at pH 7.4.

1.14. $[NEt_4][MoI(CO)_5]$

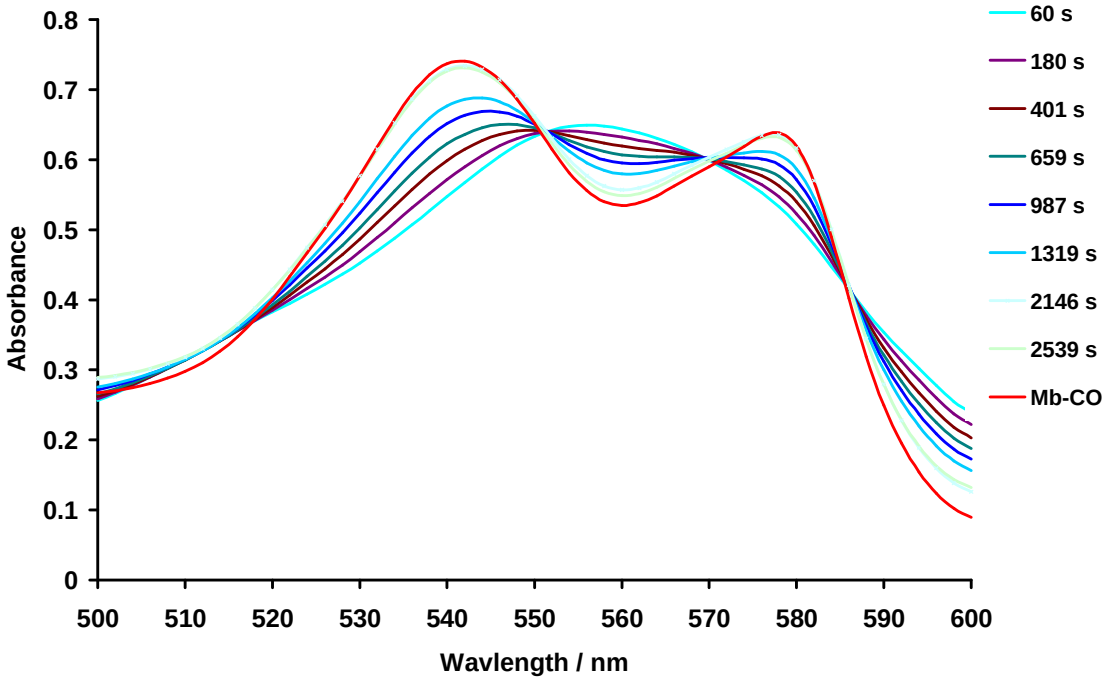

Fig. 52. The changes in the UV spectrum of myoglobin as CO is released from $[NEt_4][MoI(CO)_5]$ (60µm).

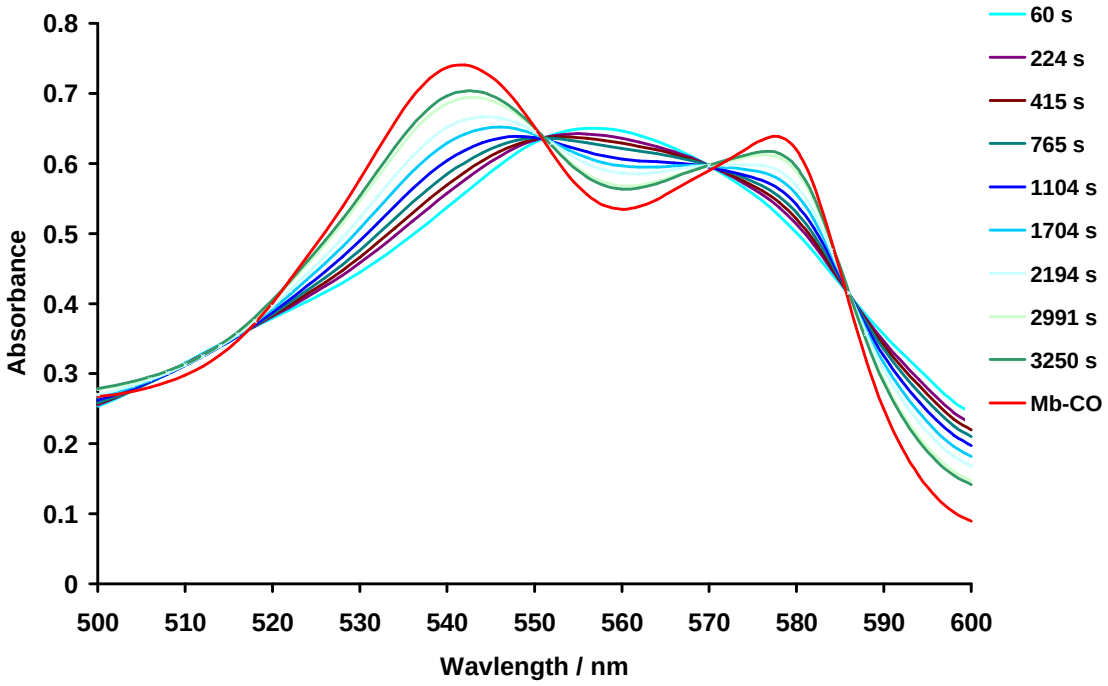

Fig. 53. The changes in the UV spectrum of myoglobin as CO is released from $[NEt_4][MoI(CO)_5]$ (40µm).

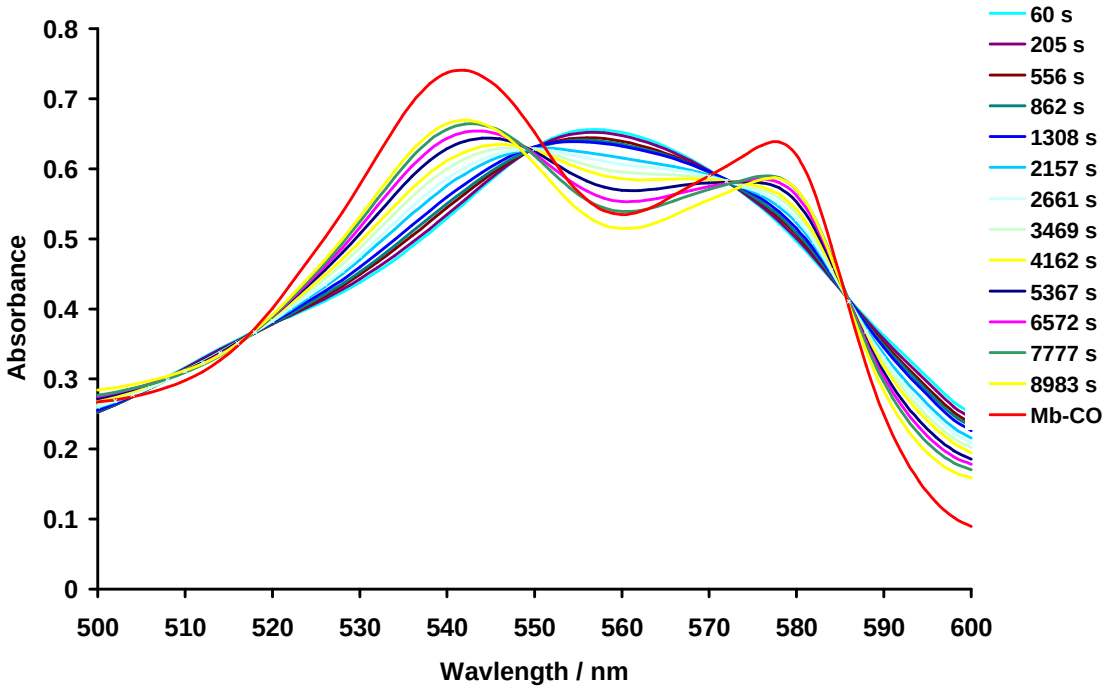

Fig. 54. The changes in the UV spectrum of myoglobin as CO is released from $[NEt_4][MoI(CO)_5]$ (20µm).

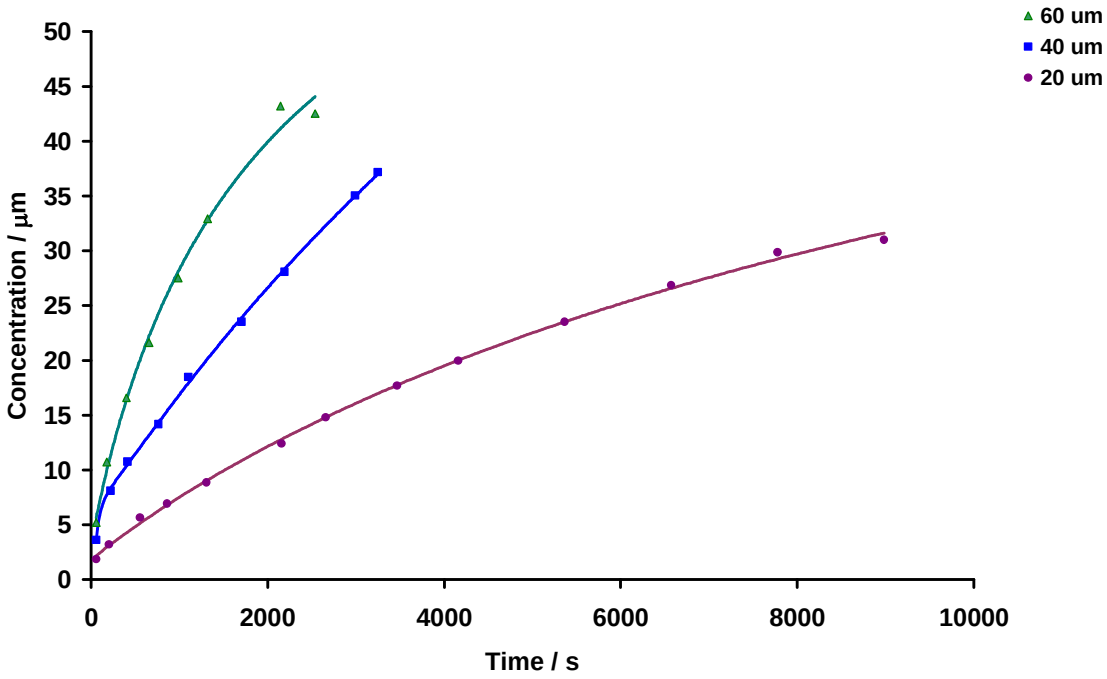

Fig 55. Formation of MbCO over time after addition of 60 µM, 40µM and 20µM of $[NEt_4][[MoI(CO)_5]$ in DMSO to an aqueous solution containing deoxy-myoglobin at pH 7.4.

1.15. $[NEt_4][WCl(CO)_5]$

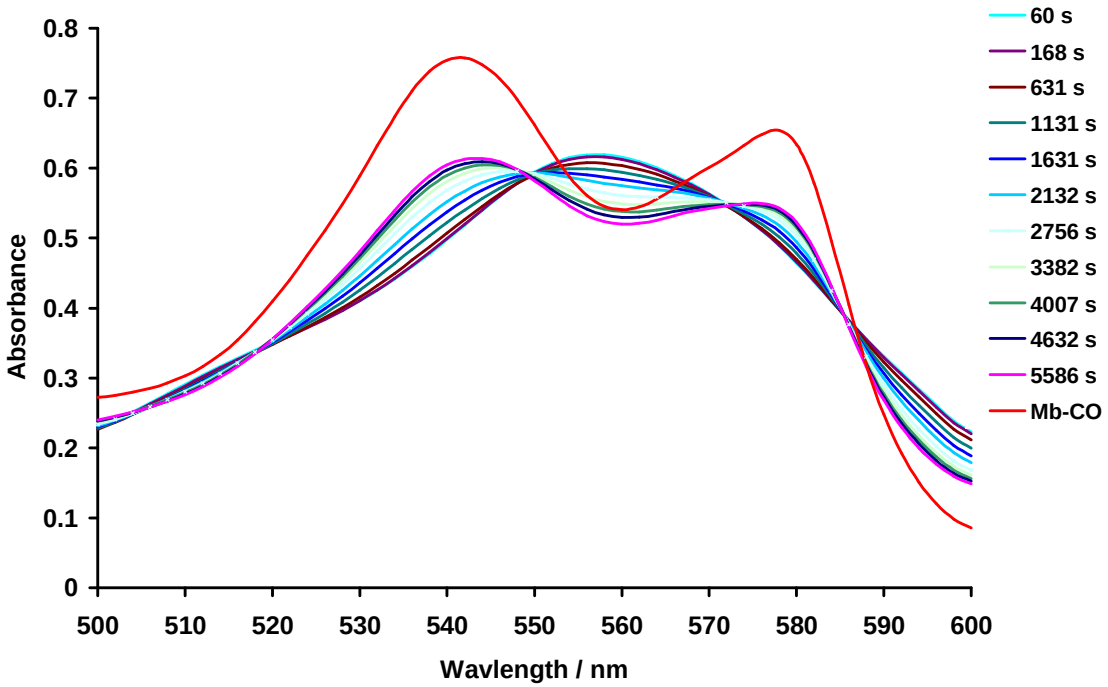

Fig. 56. The changes in the UV spectrum of myoglobin as CO is released from $[NEt_4][WCl(CO)_5]$ (60µm).

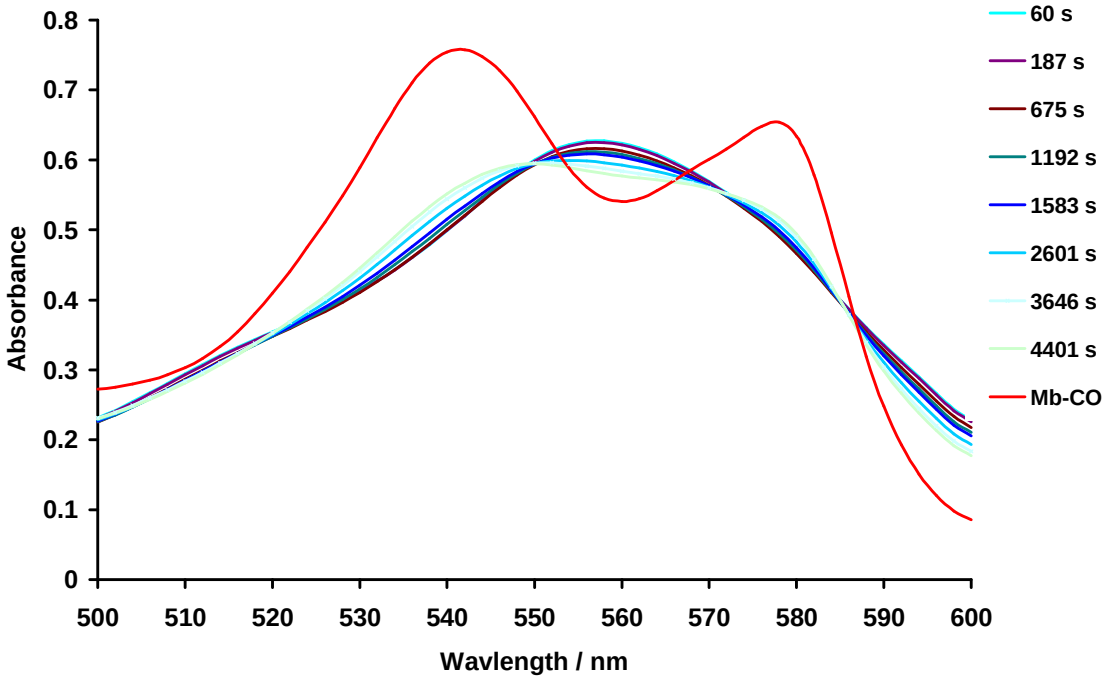

Fig. 57. The changes in the UV spectrum of myoglobin as CO is released from $[NEt_4][WCl(CO)_5]$ (40µm).

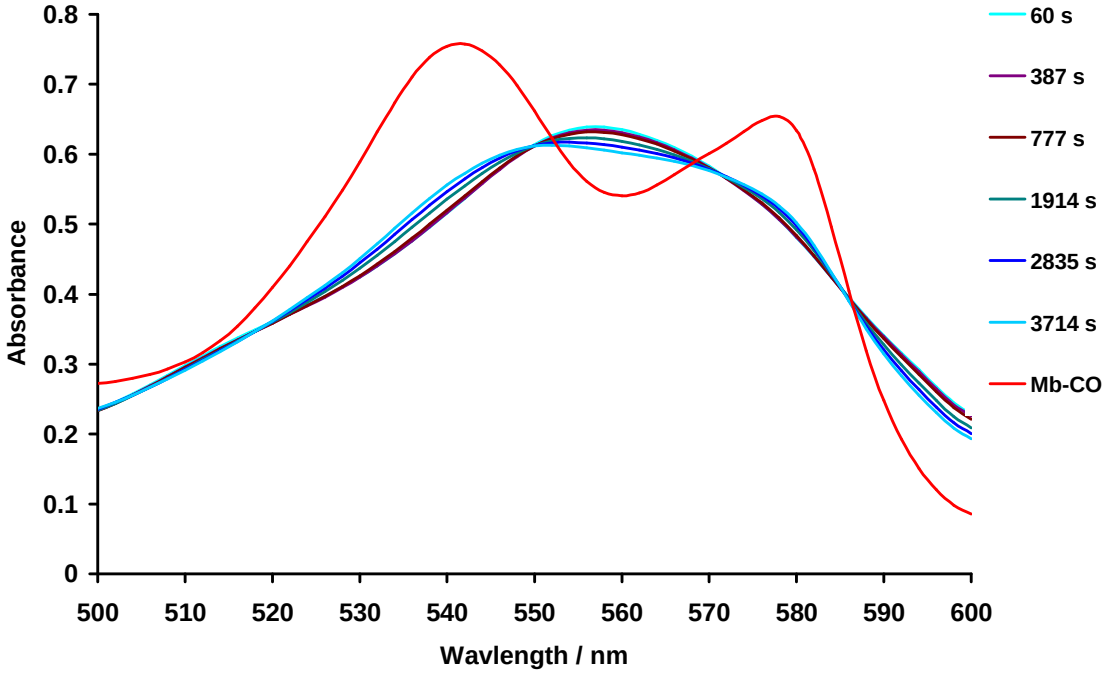

Fig. 58. The changes in the UV spectrum of myoglobin as CO is released from $[NEt_4][WCl(CO)_5]$ (20µm).

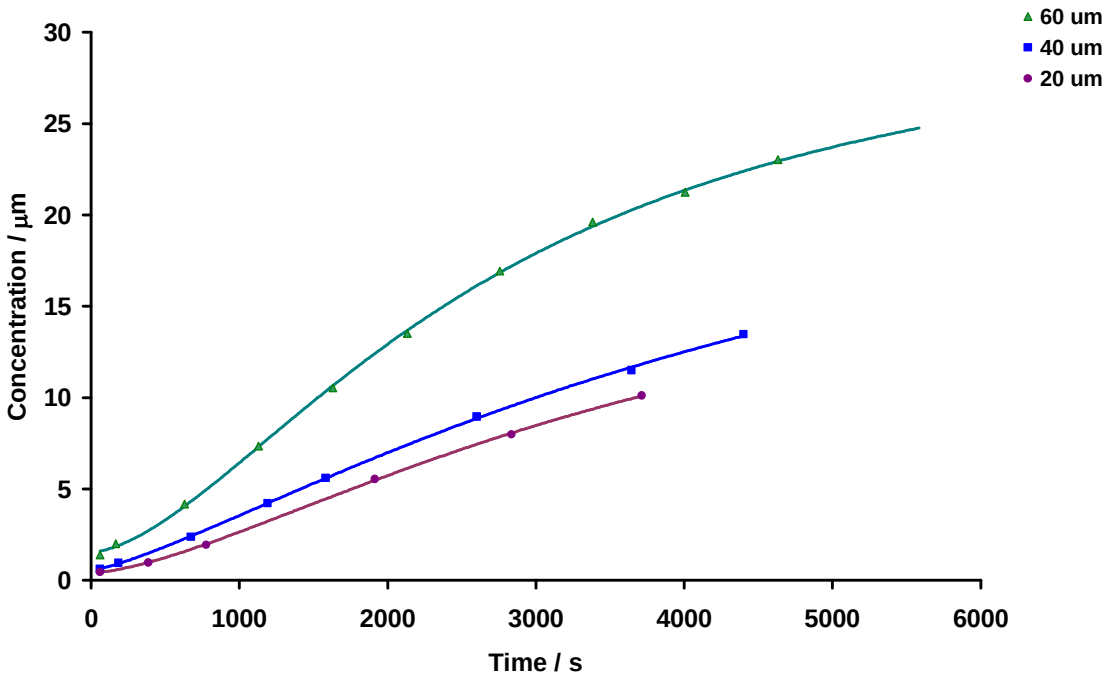

Fig 59. Formation of MbCO over time after addition of 60 µM, 40µM and 20µM of $[NEt_4][WCl(CO)_5]$ in DMSO to an aqueous solution containing deoxy-myoglobin at pH 7.4.

1.16. [NEt$_4$][WBr(CO)$_5$]

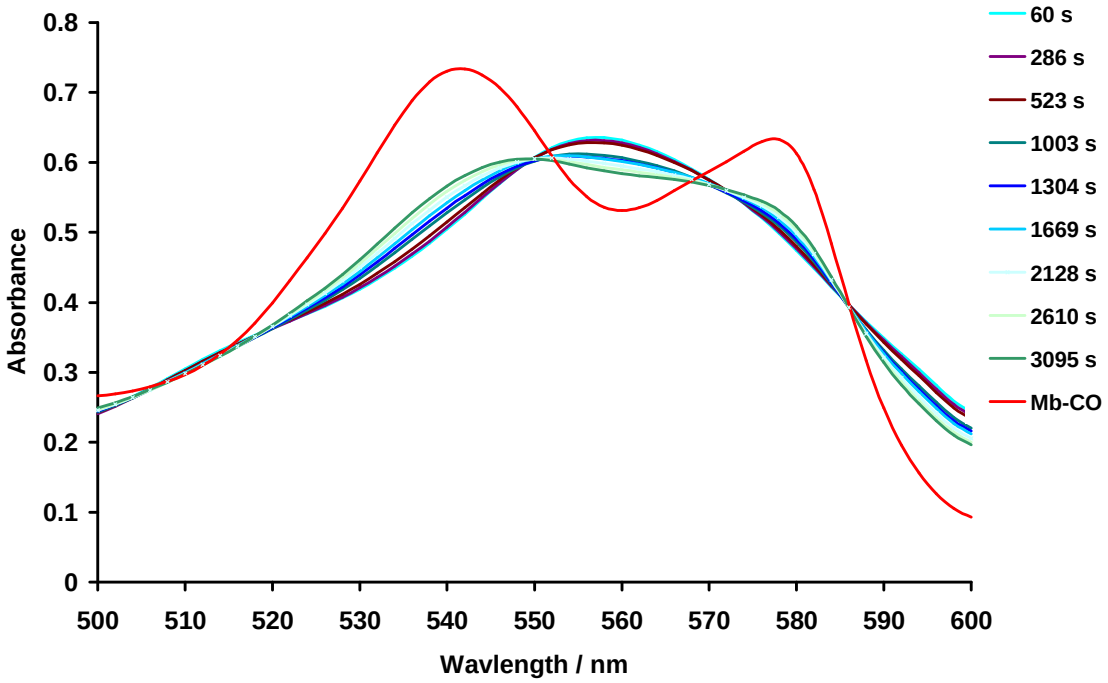

Fig. 60. The changes in the UV spectrum of myoglobin as CO is released from [NEt$_4$][WBr(CO)$_5$] (60µm).

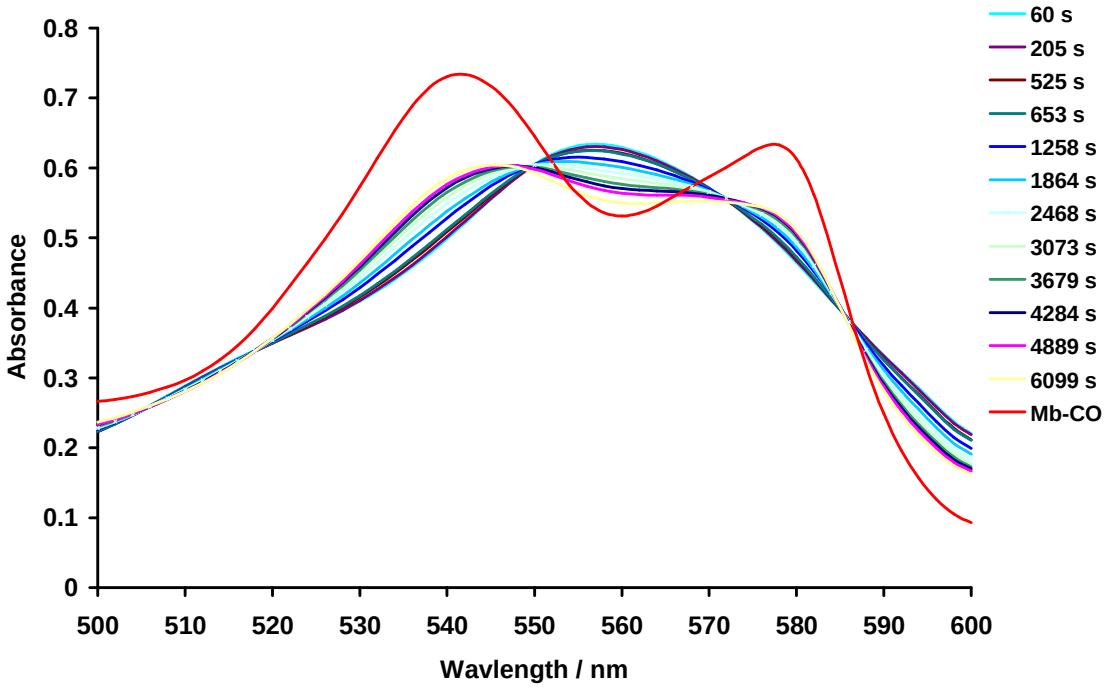

Fig. 61. The changes in the UV spectrum of myoglobin as CO is released from [NEt$_4$][WBr(CO)$_5$] (40µm).

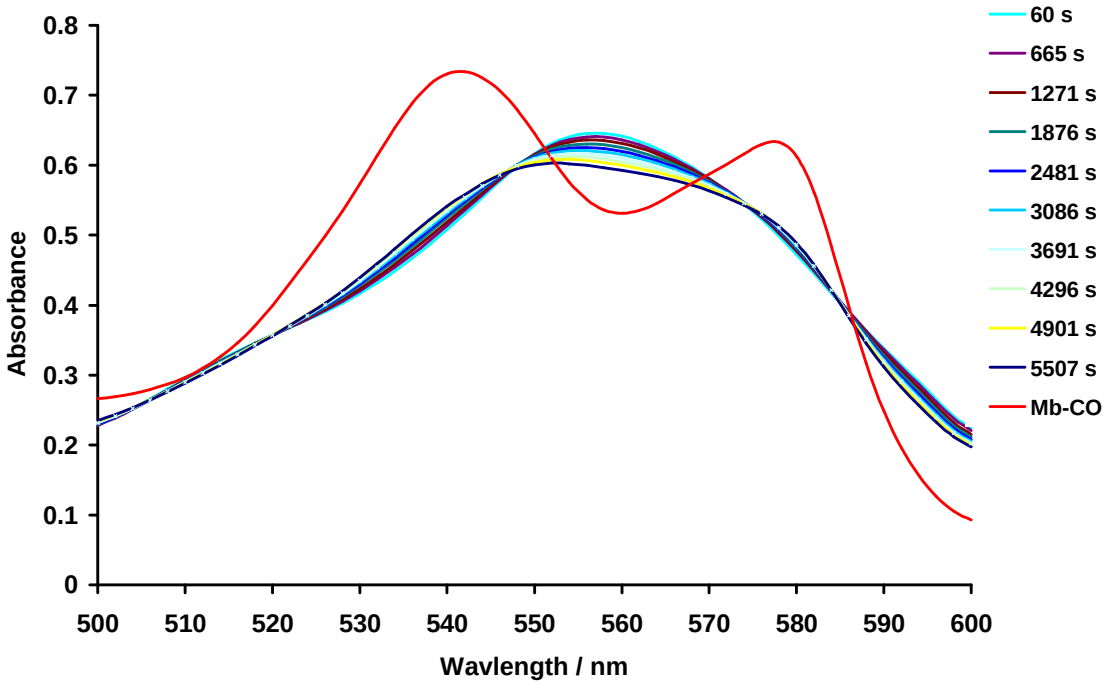

Fig. 62. The changes in the UV spectrum of myoglobin as CO is released from $[NEt_4][WBr(CO)_5]$ (20µm).

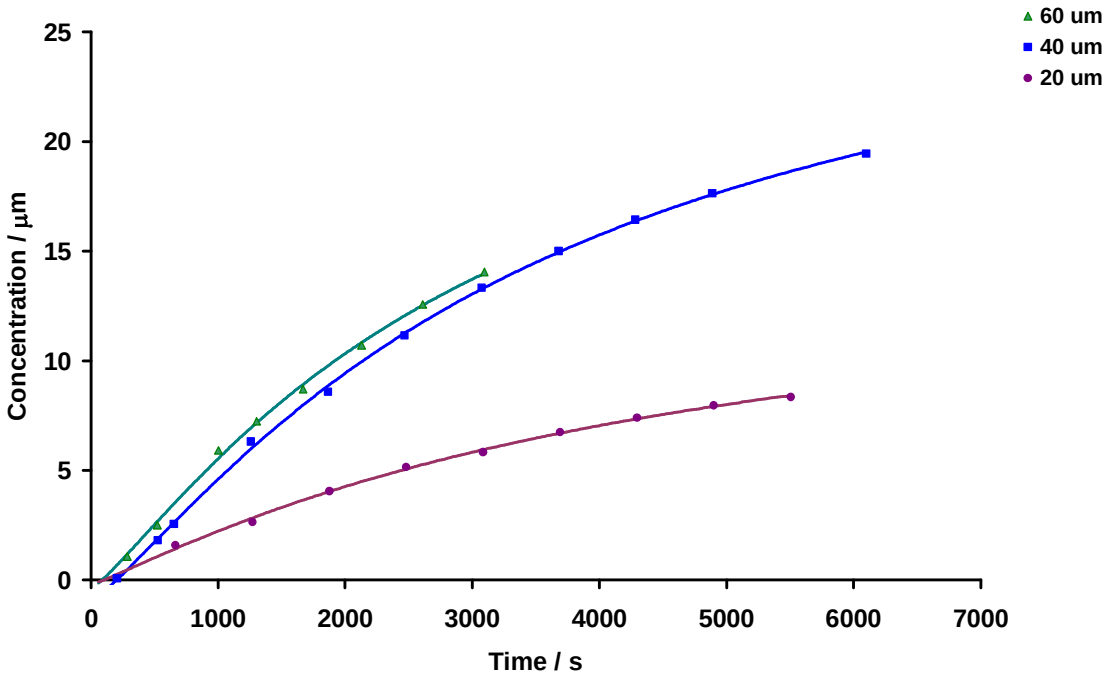

Fig 63. Formation of MbCO over time after addition of 60 µM, 40µM and 20µM of $[NEt_4][WBr(CO)_5]$ in DMSO to an aqueous solution containing deoxy-myoglobin at pH 7.4.

1.17. [NEt$_4$][WI(CO)$_5$]

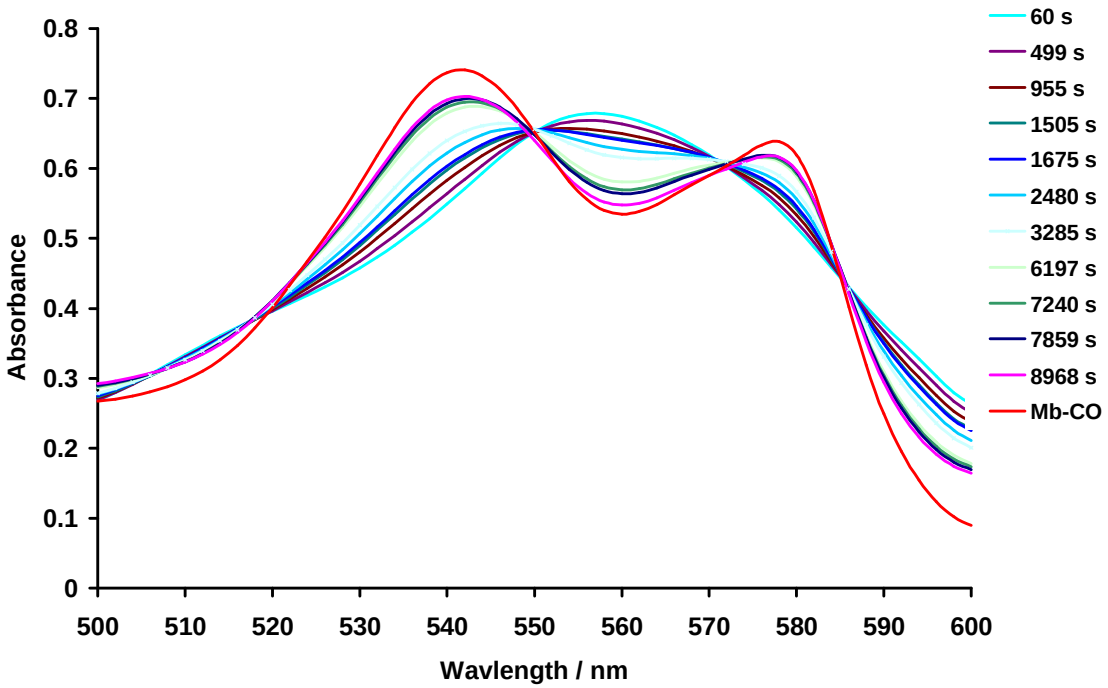

Fig. 64. The changes in the UV spectrum of myoglobin as CO is released from [NEt$_4$][WI(CO)$_5$] (60µm).

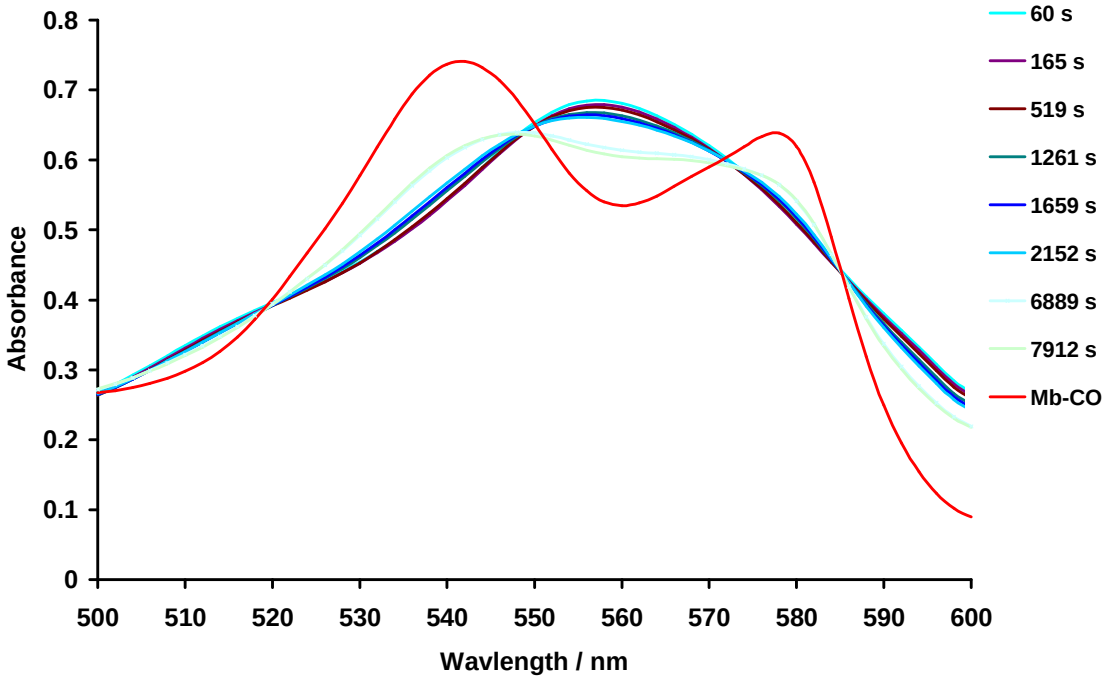

Fig. 65. The changes in the UV spectrum of myoglobin as CO is released from [NEt$_4$][WI(CO)$_5$] (40µm).

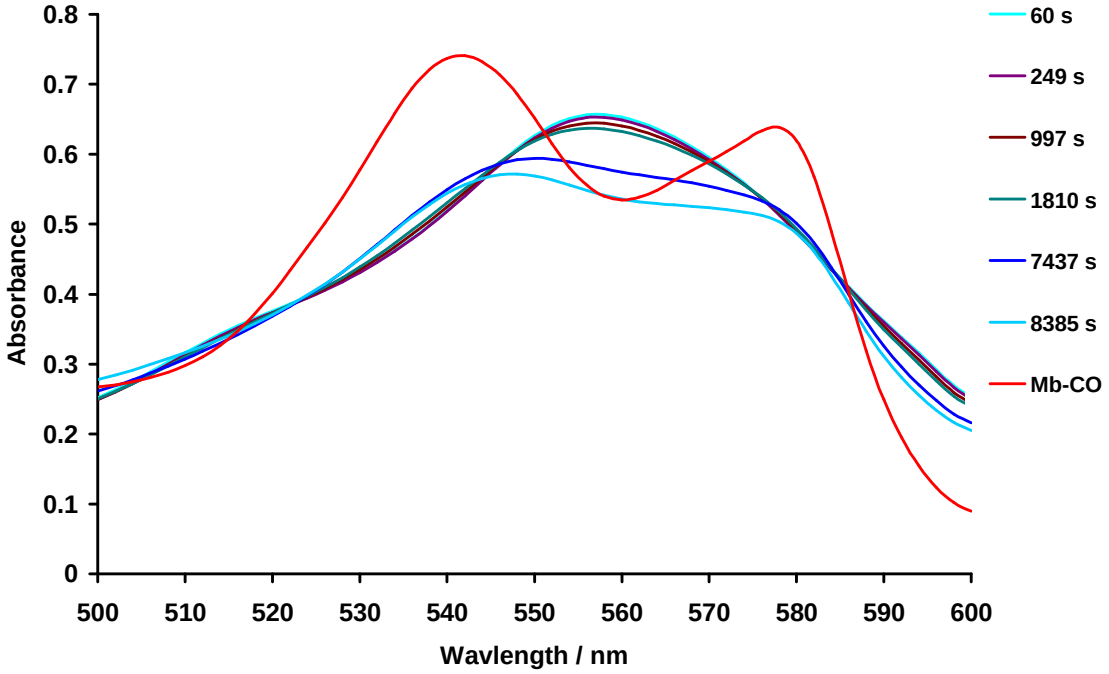

Fig. 66. The changes in the UV spectrum of myoglobin as CO is released from $[NEt_4][WI(CO)_5]$ (20µm).

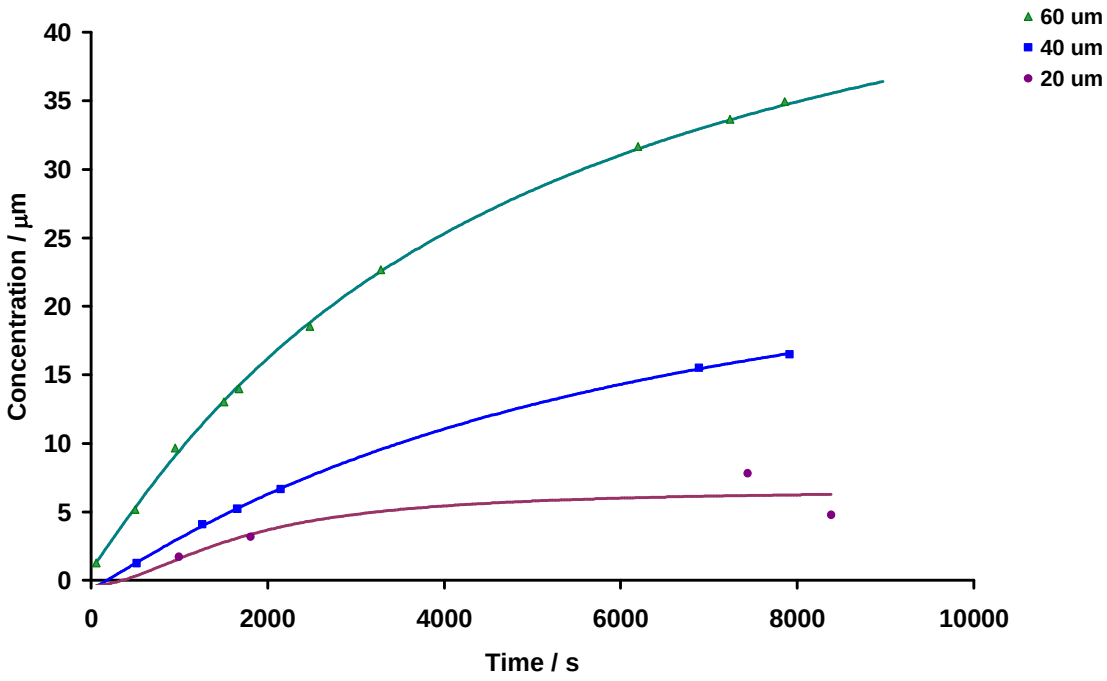

Fig 67. Formation of MbCO over time after addition of 60 µM, 40µM and 20µM of $[NEt_4][WI(CO)_5]$ in DMSO to an aqueous solution containing deoxy-myoglobin at pH 7.4.

1.18. [NEt$_4$][{Cr(CO)$_5$}$_2$(μ-Cl)]

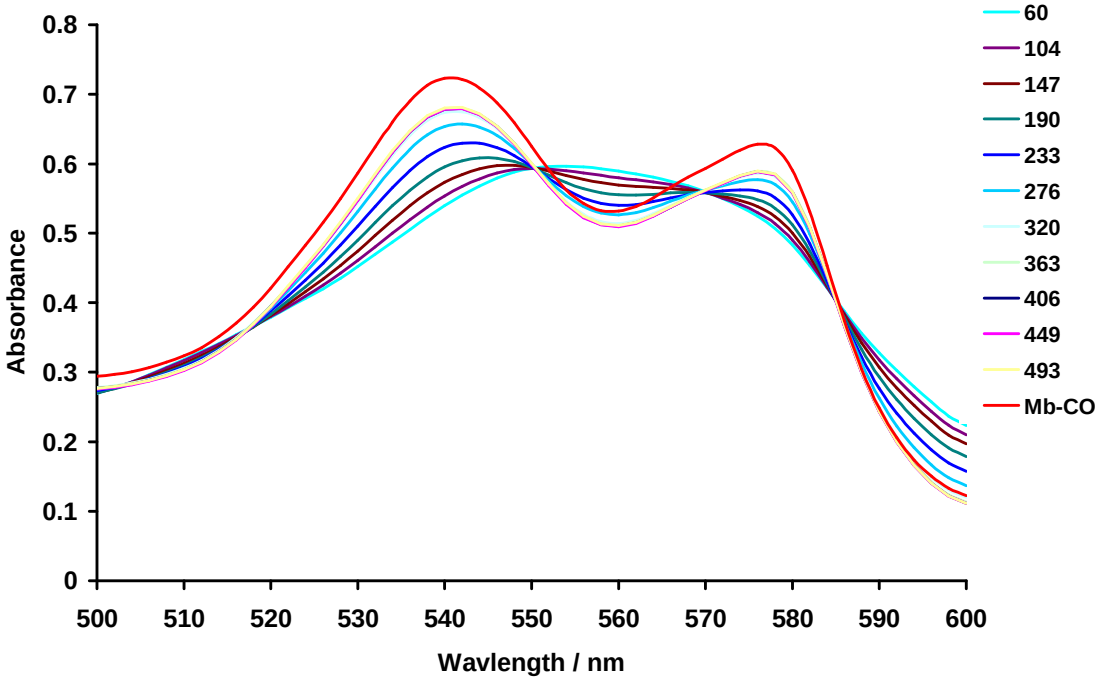

Fig. 68. The changes in the UV spectrum of myoglobin as CO is released from [NEt$_4$][{Cr(CO)$_5$}$_2$(μ-Cl)] (60μm).

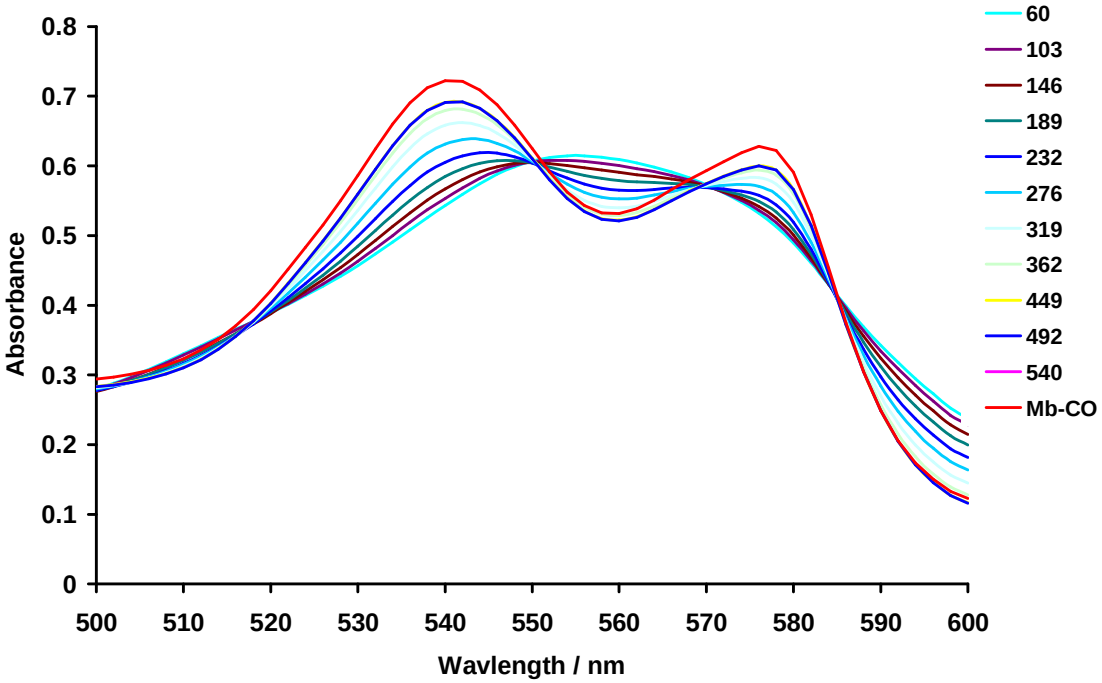

Fig. 69. The changes in the UV spectrum of myoglobin as CO is released from [NEt$_4$][{Cr(CO)$_5$}$_2$(μ-Cl)] (40μm).

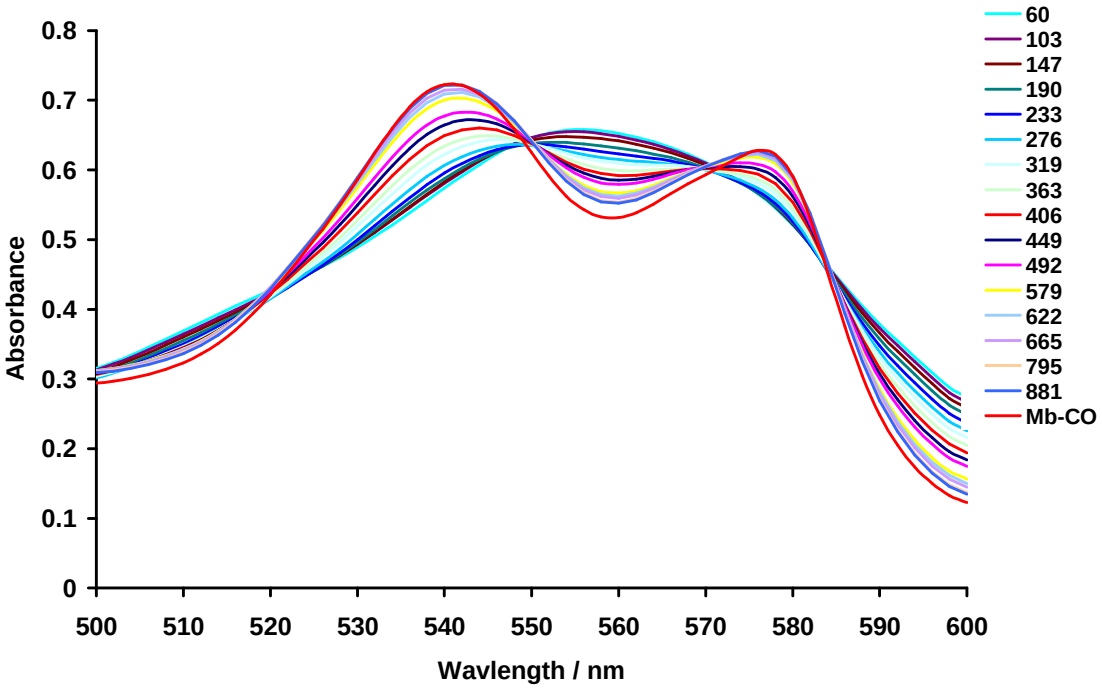

Fig. 70. The changes in the UV spectrum of myoglobin as CO is released from $[NEt_4][\{Cr(CO)_5\}_2(\mu\text{-}Cl)]$

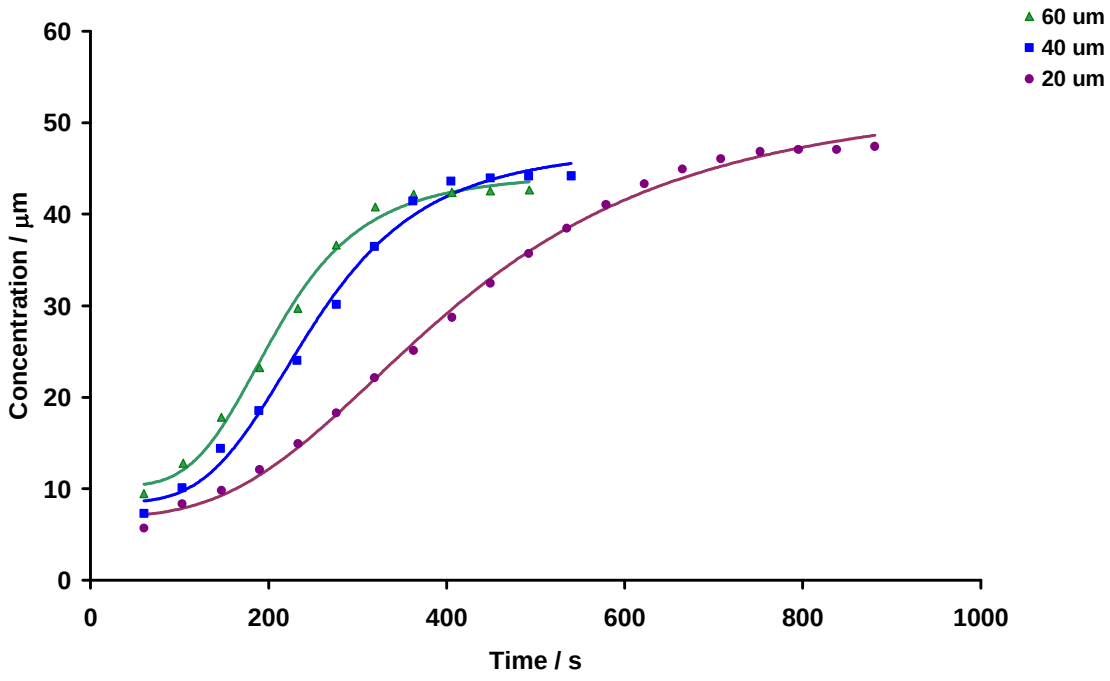

Fig 71. Formation of MbCO over time after addition of 60 µM, 40µM and 20µM of $[NEt_4][\{Cr(CO)_5\}_2(\mu\text{-}Cl)]$ in DMSO to an aqueous solution containing deoxy-myoglobin at pH 7.4.

1.19. [NEt$_4$][{Cr(CO)$_5$}$_2$(μ-Br)]

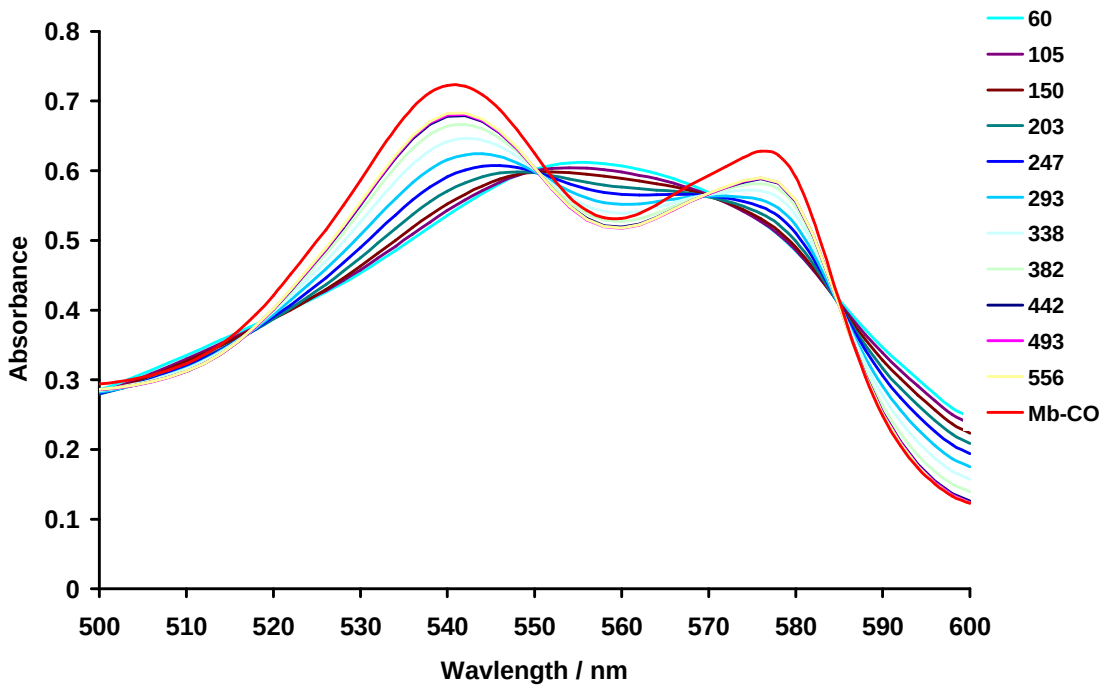

Fig. 72. The changes in the UV spectrum of myoglobin as CO is released from [NEt$_4$][{Cr(CO)$_5$}$_2$(μ-Br)] (60μm).

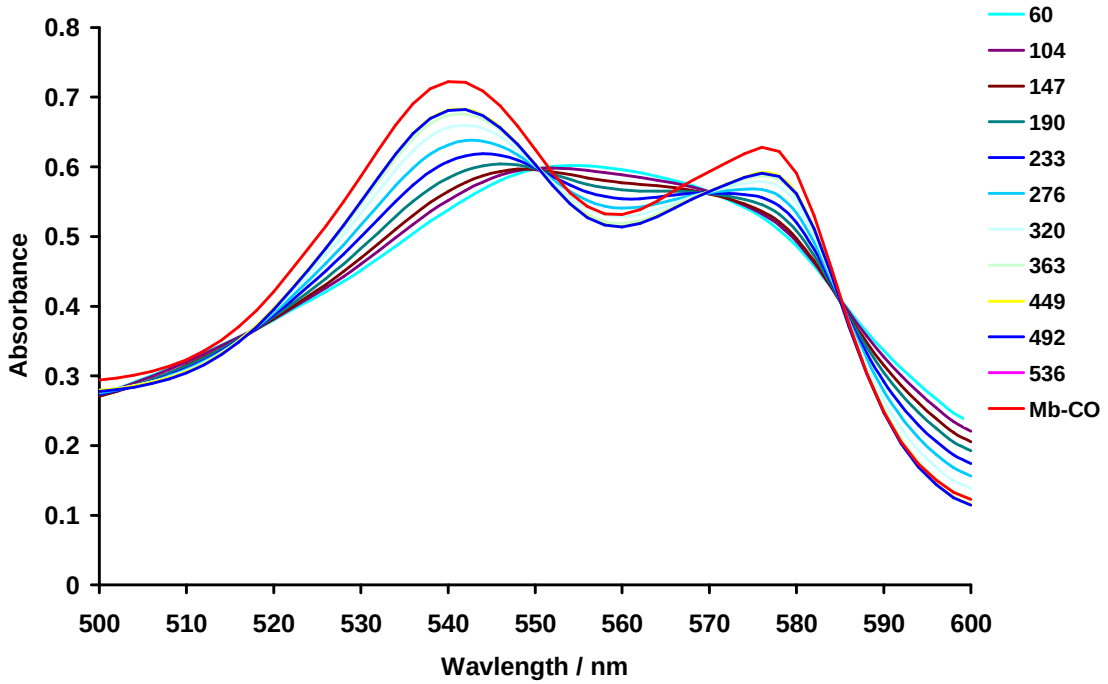

Fig. 73. The changes in the UV spectrum of myoglobin as CO is released from [NEt$_4$][{Cr(CO)$_5$}$_2$(μ-Br)] (40μm).

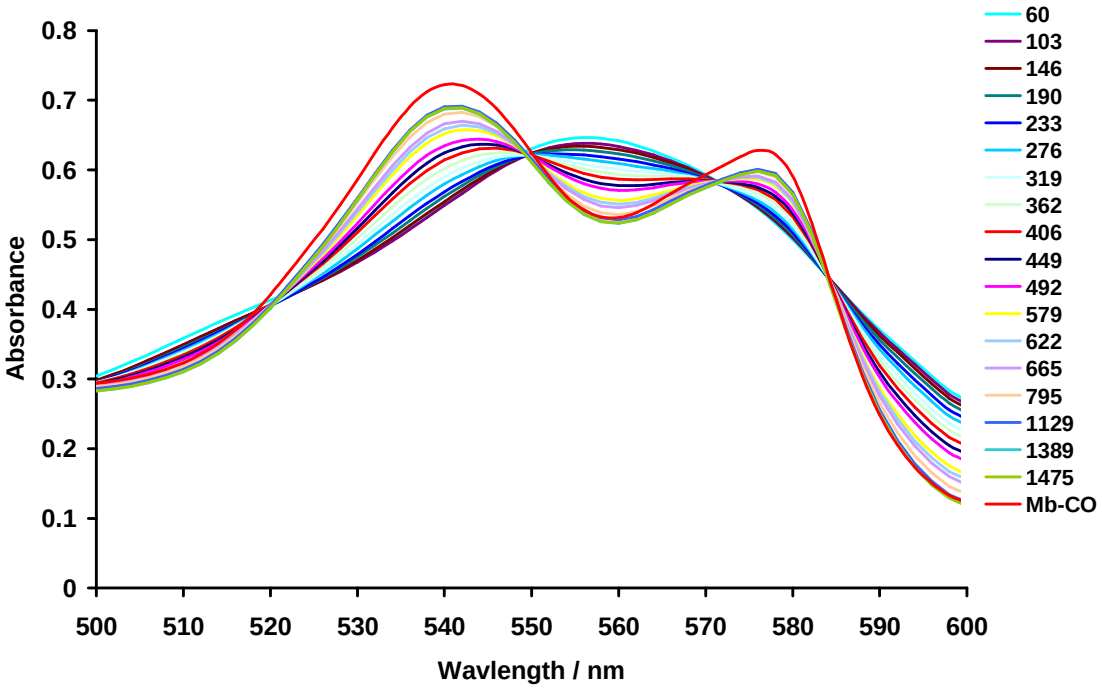

Fig. 74. The changes in the UV spectrum of myoglobin as CO is released from $[NEt_4][\{Cr(CO)_5\}_2(\mu\text{-Br})]$

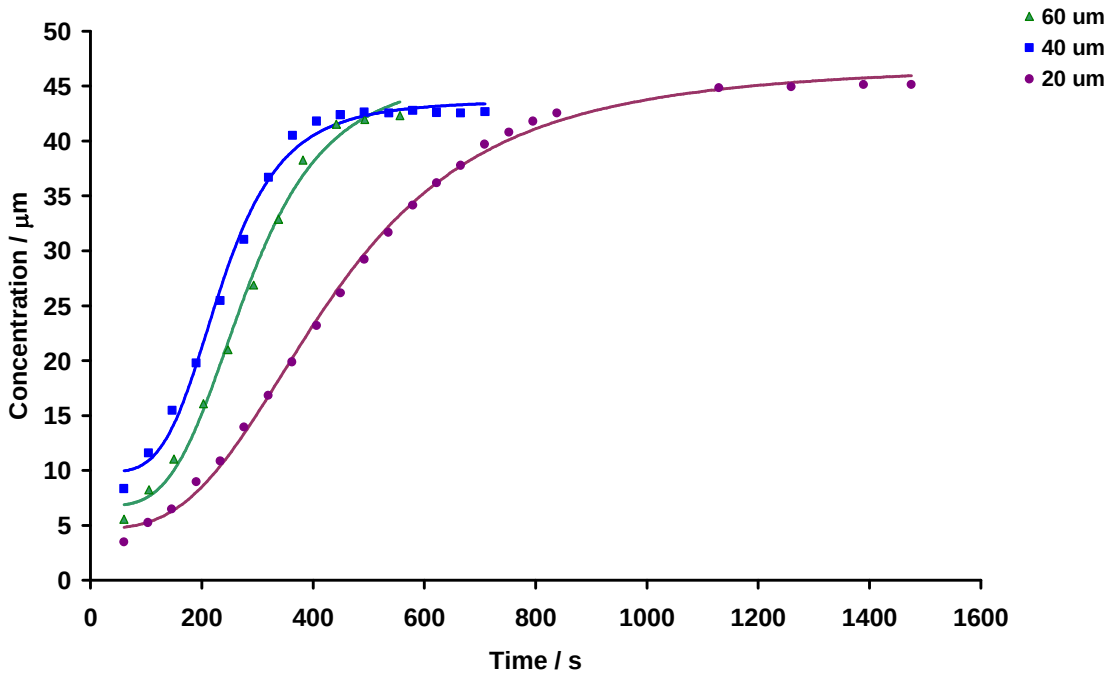

Fig 75. Formation of MbCO over time after addition of 60 µM, 40µM and 20µM of $[NEt_4][\{Cr(CO)_5\}_2(\mu\text{-Br})]$ in DMSO to an aqueous solution containing deoxy-myoglobin at pH 7.4.

1.20. [NEt$_4$][{Cr(CO)$_5$}$_2$(μ-Br)] incubated in DMSO for 6 min

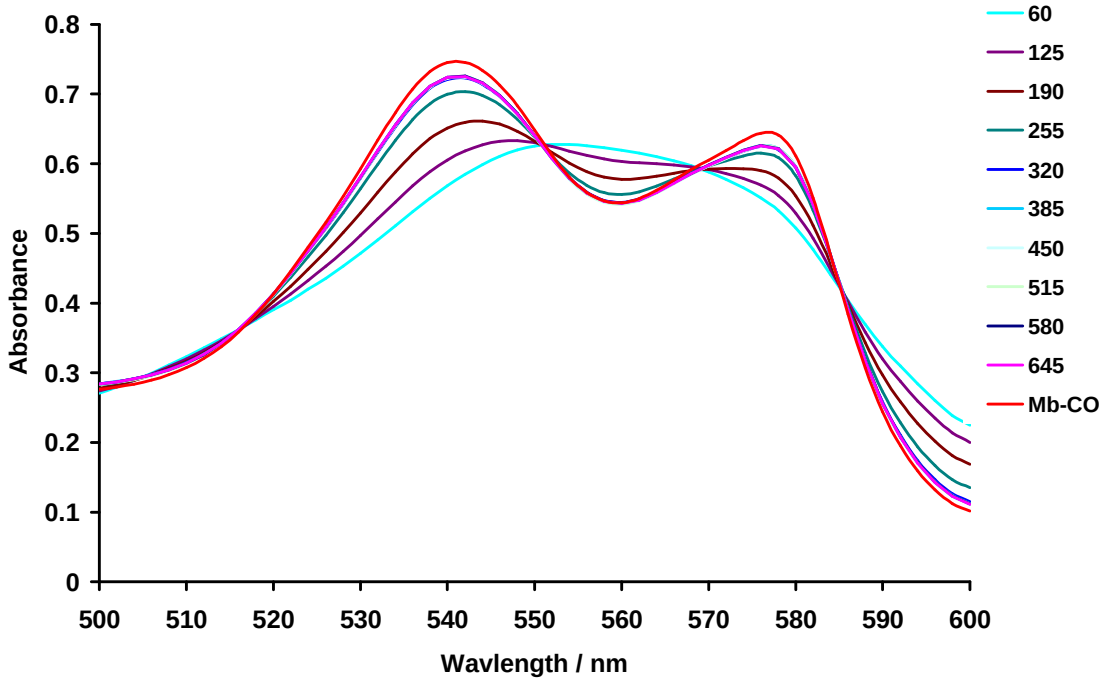

Fig. 76. The changes in the UV spectrum of myoglobin as CO is released from [NEt$_4$][{Cr(CO)$_5$}$_2$(μ-Br)] after incubation in DMSO for 6 min (60μm).

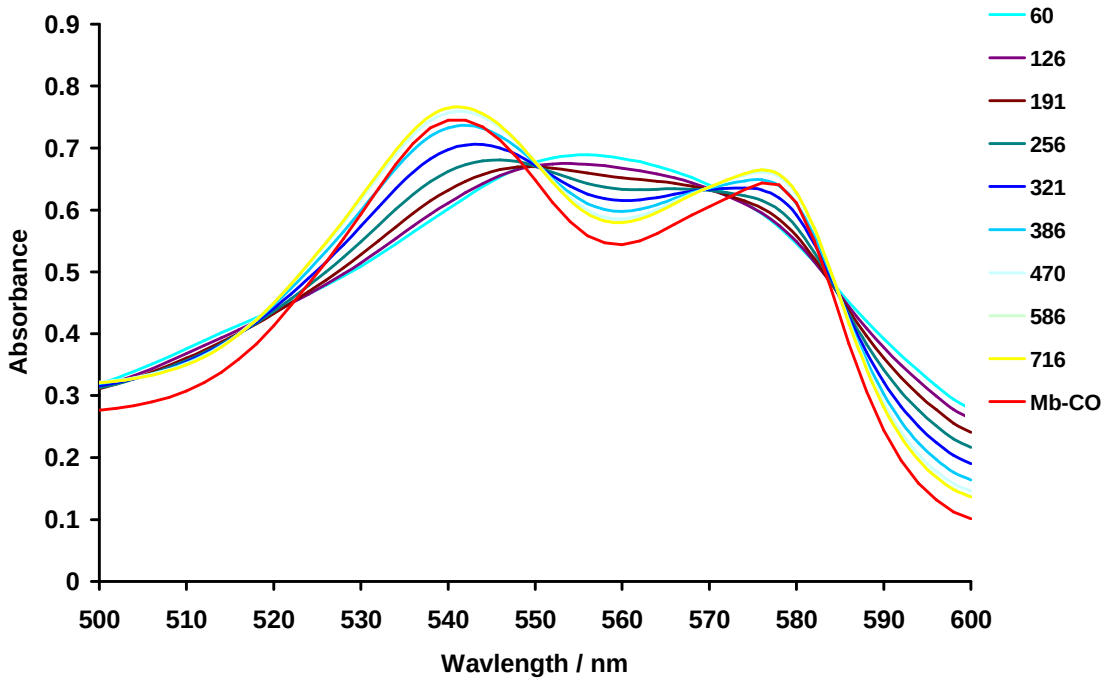

Fig. 77. The changes in the UV spectrum of myoglobin as CO is released from [NEt$_4$][{Cr(CO)$_5$}$_2$(μ-Br)] after incubation in DMSO for 6 min (40μm).

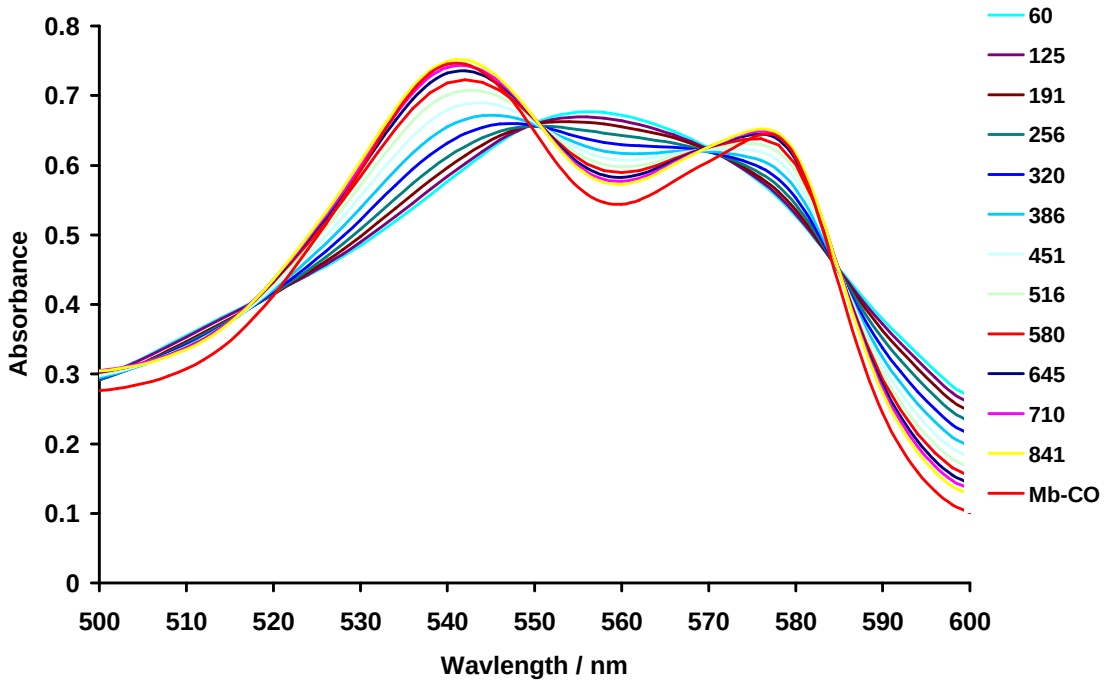

Fig. 78. The changes in the UV spectrum of myoglobin as CO is released from $[NEt_4][\{Cr(CO)_5\}_2(\mu\text{-}Br)]$ after incubation in DMSO for 6 min (20 µm)

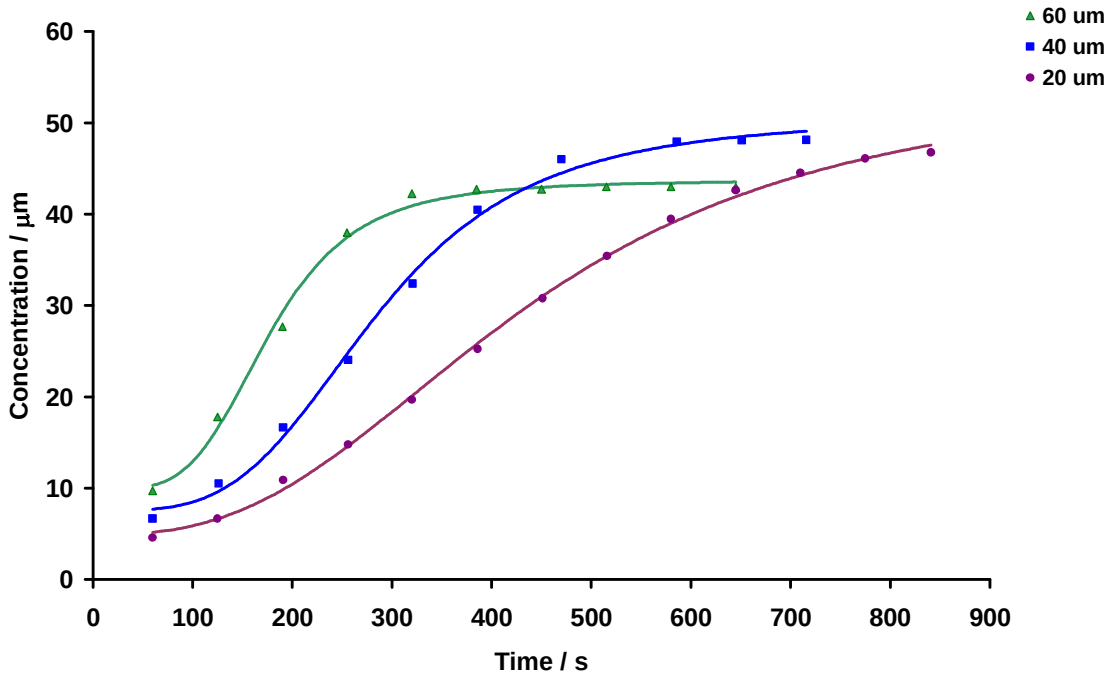

Fig 79. Formation of MbCO over time after addition of 60 µM, 40µM and 20µM of $[NEt_4][\{Cr(CO)_5\}_2(\mu\text{-}Br)]$ after incubation in DMSO for 6 min to an aqueous solution containing deoxy-myoglobin at pH 7.4.

1.21. $[NEt_4][\{Cr(CO)_5\}_2(\mu\text{-}Br)]$ incubated in DMSO for 30 min

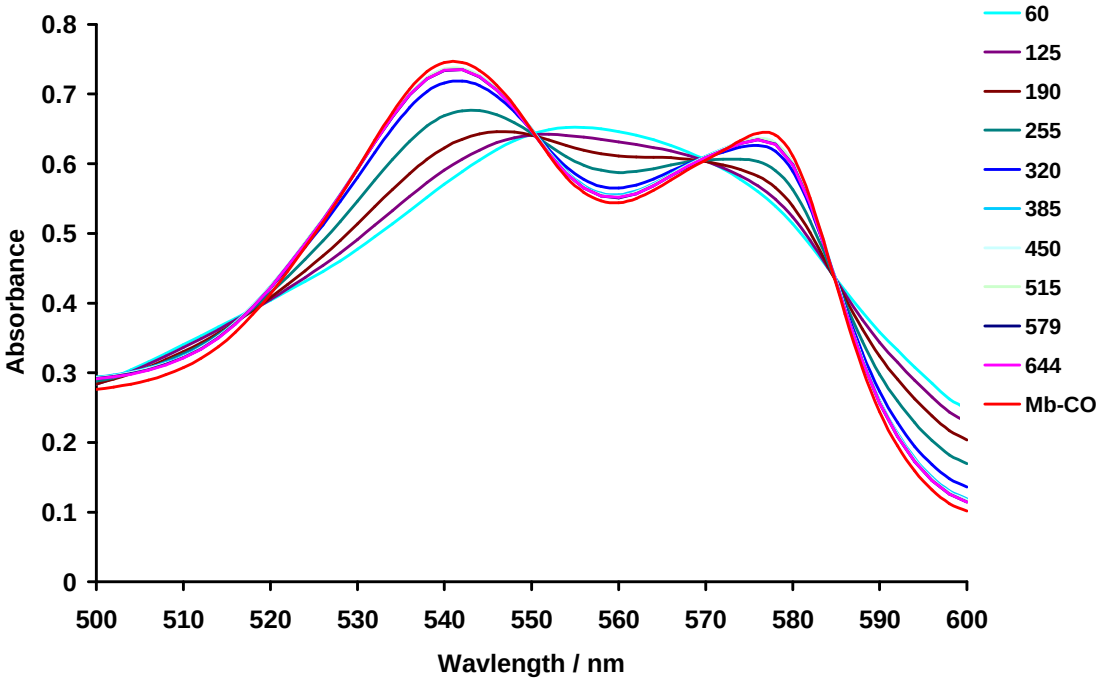

Fig. 80. The changes in the UV spectrum of myoglobin as CO is released from $[NEt_4][\{Cr(CO)_5\}_2(\mu\text{-}Br)]$ after incubation in DMSO for 30 min (60µm).

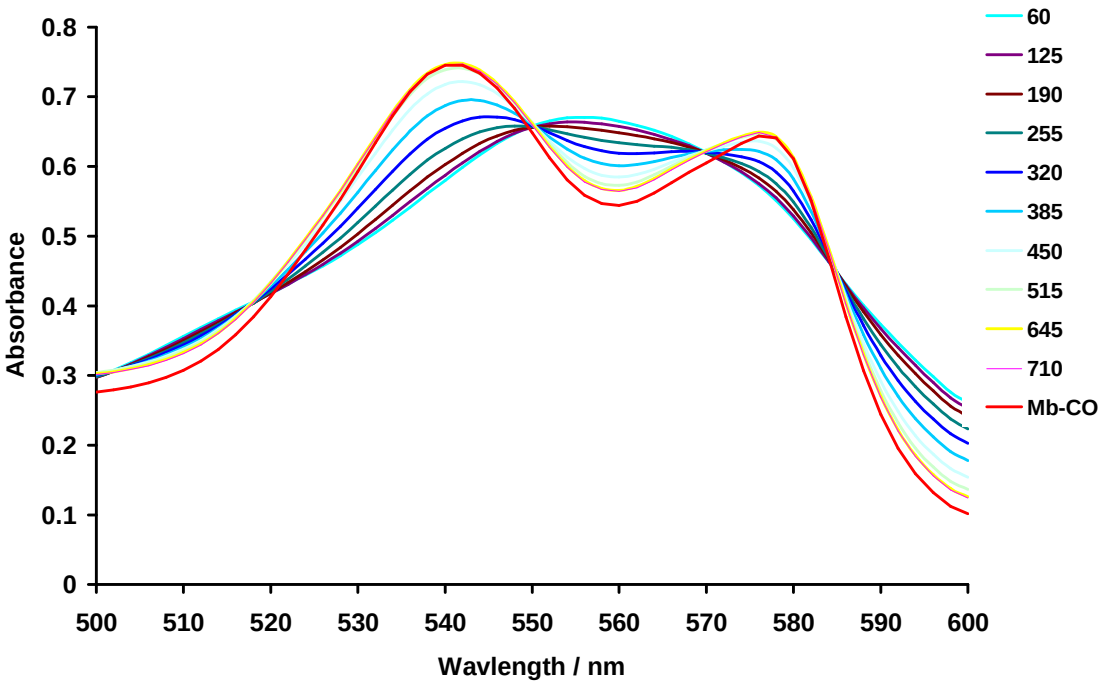

Fig. 81. The changes in the UV spectrum of myoglobin as CO is released from $[NEt_4][\{Cr(CO)_5\}_2(\mu\text{-}Br)]$ after incubation in DMSO for 30 min (40µm).

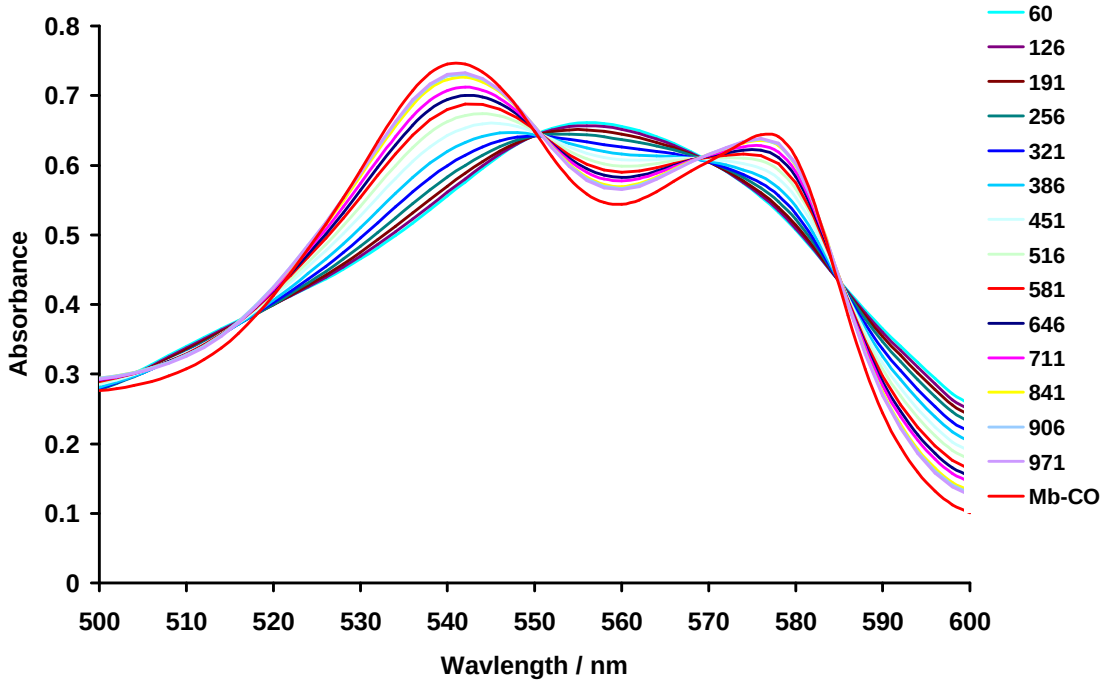

Fig. 82. The changes in the UV spectrum of myoglobin as CO is released from $[NEt_4][\{Cr(CO)_5\}_2(\mu\text{-Br})]$ after incubation in DMSO for 30 min (20 µm)

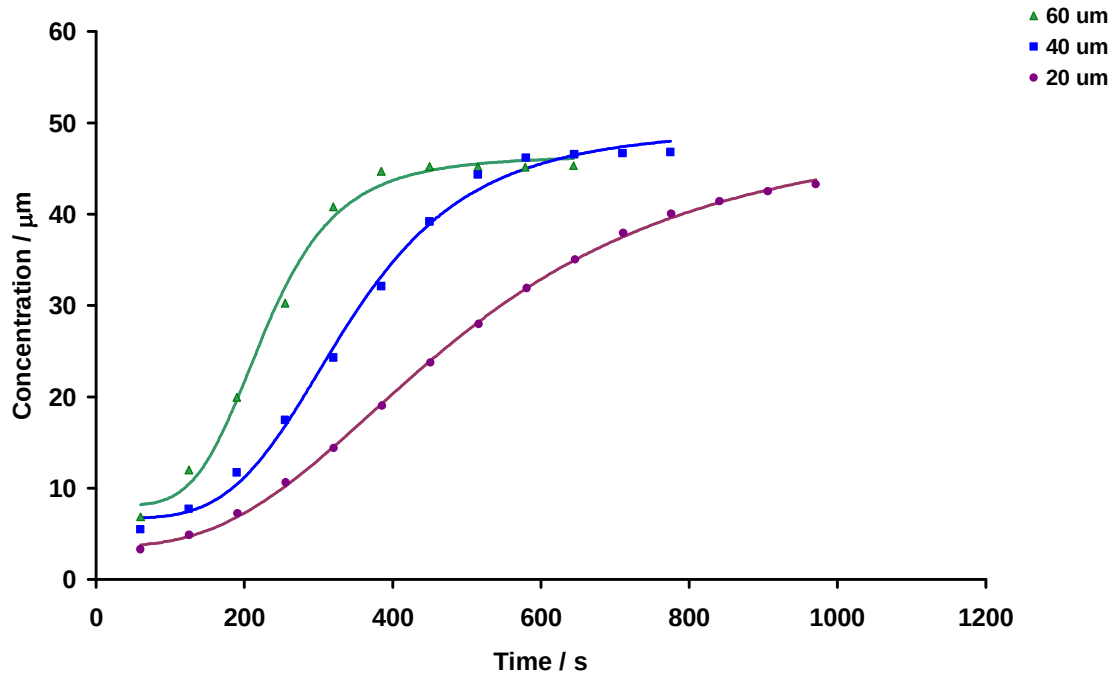

Fig 83. Formation of MbCO over time after addition of 60 µM, 40µM and 20µM of $[NEt_4][\{Cr(CO)_5\}_2(\mu\text{-Br})]$ after incubation in DMSO for 30 min to an aqueous solution containing deoxy-myoglobin at pH 7.4.

1.22. Comparison of CO-release from [NEt$_4$][{Cr(CO)$_5$}$_2$(μ-Br)] after incubated in DMSO.

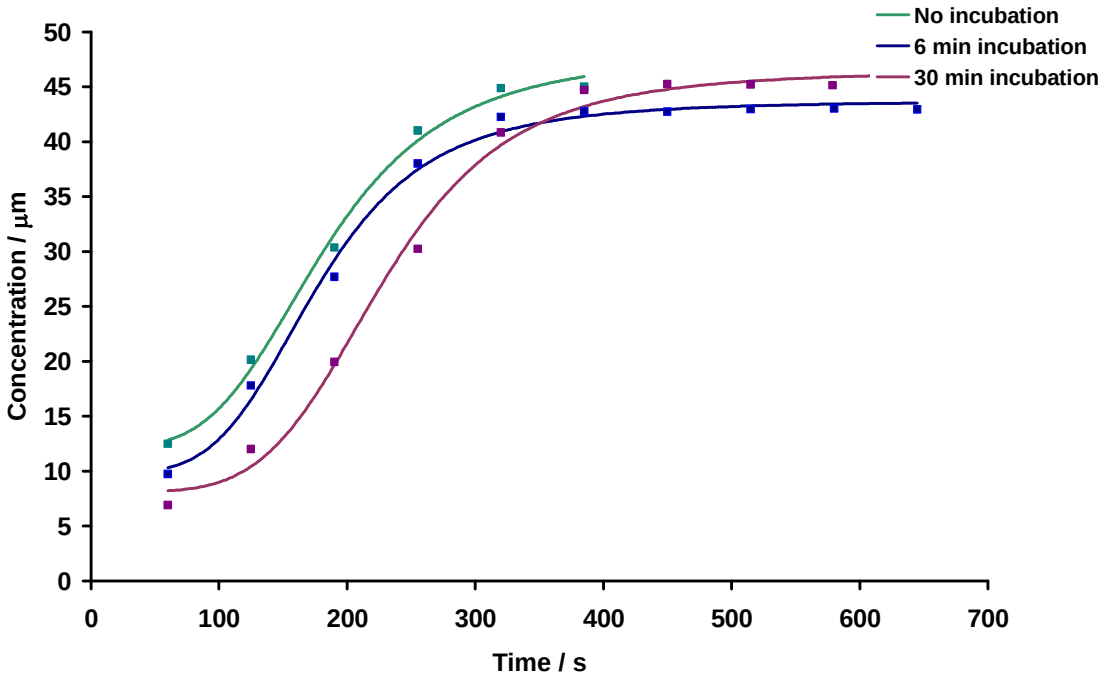

Fig. 84. Formation of MbCO over time after addition of 60 μM solutions of [NEt$_4$][{Cr(CO)$_5$}$_2$(μ-Br)] after incubated in DMSO for various time periods to an aqueous solution containing deoxy-myoglobin at pH 7.4.

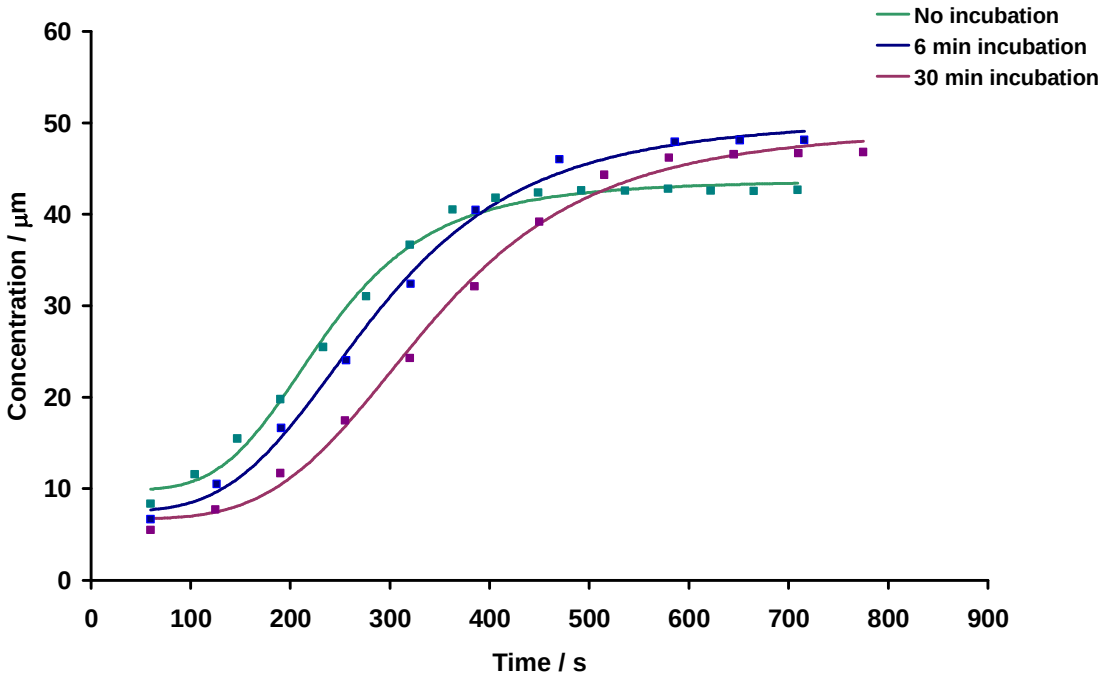

Fig. 85. Formation of MbCO over time after addition of 40 μM solutions of [NEt$_4$][{Cr(CO)$_5$}$_2$(μ-Br)] after incubated in DMSO for various time periods to an aqueous solution containing deoxy-myoglobin at pH 7.4.

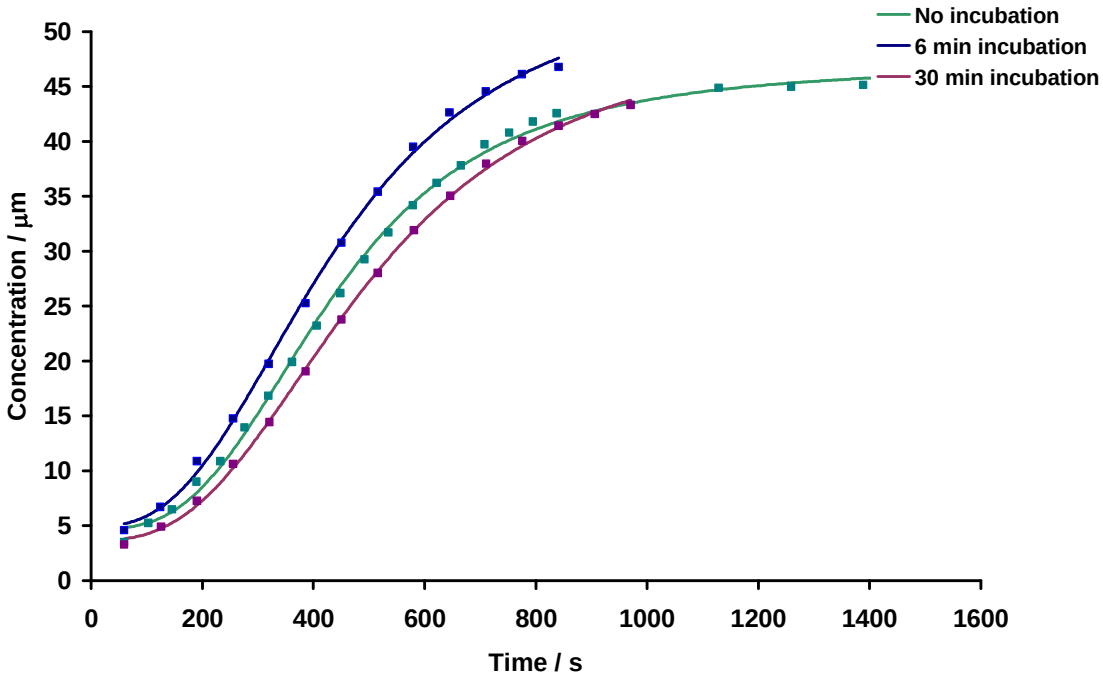

Fig. 86. Formation of MbCO over time after addition of 40 µM solutions of $[NEt_4][\{Cr(CO)_5\}_2(\mu\text{-}Br)]$ after incubated in DMSO for various time periods to an aqueous solution containing deoxy-myoglobin at pH 7.4.

1.23. $Cr(=C\{OCH_3\}CH_3)(CO)_5$

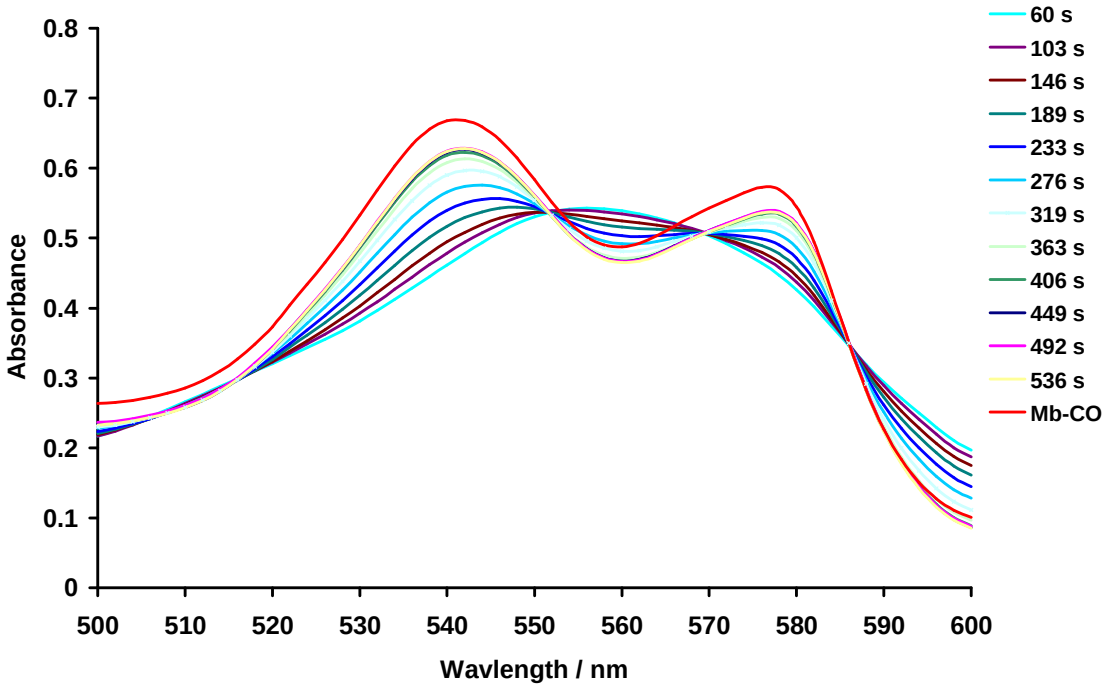

Fig. 87. The changes in the UV spectrum of myoglobin as CO is released from $Cr(=C\{OCH_3\}CH_3)(CO)_5$ (60µm).

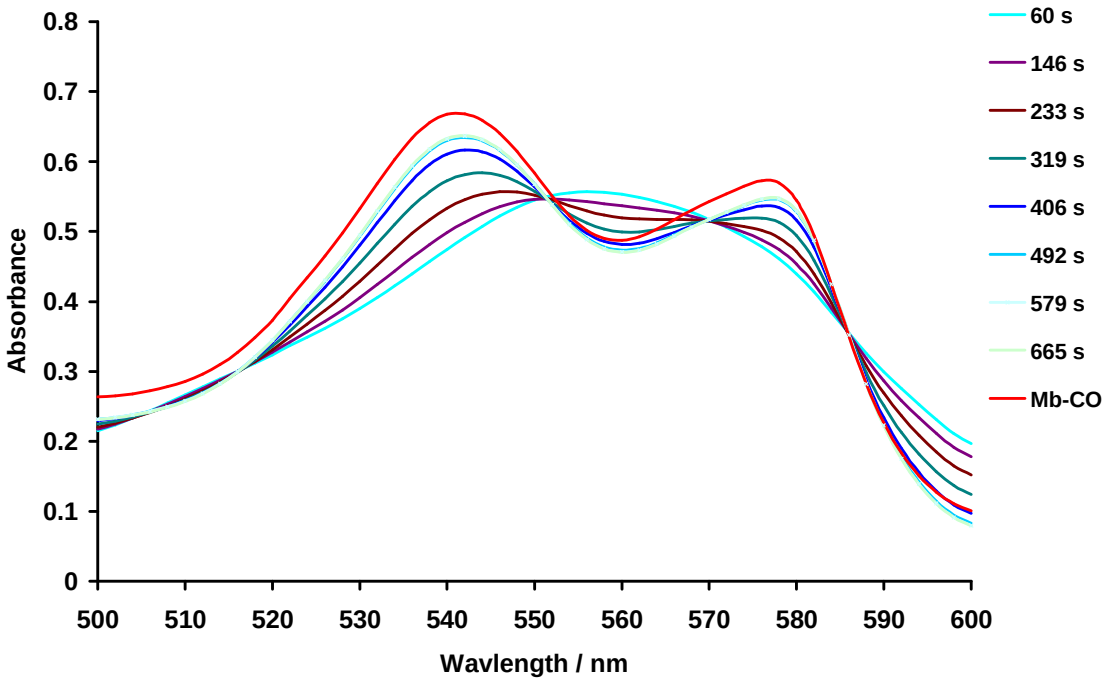

Fig. 88. The changes in the UV spectrum of myoglobin as CO is released from $Cr(=C\{OCH_3\}CH_3)(CO)_5$ (40µm).

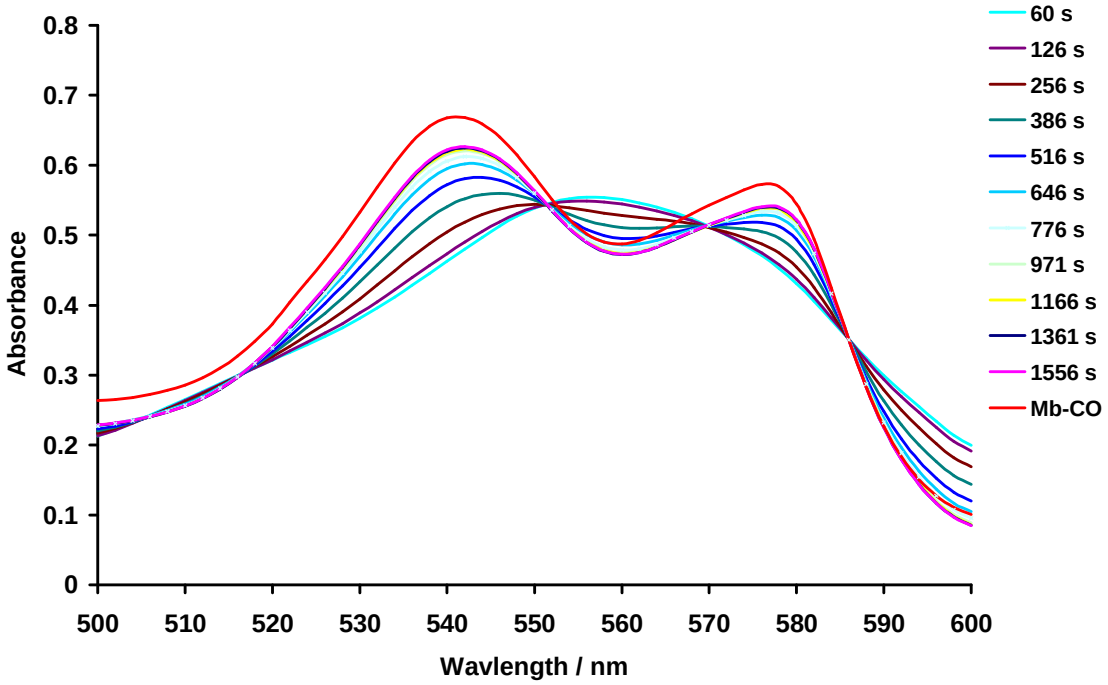

Fig. 89. The changes in the UV spectrum of myoglobin as CO is released from $Cr(=C\{OCH_3\}CH_3)(CO)_5$ (20μm).

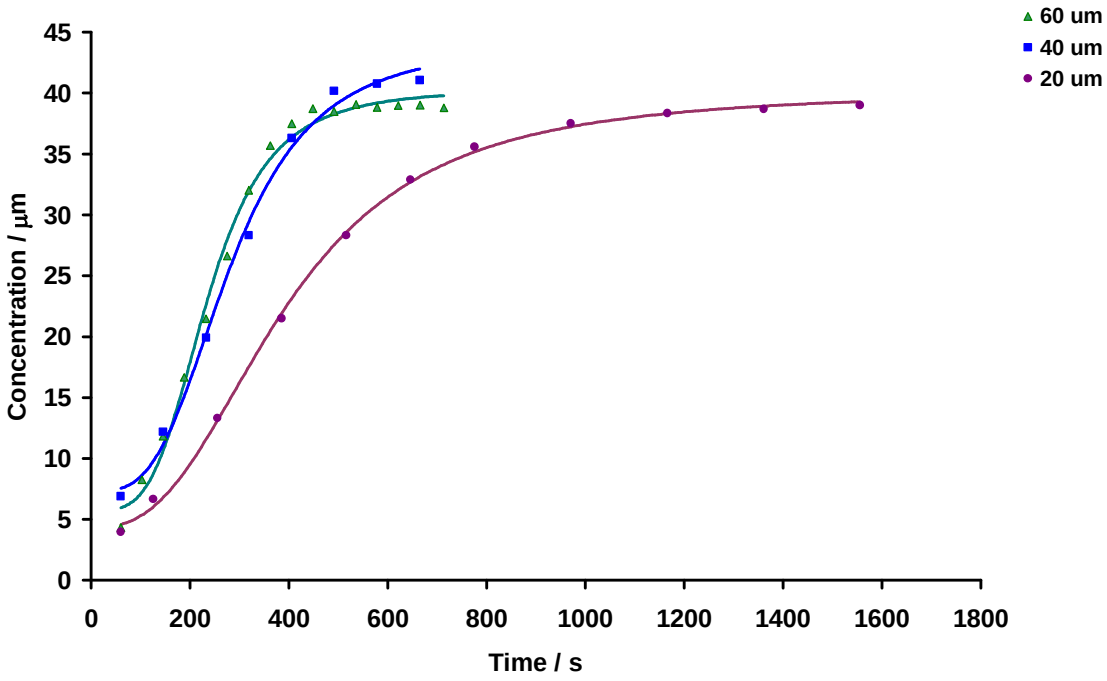

Fig 90. Formation of MbCO over time after addition of 60 μM, 40μM and 20μM of $Cr(=C\{OCH_3\}CH_3)(CO)_5$ in DMSO to an aqueous solution containing deoxy-myoglobin at pH 7.4.

1.24. Mo(=C{OCH$_3$}CH$_3$)(CO)$_5$

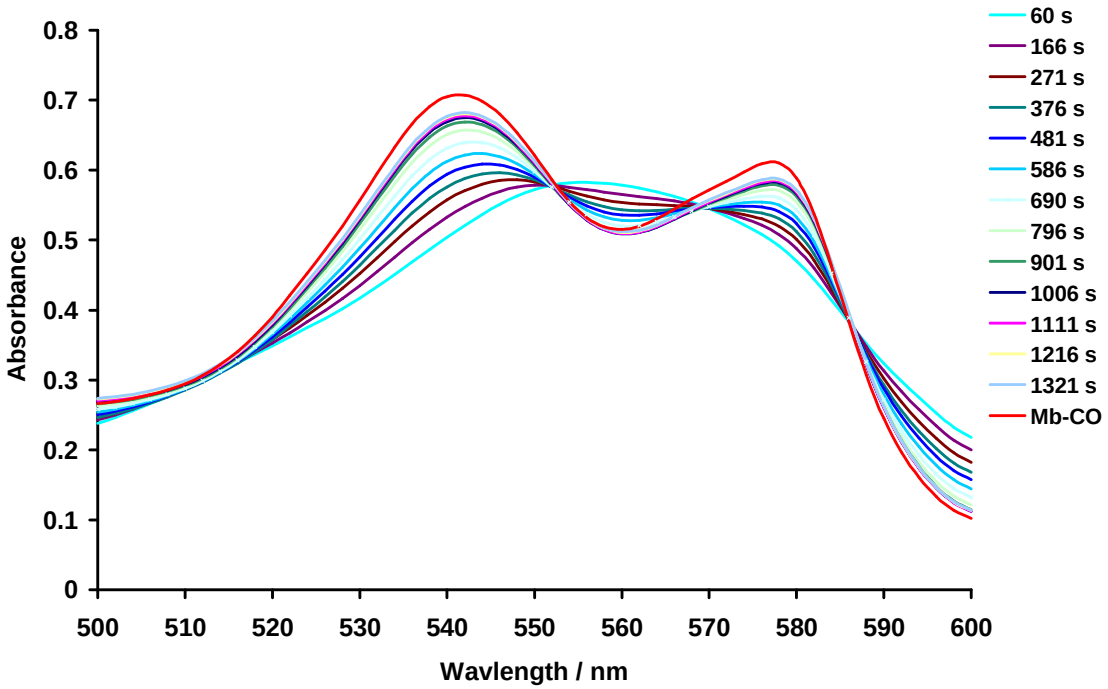

Fig. 91. The changes in the UV spectrum of myoglobin as CO is released from Mo(=C{OCH$_3$}CH$_3$)(CO)$_5$ (60μm).

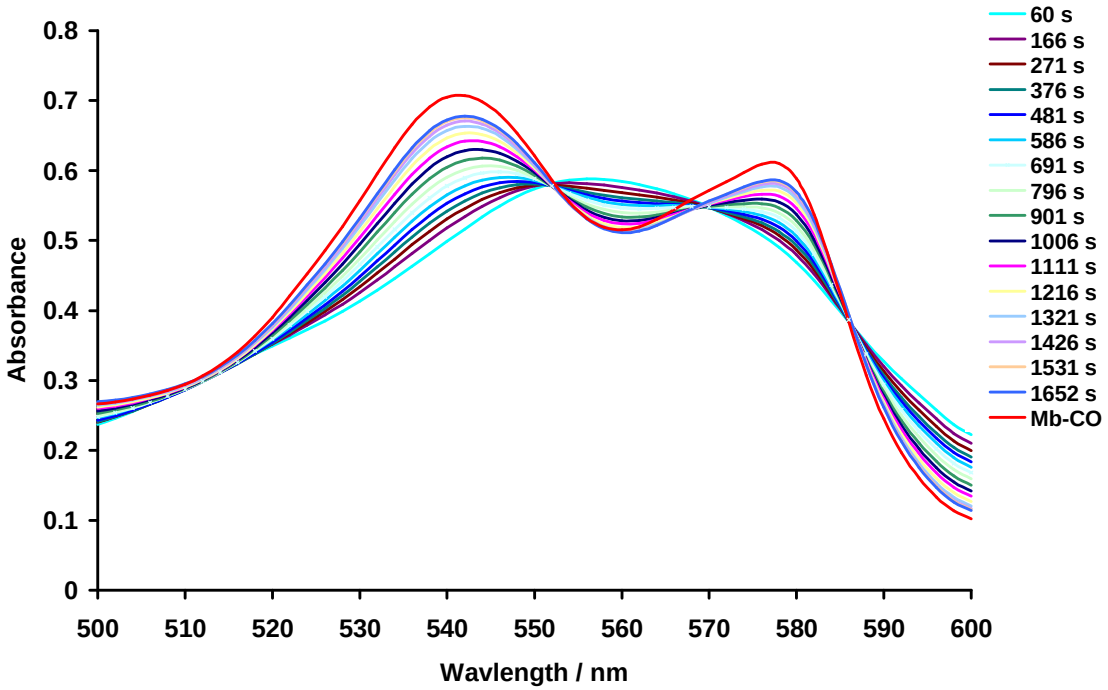

Fig. 92. The changes in the UV spectrum of myoglobin as CO is released from Mo(=C{OCH$_3$}CH$_3$)(CO)$_5$ (40μm).

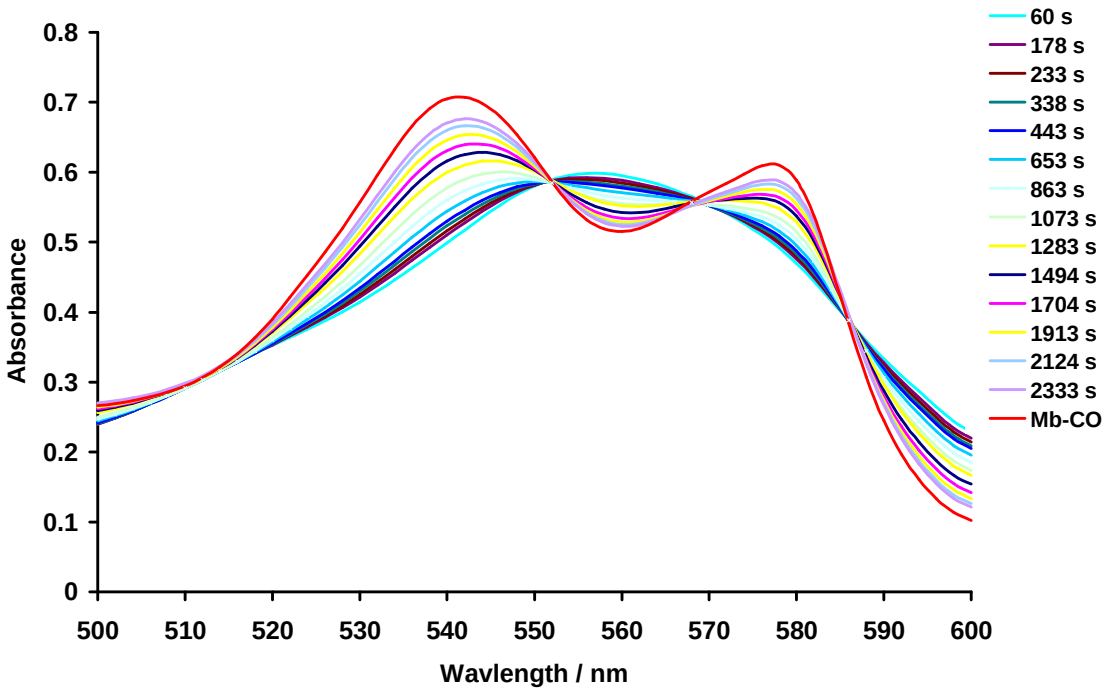

Fig. 93. The changes in the UV spectrum of myoglobin as CO is released from $Mo(=C\{OCH_3\}CH_3)(CO)_5$ (20μm).

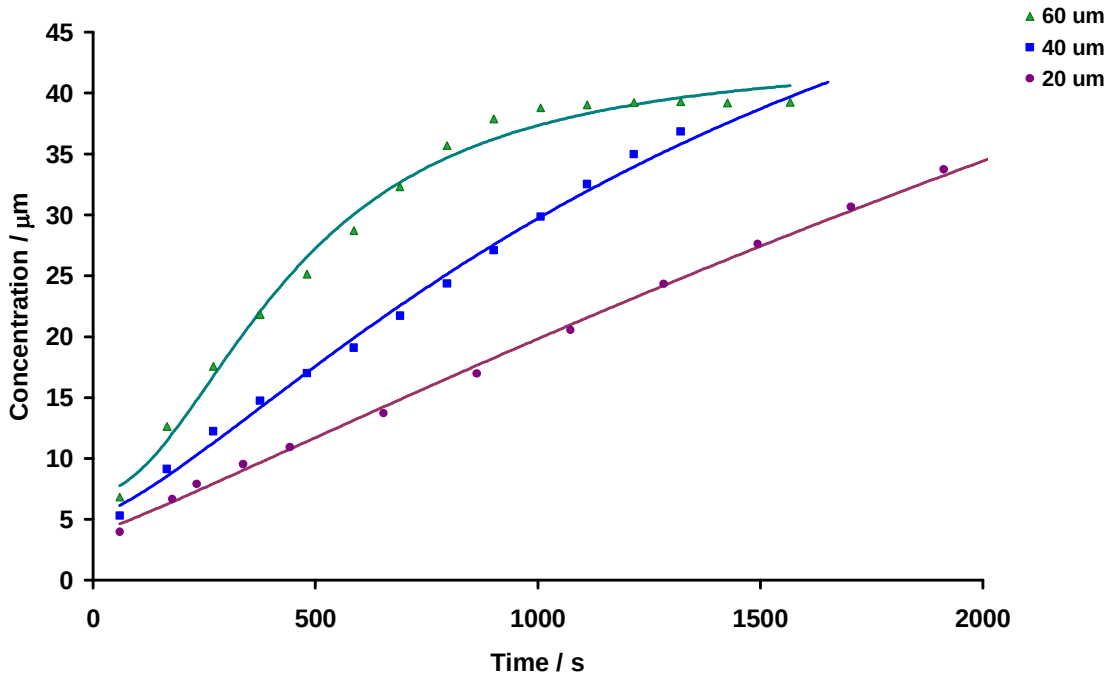

Fig 94. Formation of MbCO over time after addition of 60 μM, 40μM and 20μM of $Mo(=C\{OCH_3\}CH_3)(CO)_5$ in DMSO to an aqueous solution containing deoxy-myoglobin at pH 7.4.

1.25. W(=C{OCH$_3$}CH$_3$)(CO)$_5$

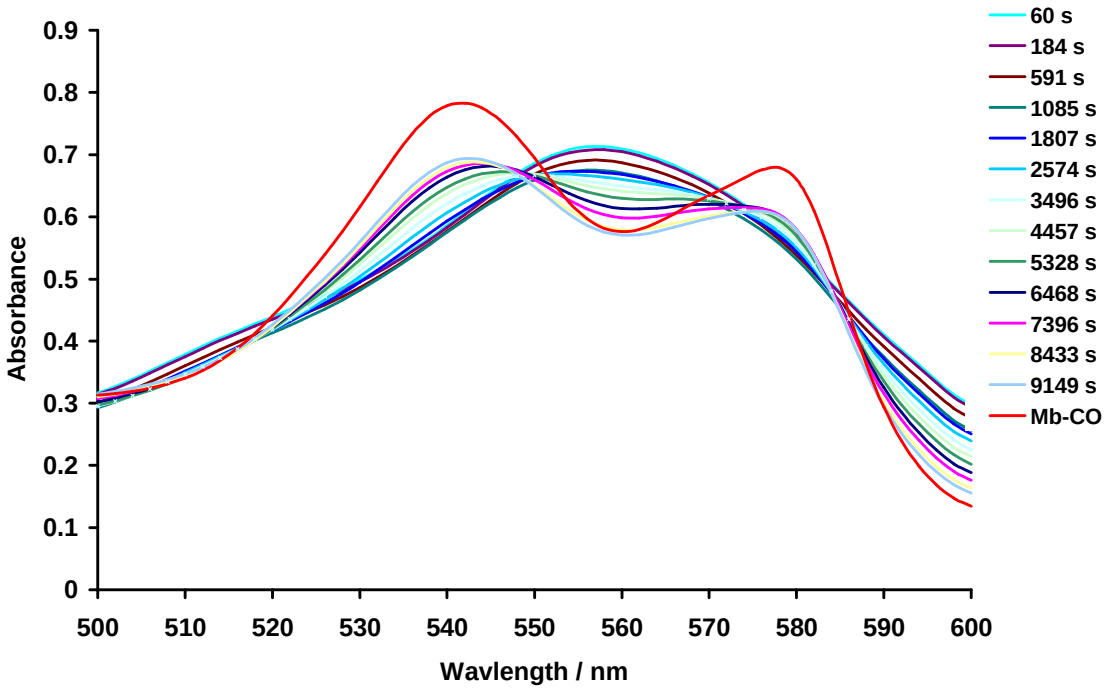

Fig. 95. The changes in the UV spectrum of myoglobin as CO is released from W(=C{OCH$_3$}CH$_3$)(CO)$_5$ (60μm).

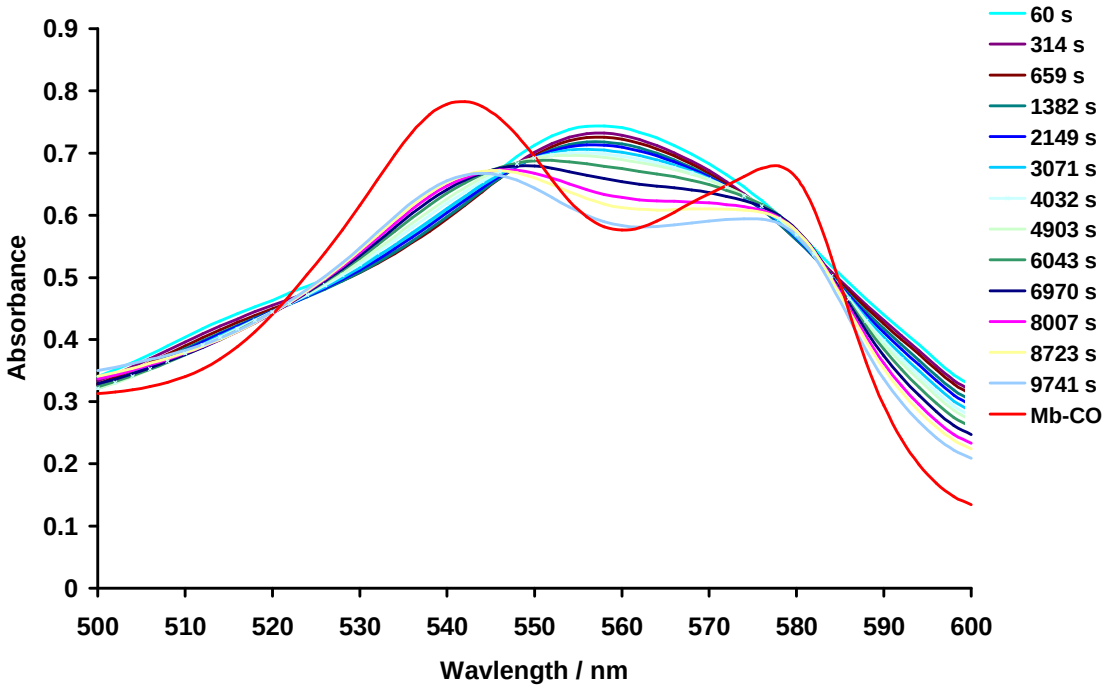

Fig. 96. The changes in the UV spectrum of myoglobin as CO is released from W(=C{OCH$_3$}CH$_3$)(CO)$_5$ (40μm).

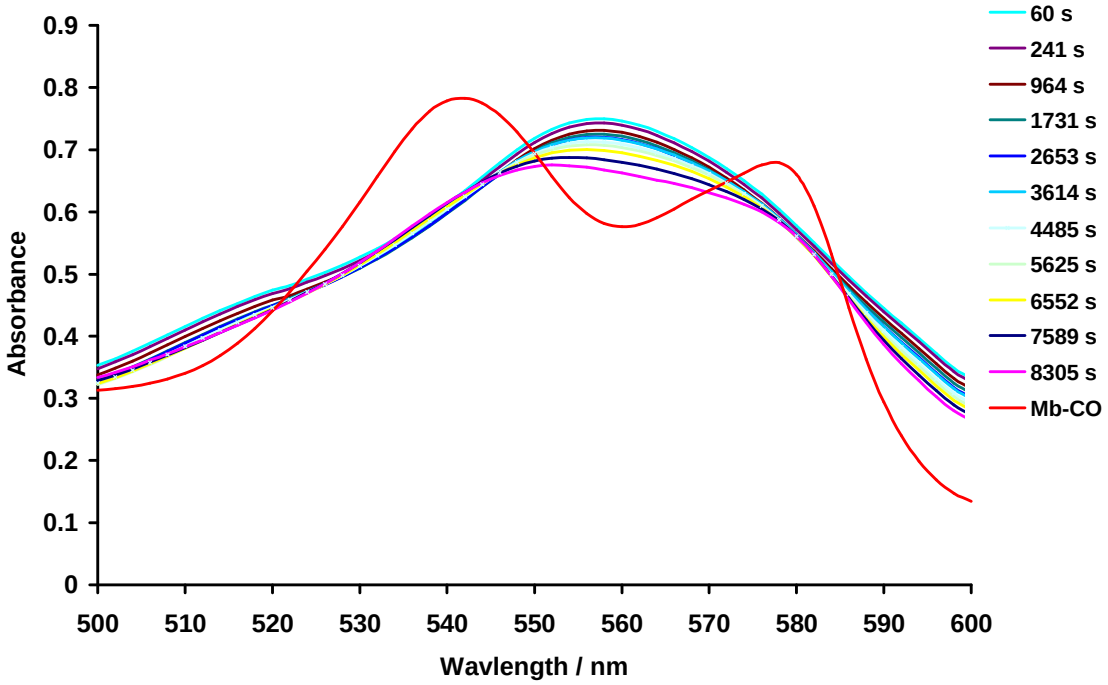

Fig. 97. The changes in the UV spectrum of myoglobin as CO is released from $W(=C\{OCH_3\}CH_3)(CO)_5$ (20μm).

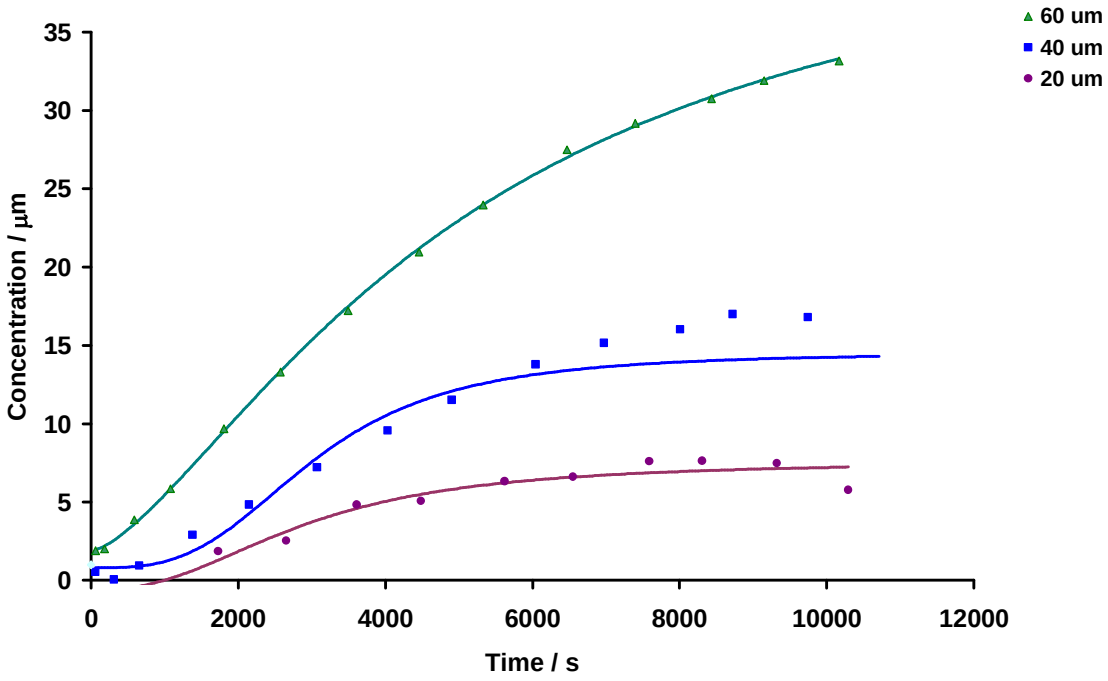

Fig 98. Formation of MbCO over time after addition of 60 μM, 40μM and 20μM of $W(=C\{OCH_3\}CH_3)(CO)_5$ in DMSO to an aqueous solution containing deoxy-myoglobin at pH 7.4.

1.26. [NEt$_4$][MoI$_3$(CO)$_4$]

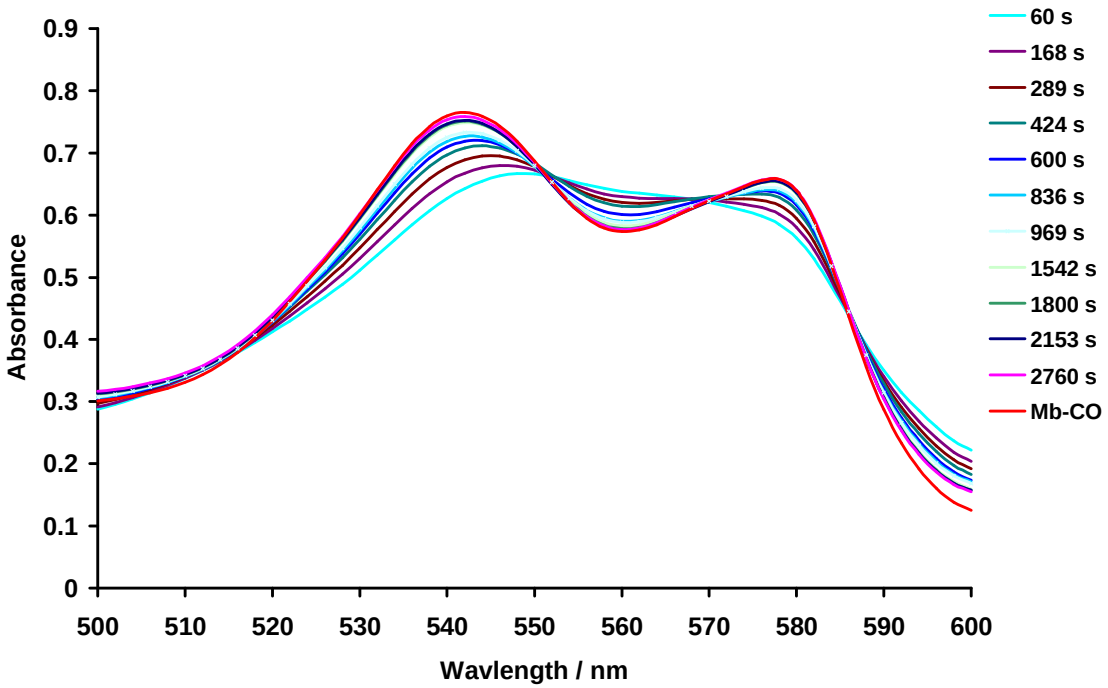

Fig. 99. The changes in the UV spectrum of myoglobin as CO is released from [NEt$_4$][MoI$_3$(CO)$_4$] (60µm).

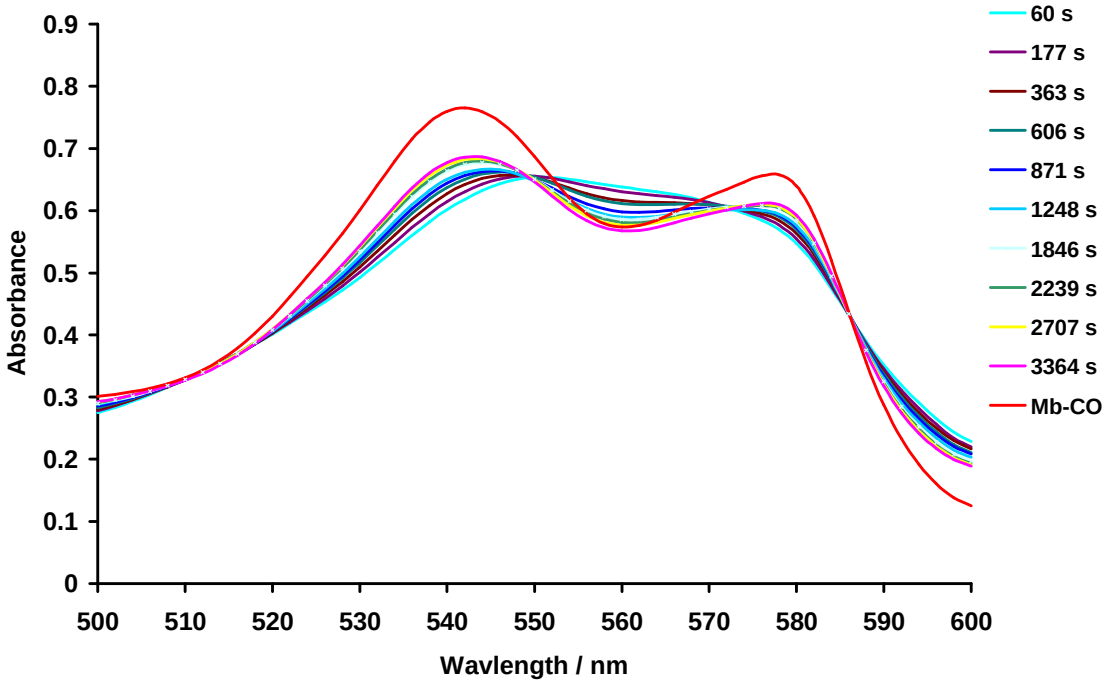

Fig. 100. The changes in the UV spectrum of myoglobin as CO is released from [NEt$_4$][MoI$_3$(CO)$_4$] (40µm).

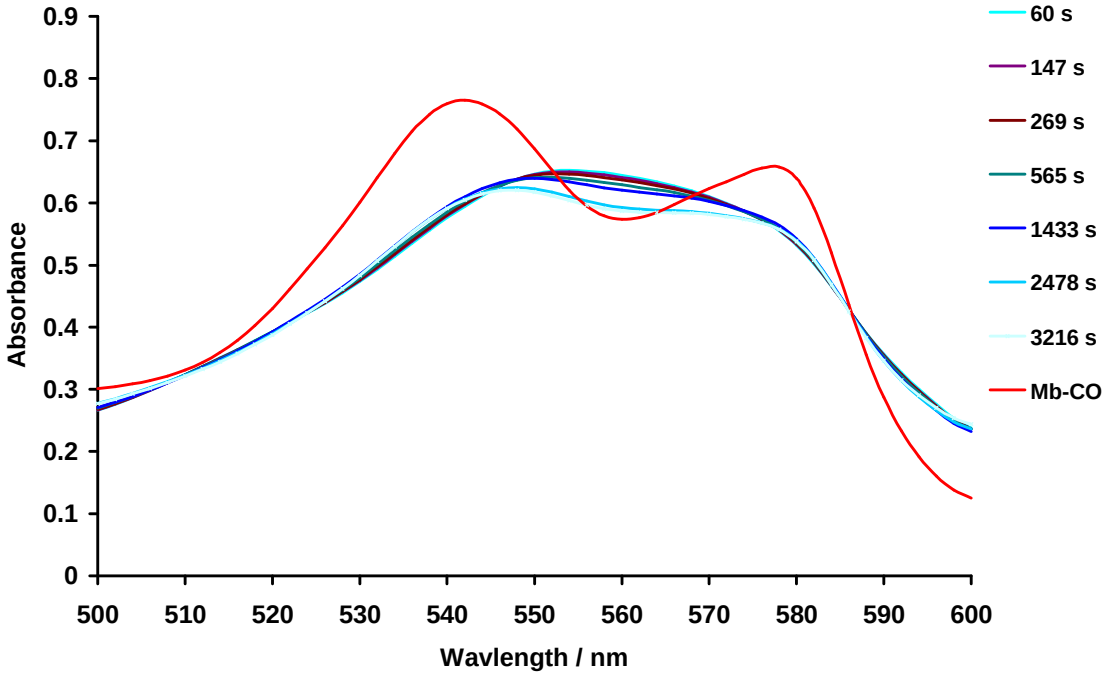

Fig. 101. The changes in the UV spectrum of myoglobin as CO is released from $[NEt_4][MoI_3(CO)_4]$ (20µm).

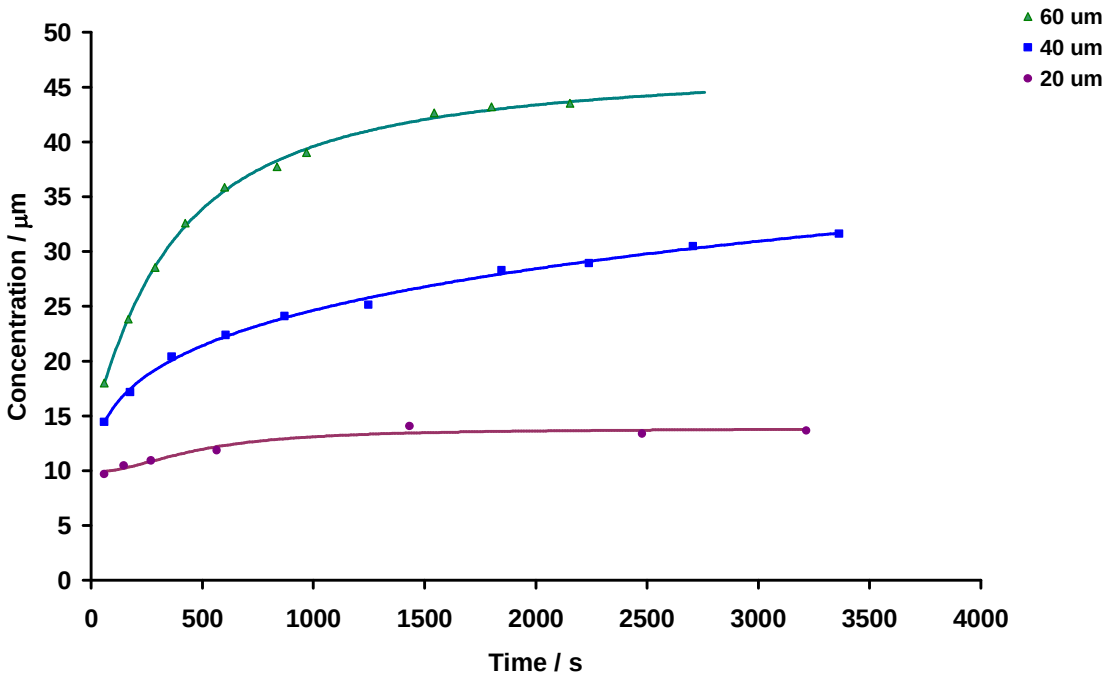

Fig 102. Formation of MbCO over time after addition of 60 µM, 40µM and 20µM of $[NEt_4][MoI_3(CO)_4]$ in DMSO to an aqueous solution containing deoxy-myoglobin at pH 7.4.

1.27. $[NEt_4][WI_3(CO)_4]$

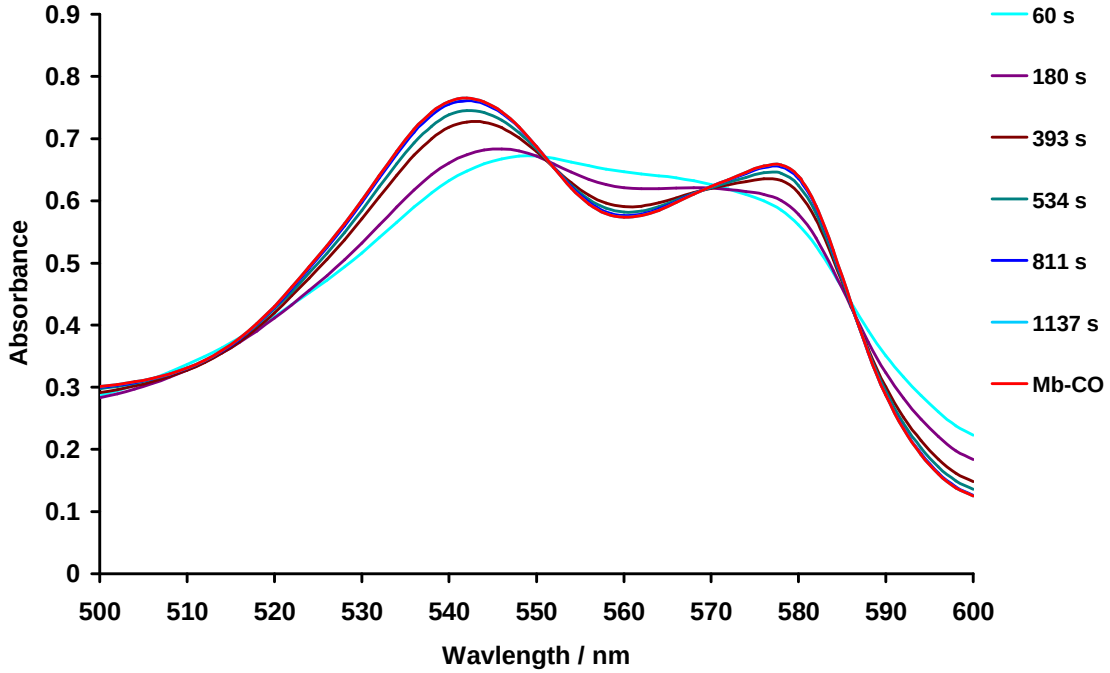

Fig. 103. The changes in the UV spectrum of myoglobin as CO is released from $[NEt_4][WI_3(CO)_4]$ (60µm).

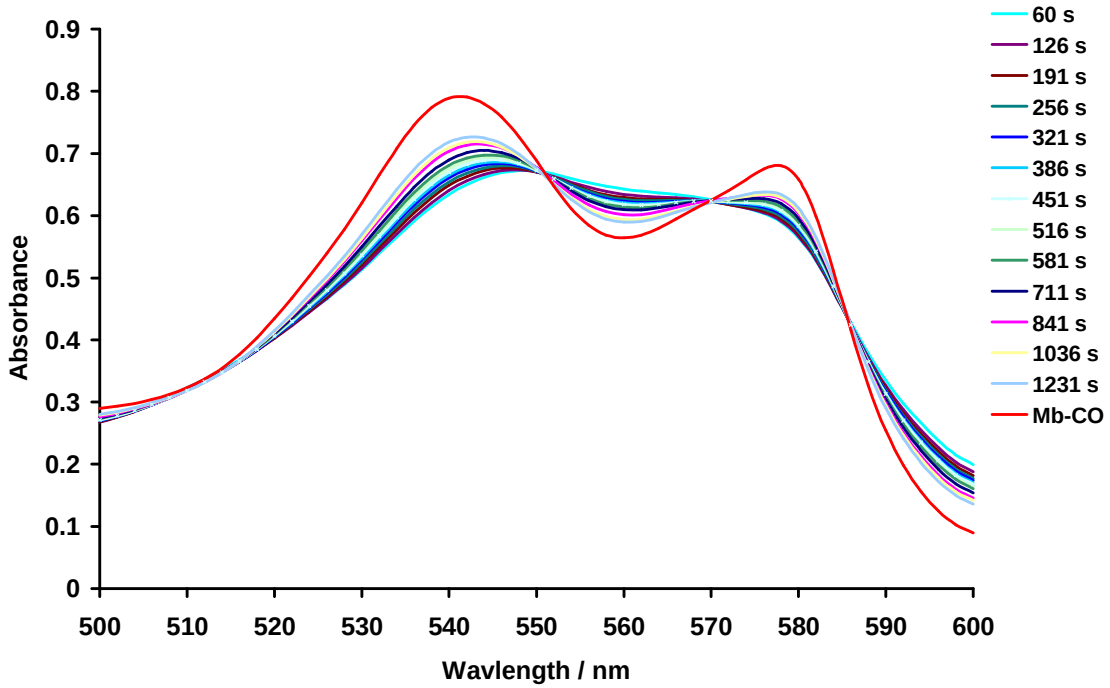

Fig. 104. The changes in the UV spectrum of myoglobin as CO is released from $[NEt_4][WI_3(CO)_4]$ (40µm).

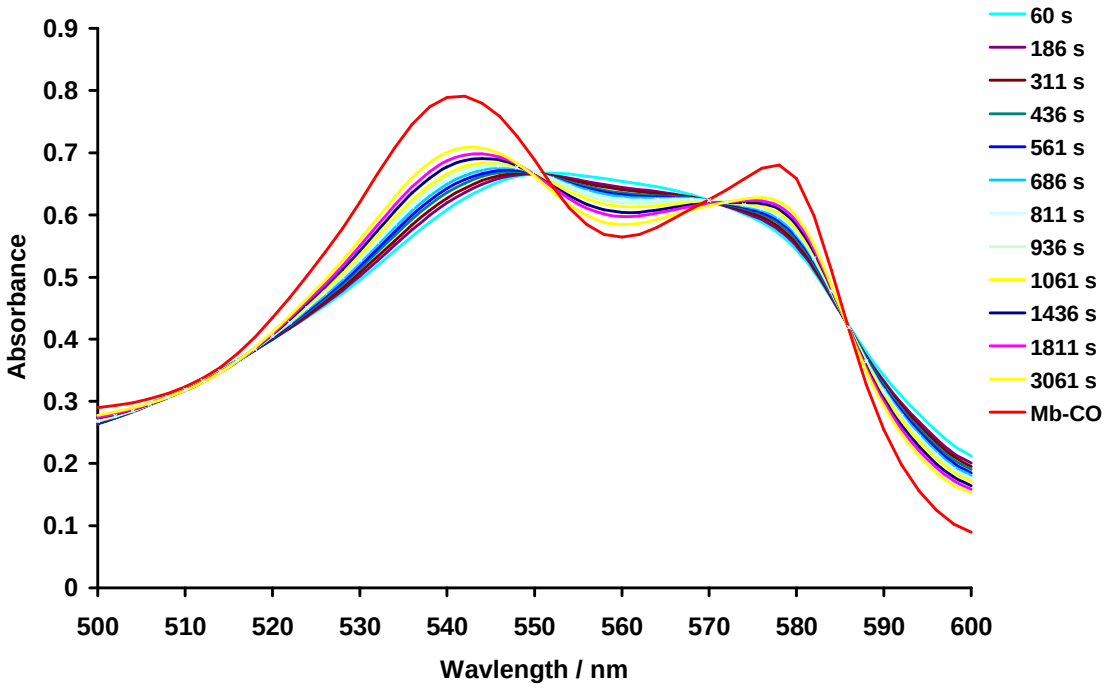

Fig. 105. The changes in the UV spectrum of myoglobin as CO is released from $[NEt_4][WI_3(CO)_4]$ (20µm).

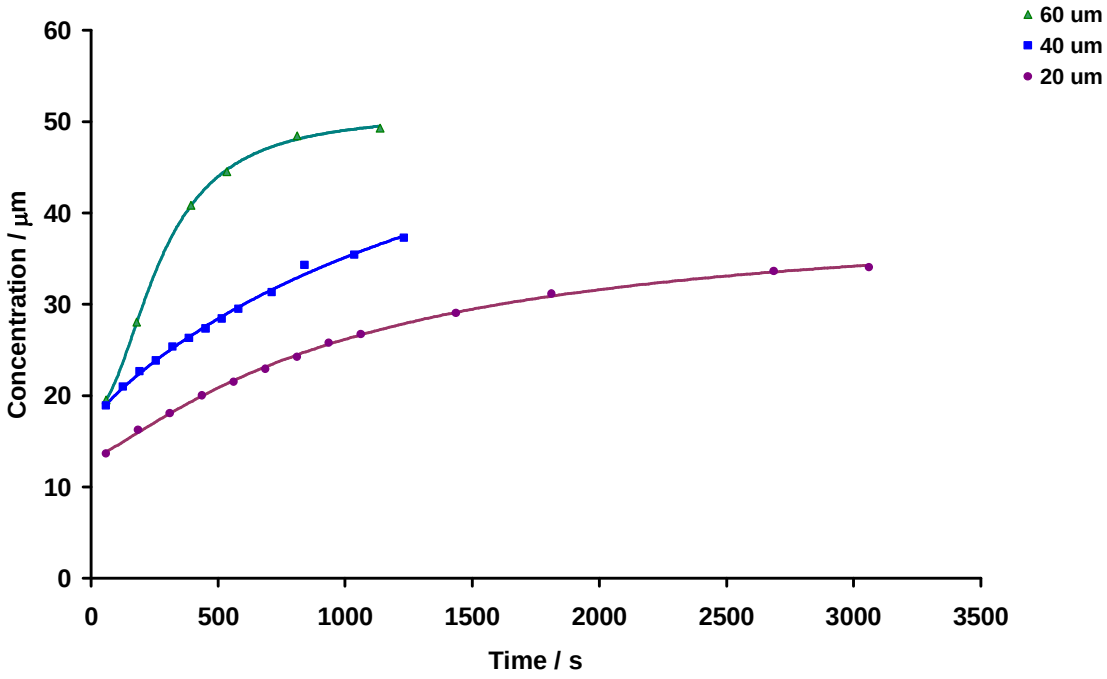

Fig 106. Formation of MbCO over time after addition of 60 µM, 40µM and 20µM of $[NEt_4][WI_3(CO)_4]$ in DMSO to an aqueous solution containing deoxy-myoglobin at pH 7.4.

1.28. W(κ²-acac)₂(CO)₃

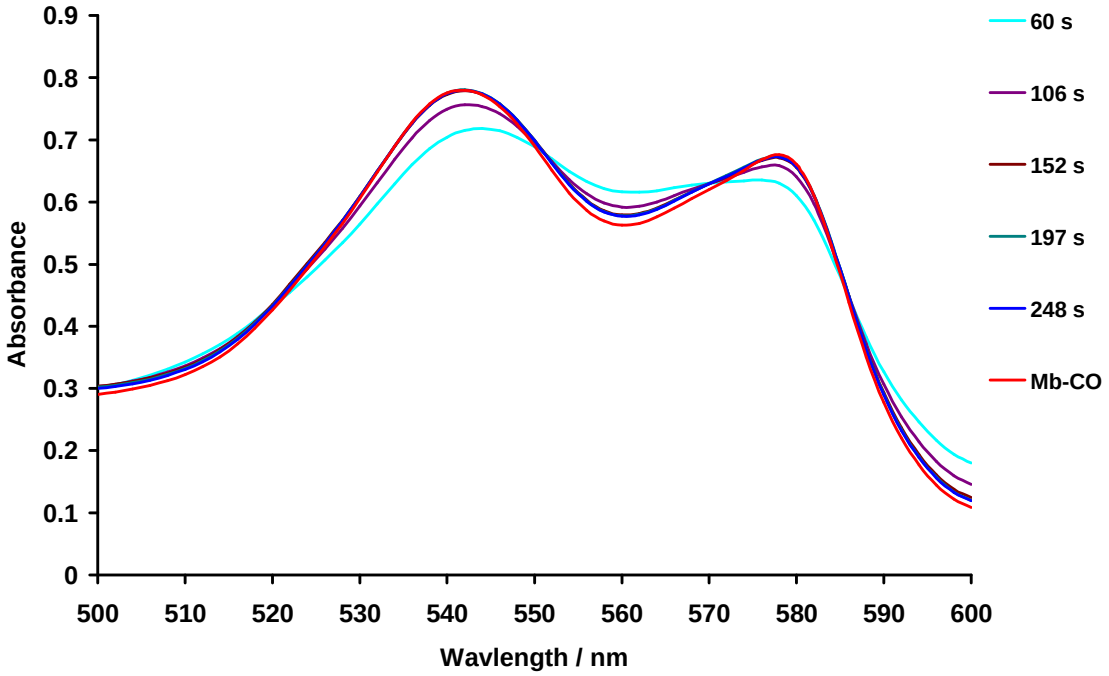

Fig. 107. The changes in the UV spectrum of myoglobin as CO is released from $W(\kappa^2\text{-acac})_2(CO)_3$ (60μm).

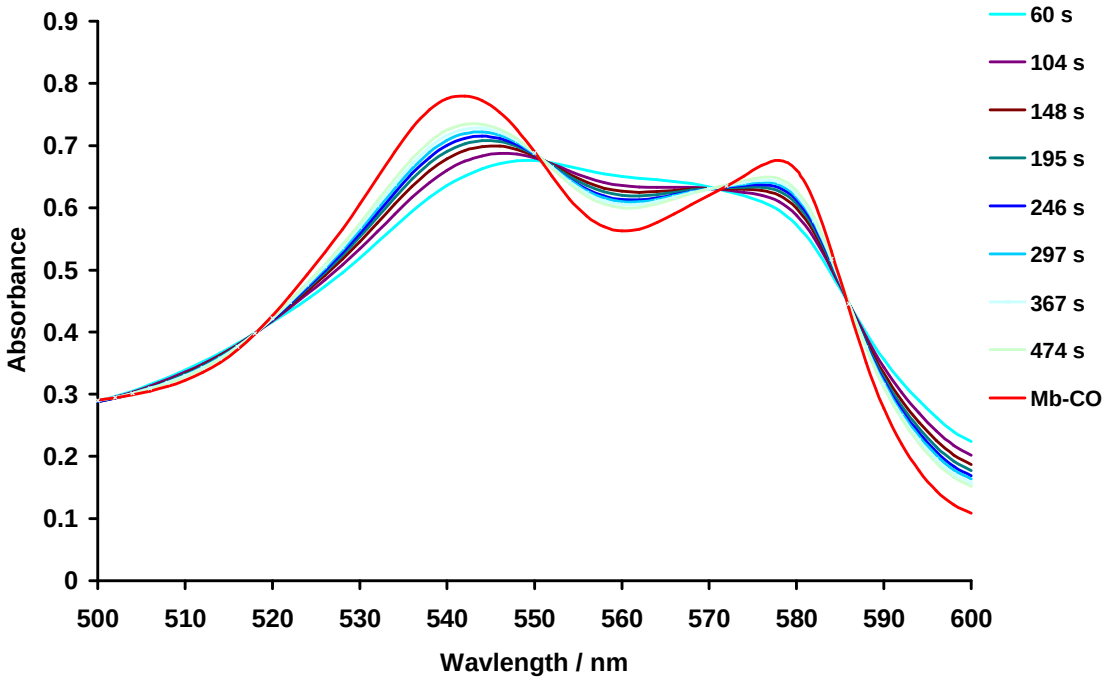

Fig. 108. The changes in the UV spectrum of myoglobin as CO is released from $W(\kappa^2\text{-acac})_2(CO)_3$ (40μm).

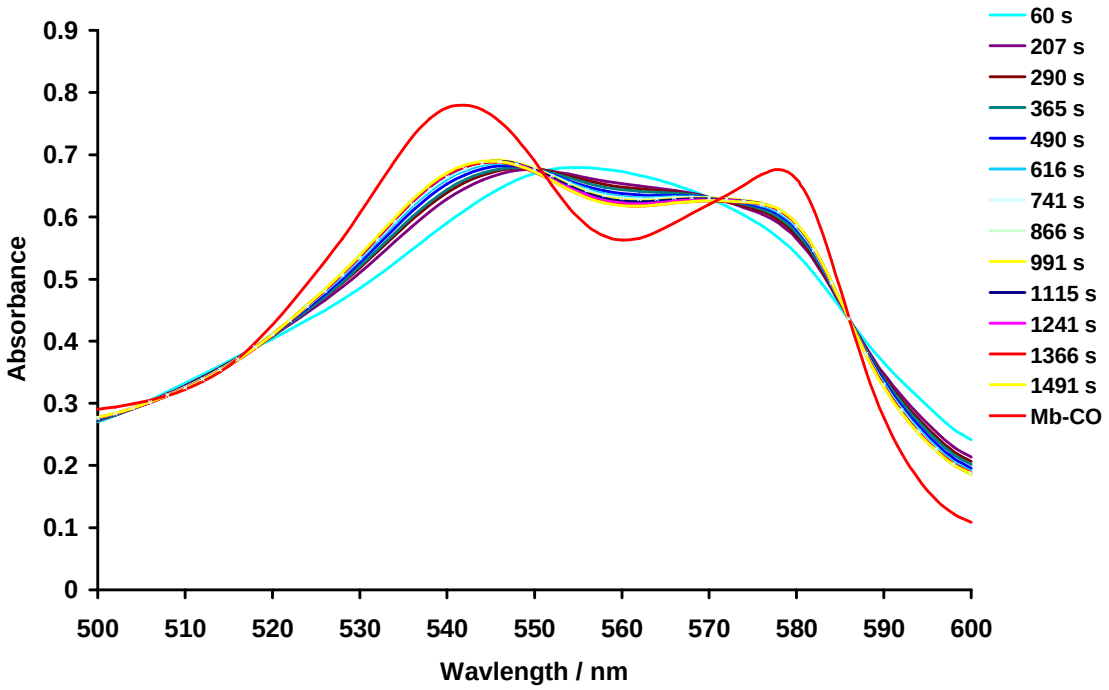

Fig. 109. The changes in the UV spectrum of myoglobin as CO is released from $W(\kappa^2\text{-acac})_2(CO)_3$ (20µm).

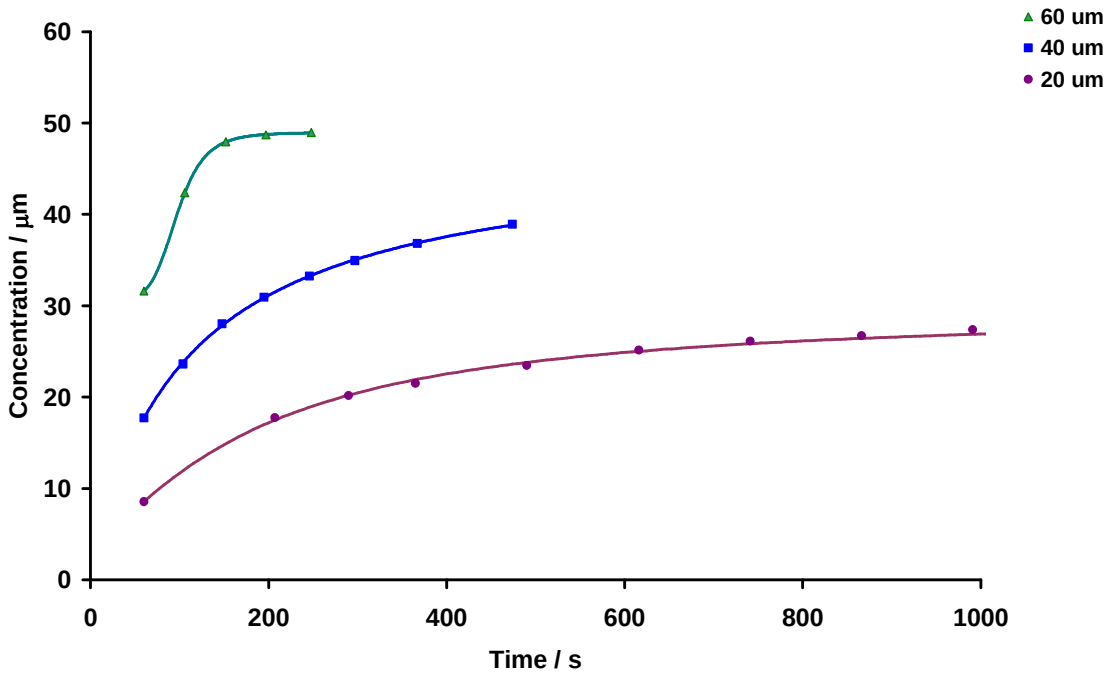

Fig 110. Formation of MbCO over time after addition of 60 µM, 40µM and 20µM of $W(\kappa^2\text{-acac})_2(CO)_3$ in DMSO to an aqueous solution containing deoxy-myoglobin at pH 7.4.

2. Degradation Tests

2.1. Degradation test of [NEt$_4$][CrBr(CO)$_5$] in DCM

The degradation of [NEt$_4$][CrBr(CO)$_5$] in DCM solution was monitored over a period of several hours by IR spectroscopy. (**Fig. 111**). The characteristic CO bands of [NEt$_4$][CrBr(CO)$_5$] was observed to decrease intensity over the period over several hours and the only new species observed was Cr(CO)$_6$.

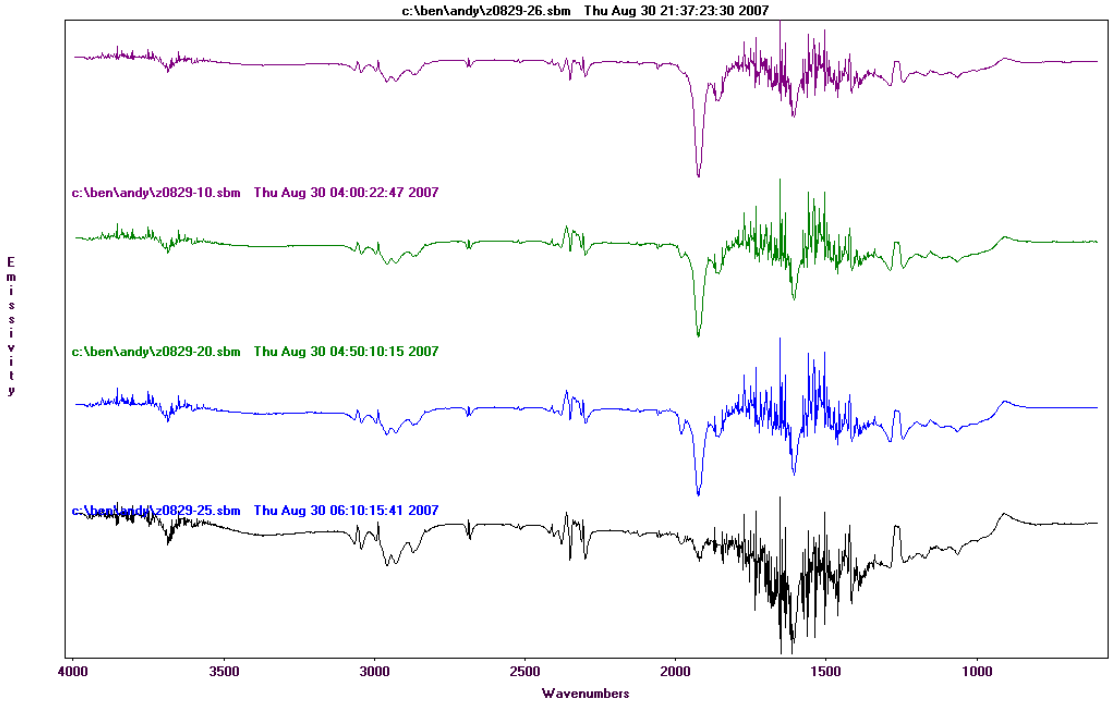

Fig 111. The decomposition of [NEt$_4$][CrBr(CO)$_5$] in DCM

A few drops of water were added into a DCM solution of [NEt$_4$][CrBr(CO)$_5$] and IR spectra recorded regularly over a 30 minute period (**Fig. 112**). The formation of Cr(CO)$_6$ was far more rapid in this instance with a strong band for Cr(CO)$_6$ being observed.

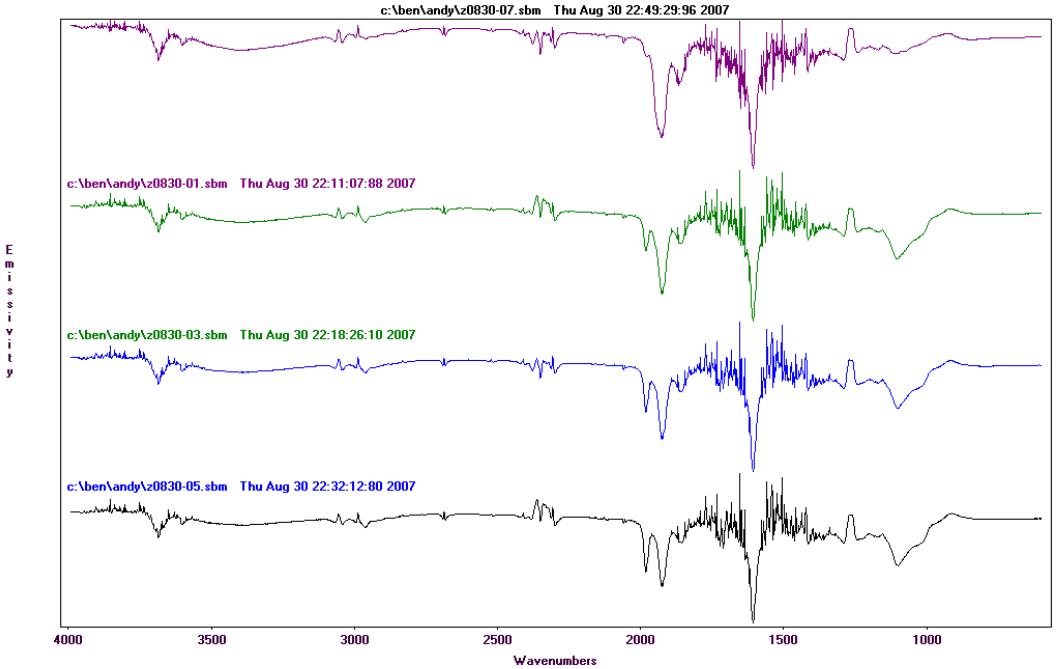

Fig 112. The degradation of [NEt$_4$][Cr(CO)$_5$Br] in DCM triggered by water over 30 min

The reaction was monitored for a further 30 minutes (**Fig 113**) by which time $Cr(CO)_6$ was the major carbonyl-containing product.

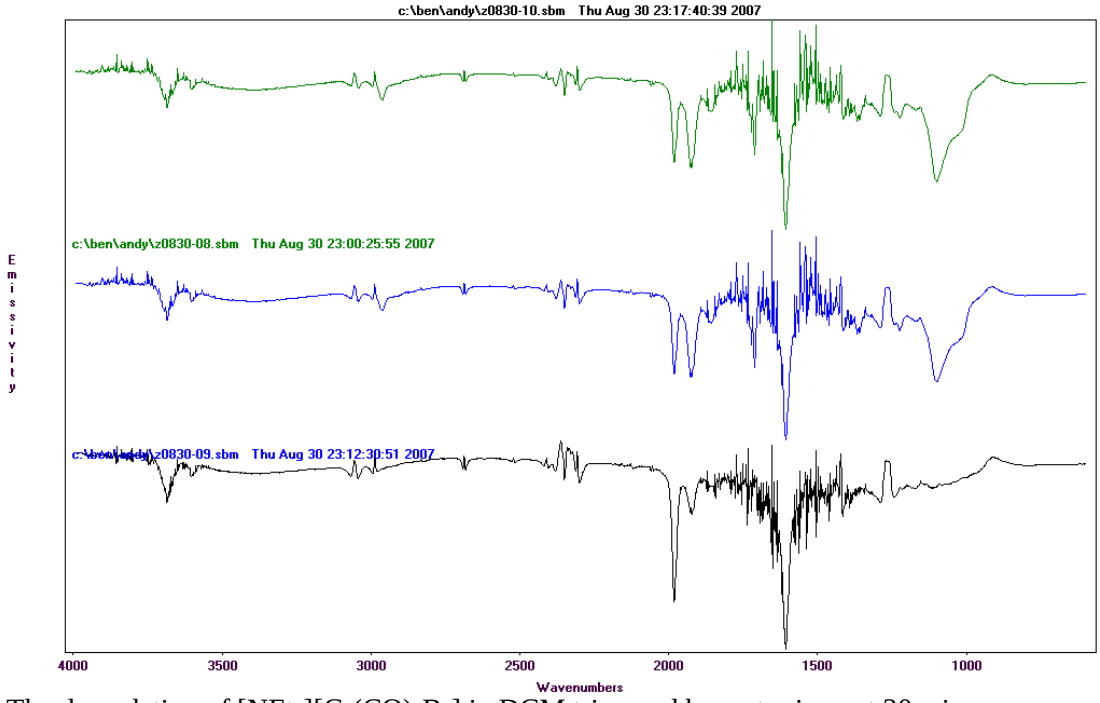

Fig 113. The degradation of $[NEt_4][Cr(CO)_5Br]$ in DCM triggered by water in next 30 min

The decomposition of $[NEt_4][CrBr(CO)_5]$ reaction was repeated and IR spectra acquired at *ca*. 2 min intervals. This allowed for the intermediate $[NEt_4][(Cr(CO)_5\}_2(\mu\text{-Br})]$, and its subsequent conversion to $Cr(CO)_6$, to be observed (Figure 2 main manuscript). Both the loss of the $[NEt_4][(Cr(CO)_5\}_2(\mu\text{-Cl})]$ and the growth of $Cr(CO)_6$ could be modeled using the SOLVER routine in Excel as obeying first order kinetic with the loss of the $[NEt_4][(Cr(CO)_5\}_2(\mu\text{-Cl})]$ and growth of $Cr(CO)_6$ having similar rate constants (**Fig. 114**).

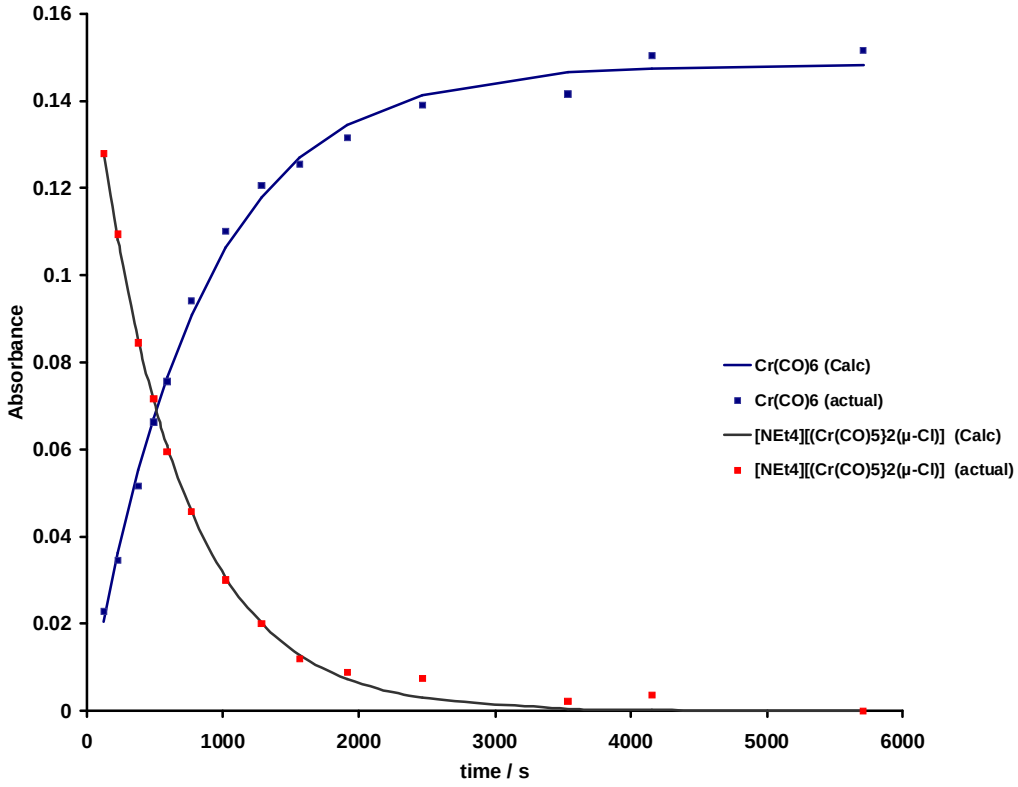

Fig 114. Loss of $[NEt_4][(Cr(CO)_5\}_2(\mu\text{-Cl})]$ and growth of $Cr(CO)_6$ with fit to first order kinetics. Rate of loss of $[NEt_4][(Cr(CO)_5\}_2(\mu\text{-Cl})] = 1.60 \times 10^{-3}\ s^{-1}$, rate of formation of $Cr(CO)_6 = 1.24 \times 10^{-3}\ s^{-1}$.

The degradation tests were repeated under using degassed solvents (**Fig 115**) and oxygenated solvents (**Fig 116**). In both cases the rate of growth of $Cr(CO)_6$ was fitted to first order kinetics and showed similar rate constants. The reaction of $[NEt_4][Cr(CO)_5Br]$ with $[Fe(\eta^5\text{-}C_5H_5)_2][PF_6]$ in DCM resulted in the formation of $[Cr(CO)_5Br]$ (**Fig 117**). Again the rate of formation of $Cr(CO)_6$ showed little variance and bands due to $[Cr(CO)_5Br]$ were only observed in the presence of the ferrocenium salt.

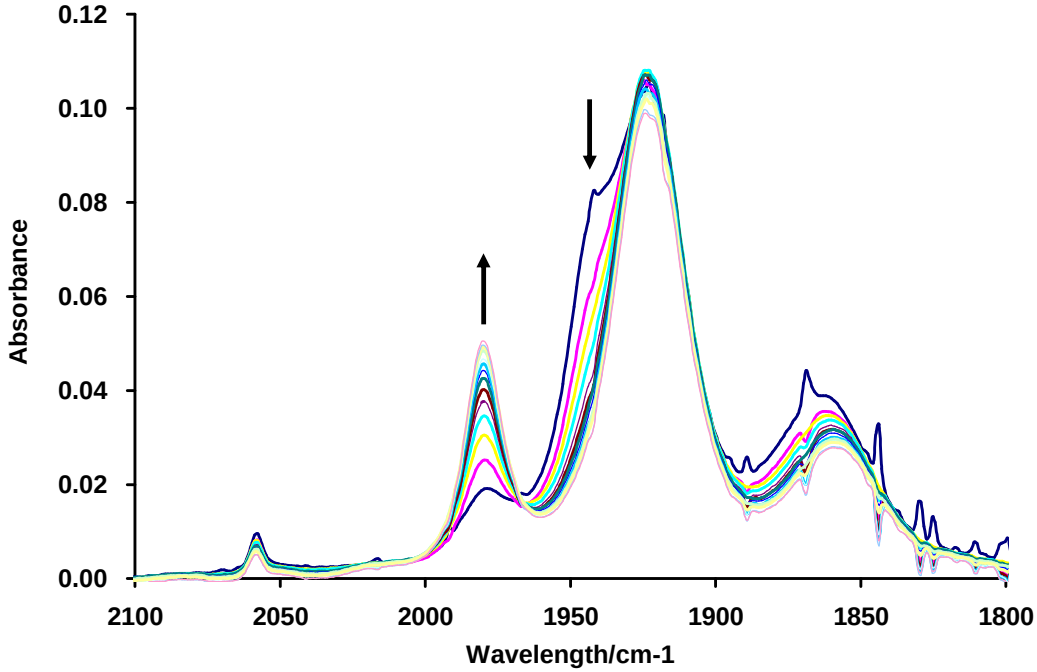

Fig 115. The degradation of $[NEt_4][Cr(CO)_5Br]$ in DCM triggered by water using degassed solvents. Rate of formation of $Cr(CO)_6 = (4.63 \pm 0.54) \times 10^{-3}\ s^{-1}$.

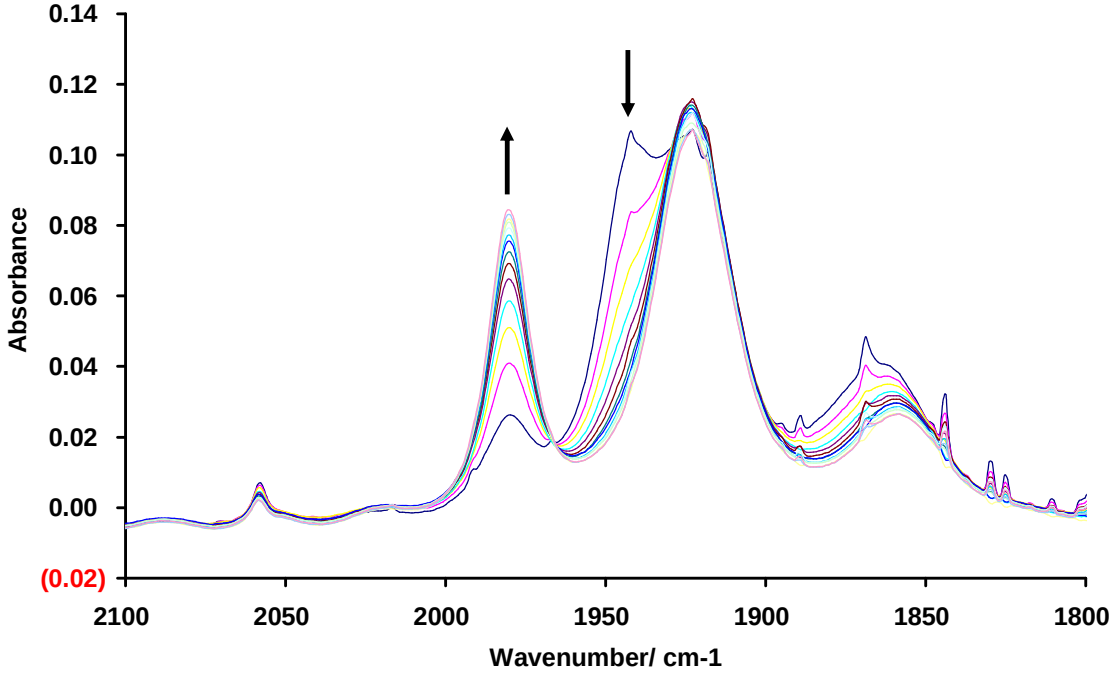

Fig 116. The degradation of $[NEt_4][Cr(CO)_5Br]$ in DCM triggered by water using oxygenated solvents. Rate of formation of $Cr(CO)_6 = (4.73 \pm 0.57) \times 10^{-3}\ s^{-1}$.

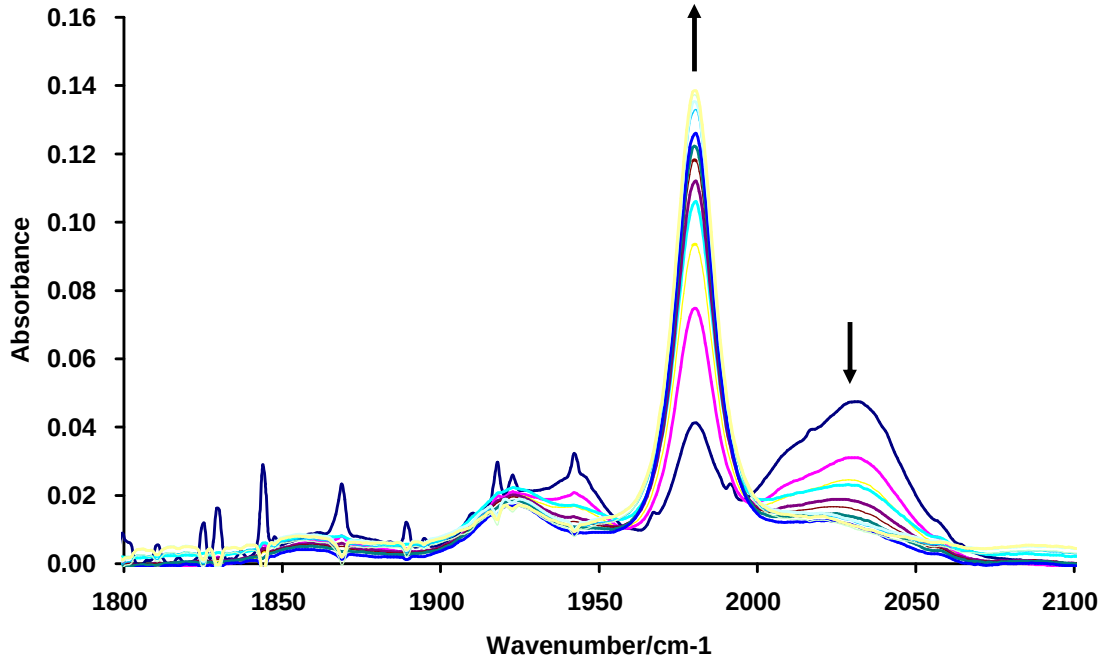

Fig 117. The degradation of $[NEt_4][Cr(CO)_5Br]$ in DCM in the presence of one equivalent of $[Fe(\eta^5\text{-}C_5H_5)_2][PF_6]$. Rate of formation of $Cr(CO)_6$ = (5.52 ± 0.66) x 10^{-3} s^{-1}.

2.2. Degradation test of $[NEt_4][CrI(CO)_5]$ in methanol

The degradation tests were carried out in same fashion as the those in DCM as described in **Section 2.1**. To a freshly prepared methanol solution of $[NEt_4][CrI(CO)_5]$ a drop of water was added and the solution mixed. The resulting reaction was monitored by IR spectroscopy with spectra recorded every 10 minutes.

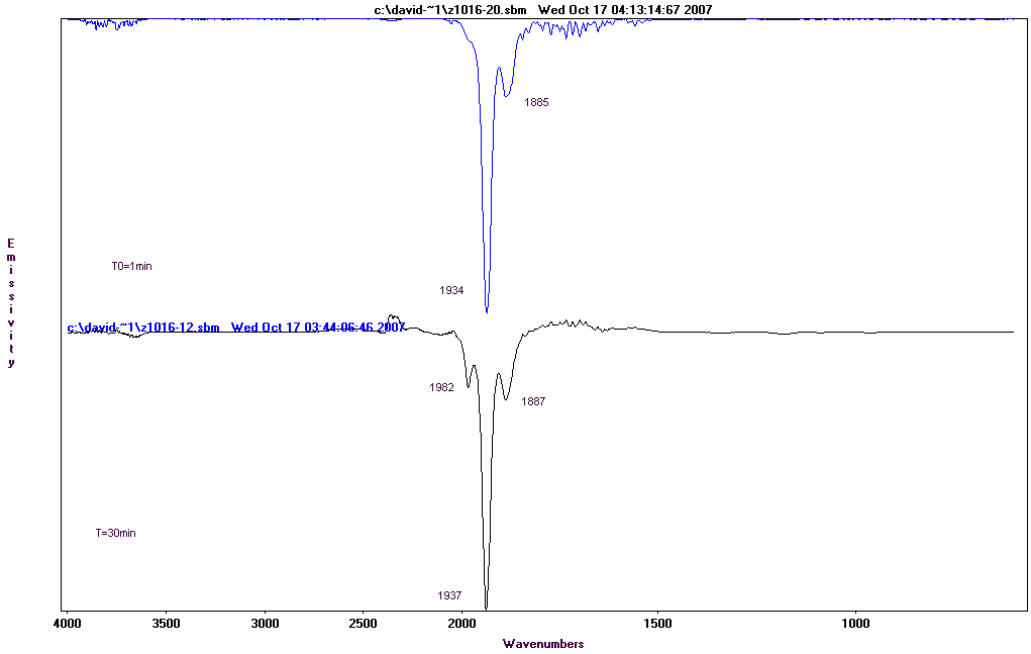

Fig 118. Spectrum recorded at t=0 min and t=30min showing the formation of $Cr(CO)_6$

2.3. Independent Carbonylation of $[NEt_4][CrI(CO)_5]$ in methanol

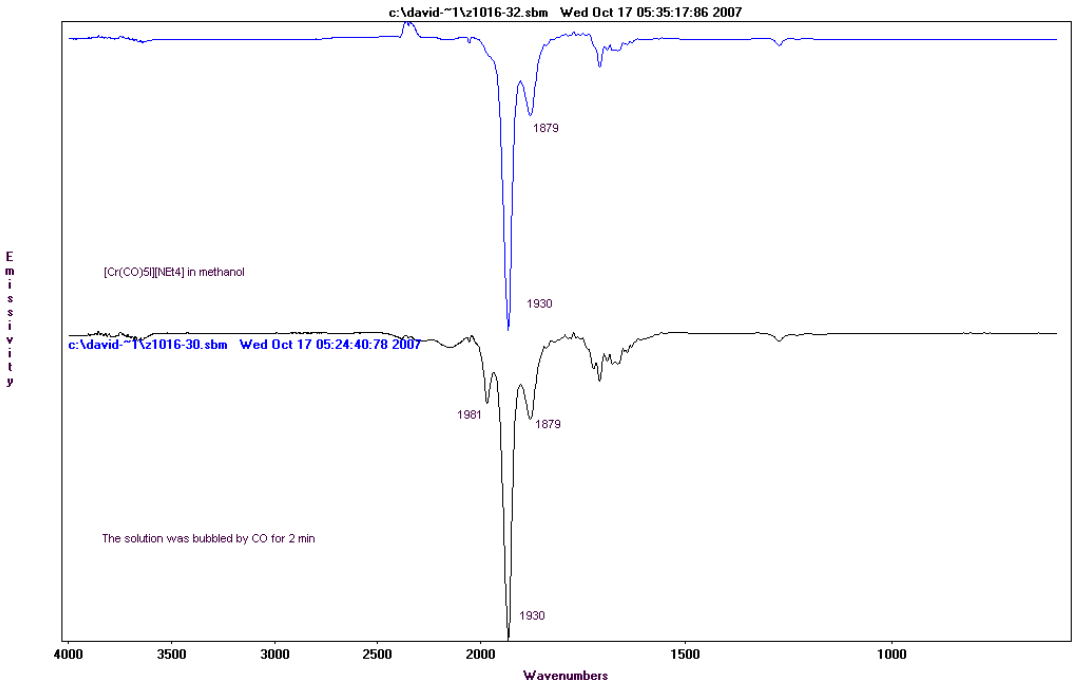

Fig 119. Independent Carbonylation of $[NEt_4][Cr(CO)_5I]$.

A methanol solution of $[NEt_4][Cr(CO)_5I]$ was purged with CO for 3 minutes. After which time the the IR spectra of the reaction mixture demonstrated that some $Cr(CO)_6$ had been formed. Further reaction with CO led to complete conversion to $Cr(CO)_6$ as the only carbonyl-containing product.

2.4. Reaction of [NEt$_4$][CrBr(CO)$_5$] and [NEt$_4$][(Cr(CO)$_5$}$_2$(μ-Br)]. With DMSO.

In a typical experiment 1 mg of [NEt$_4$][(Cr(CO)$_5$}$_2$(μ-Br)] was dissolved in 1 mL of CH_2Cl_2 and immediately afterwards a drop of DMSO was added. The reaction mixture was stirred at 20 ºC for 30 seconds. The sample was loaded in a sealed IR cell and spectra recorded at intervals. The reaction with [NEt$_4$][CrBr(CO)$_5$] was performed in an identical manner.

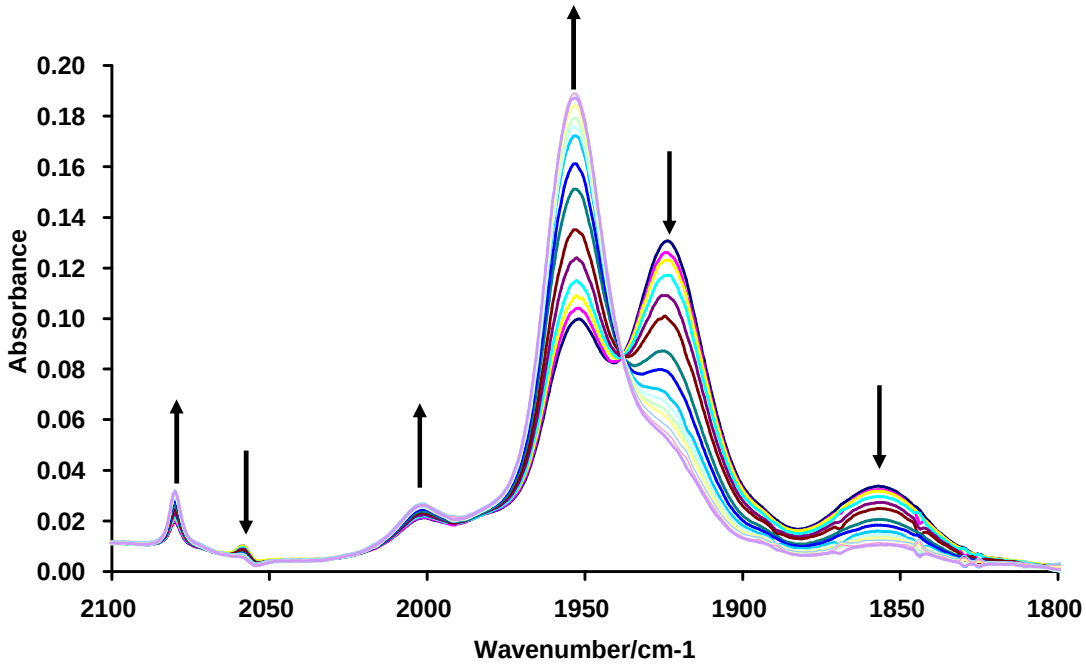

Fig 120. IR spectra illustrating the reaction of [NEt$_4$][{Cr(CO)$_5$}$_2$(μ-Br)] with DMSO.

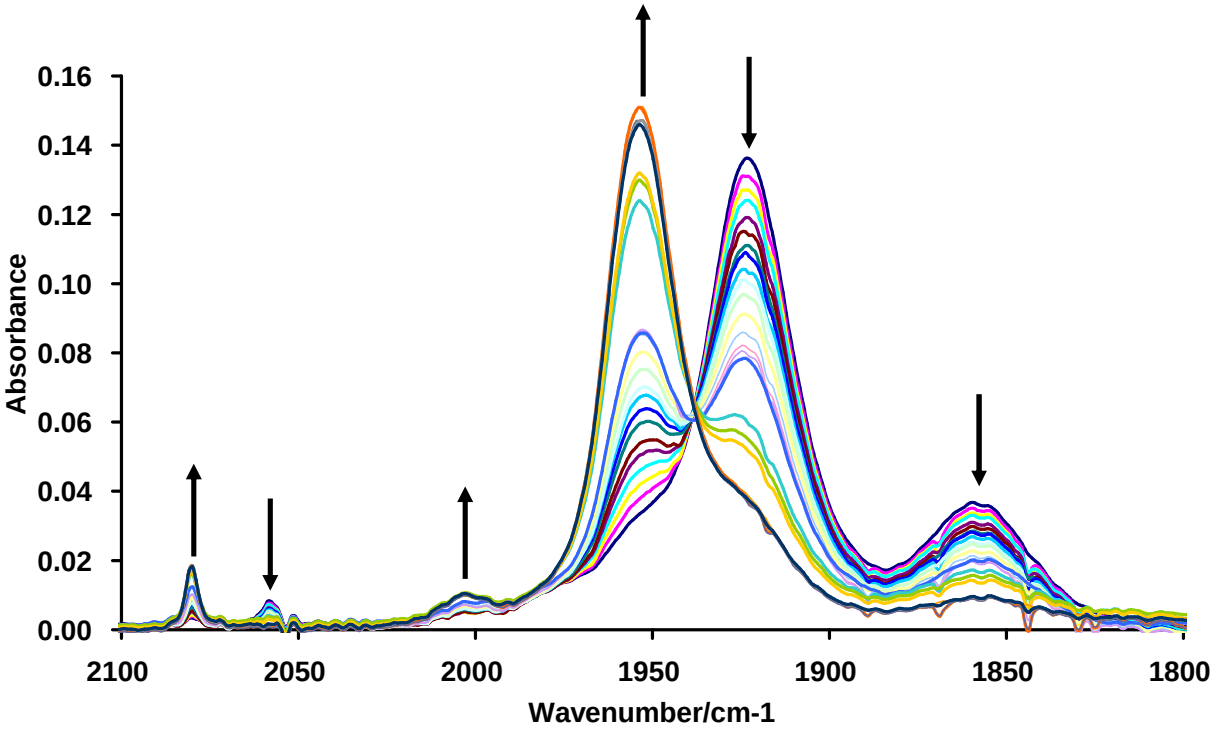

Fig 121. IR spectra illustrating the reaction of [NEt$_4$][CrBr(CO)$_5$] with DMSO.

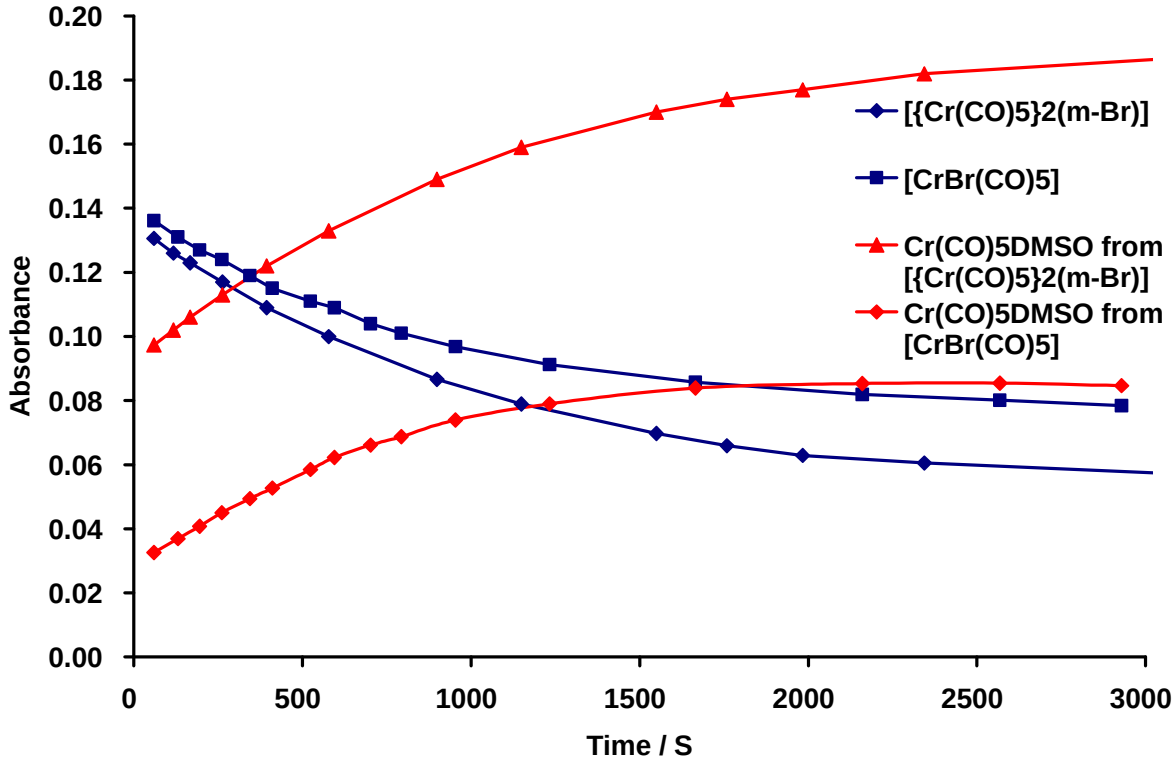

Fig 122. Comparison of the formation of $Cr(CO)_5(DMSO)$ from $[NEt_4][CrBr(CO)_5]$ and $[NEt_4][(Cr(CO)_5\}_2(\mu\text{-}Br)]$

2.5. Degradation tests of $[NEt_4][V(CO)_6]$

The degradation of $[NEt_4][V(CO)_6]$ in water was studied using the ReactIR system. Infra-red spectra of a 1.6 mM solution of $[NEt_4][V(CO)_6]$ thermostated at 37 °C were recorded at 30 s intervals. The band at $V(CO)_6^-$ at 1830 cm^{-1} was observed to decrease intensity over a period of approximately 2 hours, sample spectra are shown in **Fig. 98**.

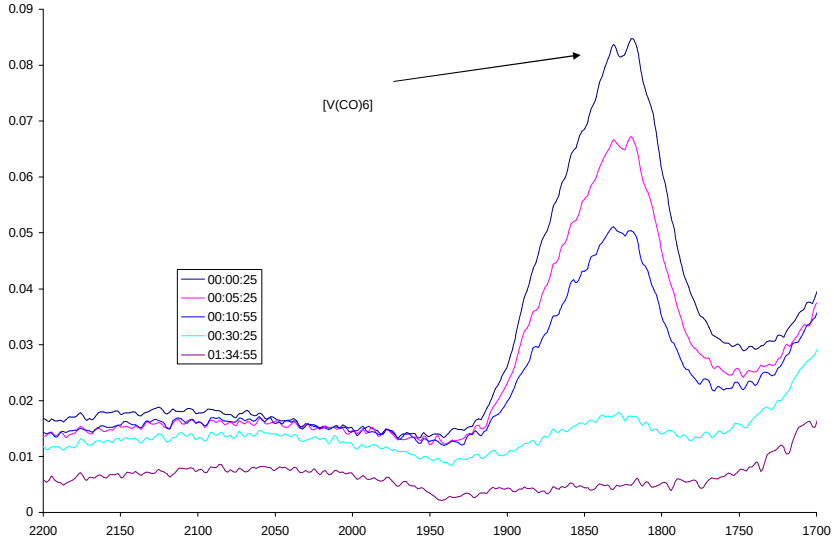

Fig 123. Infra-red spectra monitoring the degradation of $[NEt_4][V(CO)_6]$ (1.6mM) in H_2O.

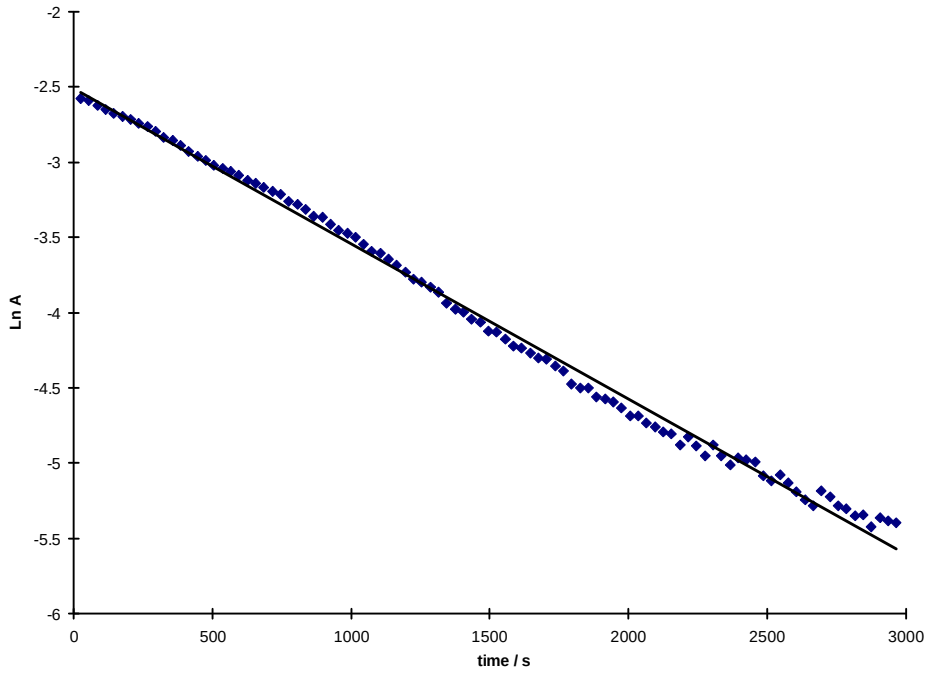

Fig 124. Degradation of $[V(CO)_6][N(C_2H_5)_4]$ in H_2O at 37.8°C, modeled with first-order kinetics with k = (1.03±0.01) x 10^{-3} s^{-1}. R^2 = 0.995